A model for predicting mangrove forest dynamics under variable environmental conditions - A Case study of the Estuary of Dongnai - Saigon River system, Vietnam

Von der

Fakultät Architektur, Bauingenieurwesen und Umweltwissenschaften

der Technischen Universität Carolo-Wilhelmina

zu Braunschweig

zur Erlangung des Grades einer

Doktorin der Naturwissenschaften (Dr. rer. nat.)

genehmigte

Dissertation

von

Hoang Anh Nguyen

geboren am 18.01.1978

aus Vietnam

Eingereicht am	26.Mai 2011
Disputation am	13.Juli 2011
Berichterstatter	Prof. Dr. Otto Richter
Berichterstatterin	Prof. Dr. Uta Berger

2011

Dedication

This work is respectfully dedicated to Prof. Dr. Huynh, Thi Minh Hang.
Prof. Dr. Huynh, Thi Minh Hang was my former supervisor and was the person who had deep influence on my career, who transferred me the love on doing scientific research.

Acknowledgment

I finish this dissertaion with many supports and helps from my sincere Professor, friends, colleagues and my family.

I would like to thank Prof. Dr. Otto Richter for supervising me and for kindly helping me. During my study, I have learnt from you the skill of working and thinking, especially I have learnt from you the patient character in understanding your students to transfer the knowledge to your students.

The memories about the time I have spent with the friends and the colleagues will always be with me, which are the sincere feelings that you have done for me. Thank to the friends and colleagues at the Department of Environmental System Analysis for the warm attentions to me and helping me. I really do not know how to express my feelings because for some situation it is not easy to tell what one really feels, but the only thing I want to tell is that I want to continue to work with all of you in this warm condition of our Department.

I would like to thank Prof. Dr. Nguyen, Van Phuoc and the colleagues at the Institute for Environment & Resources for supporting me with my work.

A special thank to my family, especially my mother, my uncle and my cousins, who always take care of me and worry for me.

Acronyms

ASVM	Aggregated state variable model
CGMM	CanGio Mangrove Forest model
CGProFMB	CanGio Protection Forest Management Board
DEM	Digital elevation model
EROS	Earth Resources Observation and Science Center (http://eros.usgs.gov/)
ERSDAC	Earth Remote Sensing Data Analysis Center
HCMC	HoChiMinh City, Vietnam
IBM	Individual based model
IER	Institute for Environment and Resources, Vietnam
LAI	Leaf area index
LBM	Landscape based model
MCMC	Markov chain Monte Carlo
NDVI	Normalized Difference Vegetation Index
ODE	Ordinary differential equation
SRHC	Sourthern Regional Hydrometeorological Center

Contents

List of Tables **VIII**

List of Figures **X**

I. General **1**

1. Introduction **2**
1.1. Statement of the problem . . . 2
1.2. Forest models and Mangrove forest models . . . 3
1.2.1. Scale in forest models . . . 4
1.2.2. Theories and methods of forest models . . . 5
1.2.3. Mangrove forest models . . . 6
1.3. Objectives and presentation of the thesis . . . 7
1.4. Data used in the thesis . . . 9

2. The Mangrove **10**
2.1. The Mangrove . . . 10
2.1.1. Mangroves and their environment . . . 10
2.1.2. Interaction between mangroves and the environment . . . 12
2.1.3. Impacts on mangroves . . . 12
2.2. The Mangrove in Vietnam . . . 12
2.3. The CanGio Mangrove Forest, Vietnam . . . 15
2.3.1. Natural conditions . . . 15
2.3.2. Social and economic activities . . . 17
2.3.3. The CanGio Mangrove forest . . . 18
2.4. Data analysis (apply for *Rhizophora apiculata*) . . . 18
2.4.1. The data . . . 18
2.4.2. Correlation between tree size and tree density . . . 24
2.4.3. Tree size along a gradient of salinity . . . 25
2.4.4. Tree size at the same zone of salinity . . . 26
2.4.5. Tree size and tree growth rate in different zones of salinity . . . 27
2.4.6. Tree size and tree growth rate along gradient of salinity . . . 28
2.5. Conclusion . . . 28

II. Modelling the dynamics of CanGio Mangrove forest **32**

3. Understanding Mangrove Dynamics using IBM **33**
3.1. Individual Based Model for simulating the CanGio Mangrove forest dynamics 33

3.2. Mangrove dynamics models . . . 34
3.2.1. Growth model . . . 34
3.2.2. Reproduction and seedling dispersal . . . 39
3.2.3. Tree mortality . . . 39
3.3. Parameter estimation for growth model (apply for *Rhizophora apiculata*) . . . 40
3.3.1. General statement of the problem . . . 40
3.3.2. Estimation strategy . . . 41
3.3.3. Parameterization using real data . . . 42
3.3.4. Parameterization for competition factor multiplier by combining real data and artificial data . . . 44
3.3.5. Test of the estimated parameters . . . 49
3.4. Simulating mangorve dynamics using IBM . . . 51

4. CanGio Mangrove Forest Model (CGMM) 60
4.1. The CanGio Mangrove Forest Model . . . 60
4.1.1. Purpose . . . 60
4.1.2. Design concept of CGMM . . . 60
4.1.3. Entities, variables and scales . . . 61
4.1.4. Process overview and scheduling . . . 62
4.1.5. Interaction . . . 62
4.1.6. Initialization and input data . . . 63
4.1.7. Submodels . . . 63
4.2. The up-scaling approach from IBM to construct CGMM . . . 64
4.2.1. Aggregation of individual sizes to size structured populations . . . 66
4.2.2. Process to extract the aggregated function of competition factor FA . 66
4.2.3. Seedling dispersal . . . 69
4.3. Dynamic processes implemented in CGMM . . . 70
4.3.1. Tree life cycle . . . 70
4.3.2. Local interaction . . . 71
4.3.3. Spatial interaction . . . 71
4.4. Modelling CanGio Mangrove Forest Dynamics using CGMM . . . 71
4.5. CGMM validation . . . 80

5. Proposing a coupled model for mangrove modelling 83
5.1. Limitations of ecological models . . . 83
5.2. Another approach for obtaining data: Remotely sensed data . . . 83
5.3. Proposing a coupled model for mangrove modelling . . . 84
5.4. Conclusion . . . 86

6. Summary 88

A. Appendix A: Calculation of Multiplier from the data 89
A.0.1. When we know the age of trees in a stand . . . 89
A.0.2. We don't know the age of trees, but we know the increment of *dbh* . . 89

B. Appendix B: Reconstruction of spatial point pattern 91
B.1. Reconstruction of point patterns . . . 92

C. Appendix C: Equations, Variables and Constants **94**
C.1. Equations 94
C.1.1. Tree Growth 94
C.1.2. Tree - to - tree Competition 94
C.1.3. Reproduction 96
C.1.4. Seedling dispersal 96
C.1.5. Tree mortality 96
C.2. Parameters 97

D. Appendix D: List of Symbols **100**

List of Tables

1.1. Data used for the study 9

3.1. Data used for estimating parameters for salinity factor multiplier 42
3.2. Data used to test the estimated parameters 51

4.1. Description of components and variables of different scales of CGMM 62
4.2. Processes implemented in IBM and CGMM 65

C.1. Processes are implemented in IBM and CGMM 95
C.2. Parameters of growth equation 97
C.3. Parameters of growth multiplier of salinity factor 97
C.4. Parameters of growth multiplier of elevation factor 98
C.5. Parameters of growth multiplier of competition factor (for IBM) 98
C.6. Parameters of growth multiplier of competition factor (for CGMM) 99
C.7. Parameters of reproduction function 99
C.8. Parameters of mortality probability function 99

List of Figures

1.1. Conceptual structure of the ecological models in the thesis 8

2.1. Interrelation between mangroves and the environment 13
2.2. Map of mangrove distribution in Vietnam 14
2.3. Map of CanGio area 16
2.4. Species distribution: on Fluvisols 19
2.5. Species distribution: on Gleysols 19
2.6. Species distribution: on Arenosols 20
2.7. Salinity contour 21
2.8. Sampling positions 22
2.9. Digital elevation model (DEM) of study area 23
2.10. dbh and density relationship of *R. apiculata* 25
2.11. Growth multiplier (MUL) and density (N) relationship of *R. apiculata* . . . 26
2.12. Tree health along salinity gradient 27
2.13. Tree sizes at the same zone of salinity. Case: plots of different tree age, same salinity zone, same density (N) 28
2.14. Tree sizes at the same zone of salinity. Case: plots of same-age trees, same salinity zone and different tree number N 29
2.15. dbh and salinity relationship of *R. apiculata* 30
2.16. Growth rate (MUL) and density (N) relationship of *R. apiculata* 30
2.17. Mean dbh of *R. apiculata* along salinity gradient 31
2.18. Growth rate of *R. apiculata* along salinity gradient 31

3.1. Conceptual structure of the IBM 34
3.2. The IBM submodels 35
3.3. The curves of multipliers which affecting tree growth 38
3.4. Order and data choosing for the process of parameter estimation 41
3.5. Fitted diameter and height curves under optimal environmental conditions . . 43
3.6. Sensitivity analysis of optimal growth curve. 44
3.7. Fitted multiplier curve with data 45
3.8. A sample of a realisation of a ***'Hard-core Strauss'*** process 46
3.9. Fitted R's curve with simulated data 47
3.10. Examples of fitted curves for the relationship between f_c and FA 48
3.11. Correlation and sum of square of residual between f_c and FA from 3 examined plots (ID35, ID37 and ID41) 50
3.12. Frequency of mean diameters from 500 simulations 52
3.13. Example of frequency of tree diameters of each plot in one of 500 simulations from IBM 53
3.14. Simulated stable environmental conditions 55
3.15. Simulated environmental conditions for sea level change scenario 56

3.16. Mangrove growth and distribution under two scenarios: stable environmental conditions and sea level rise 57
3.17. Time course of total biomass of each species under stable environmental conditions 58
3.18. Time course of total biomass of each species under influence of sea level rise . 58
3.19. Species composition (%) following time under stable environmental conditions 59
3.20. Species composition (%) following time under influence of sea level rise 59

4.1. Conceptual structure of CGMM 61
4.2. Submodels of CGMM 63
4.3. Examples of fitted curves of simulated FA from focused trees against different neighbouring trees 68
4.4. Maps of simulated area 73
4.5. Scenarios of sea level rise ans salinity rise 74
4.6. Species distribution resulted from simulations of three scenarios 75
4.7. Biomass distribution resulted from simulations of three scenarios 76
4.8. Time course of biomass resulted from the simulations of stable environmental condition 77
4.9. Time course of species composition resulted from the simulations of stable environmental condition 77
4.10. Time course of biomass resulted from the simulations of the sea level increase 65 cm scenario 78
4.11. Time course of species composition resulted from the simulations of the sea level increase 65 cm scenario 78
4.12. Time course of biomass resulted from the simulations of the sea level increase 100 cm scenario 79
4.13. Time course of species composition resulted from the simulations of the sea level increase 100 cm scenario 79
4.14. NDVI images of the study area 81
4.15. Correlation between mean NDVI values and mean simulated biomass values . 82

5.1. Spectral characteristics of 3 mangrove species 85
5.2. NDVI distribution following tiem in the study area 86
5.3. Conceptual structure proposed for a coupling model to predict mangrove future 87

Part I.

General

1. Introduction

1.1. Statement of the problem

The role and the importance of mangrove ecosystems have been widely discussed in many fields of research. From the aspects of biodiversity, ecology, environment and also economics... all of which underscore the same conclusion: we need to protect and conserve the mangrove ecosystems.

In Vietnam, the issue of how to balance between economic development, mangrove ecosystems exploitation and conservation on coastal wetland areas, particularly in the context of proactively find solutions to deal with the effects of global warming, is always a matter of concern.

Discussion can be started by analyzing the situation of CanGio Mangrove Forest which is located in the South of Vietnam. CanGio mangrove forest is known as the World Biosphere Reserve area. This forest plays a very important role because it is the habitat for a myriad of ecological and economic reasons and is the screening of pollution for HoChiMinh City (HCMC), the biggest City in Vietnam. There have been many researches on this forest concerning ecology, vegetation, species composition, biomass, and so forth; some important results are given by Hong et al. (1988), Hong (1991), Nam et al. (1992), Nam et al. (1996), Nam and Thuy (1998), Nam (2000), Mochida et al. (2000), Fujimoto et al. (2000), Clough et al. (2000).

The results of these studies have inspired the sense of sustainable exploitation and management of mangrove resources, leading to researches on developing models and support tools for the management. In the year 2000, the Government of HCMC enacted the mangrove preservation act to ensure the protection and proper trimming of these trees. The call for social science and human ecology to develop a better understanding of the interaction between mangrove habitats and human activities had been issued. Since then researches focused on building and developing tools to support for mangrove ecosystem management have been conducted, among those Hang and Anh (2002), Hang et al. (2003), Hang and Anh (2003), Hang and Anh (2006b), Hang and Anh (2006a) and Anh (2007).

Results of those researches on the one hand contributed to the development of support tools for resources management, on the other hand they show their own limitations. The models and tools proposed still lack quantitative forecasts. The quantification of future status of mangrove ecosystems under different environmental settings is not feasible.

A predictive understanding can challenge our assumptions concerning the factors that control plant distribution and abundance and provide techniques for predicting rate and ranges of change of species in response to disturbances. Simulation modelling is widely recognised to be

a powerful tool for understanding the complexity of biological systems and a useful means of inference on long-term dynamics, especially given the rarity of comprehensive long-term data on vegetation dynamics. As an essential requirement of the development, we need to develop a mathematical model which can quantify the situation of mangrove ecosystems, from which we can predict mangrove changes in the future.

1.2. Forest models and Mangrove forest models

Practical demands of a mathematical model which can reconstruct, simulate and predict the development of forest ecosystems in general, and mangrove ecosystems, in particular, do not concern only Vietnam, but also the general situation in the world.

Initially, models for forest ecosystems primarily focused on calculating yield and productivity of forest (wood production), ***Forest Growth and Yield Models***. This is the oldest and broadest class, dating from the first yield tables in the 18^{th}-19^{th} centuries (Monserud, 2003). They were developed aiming to predict growth and yield using statistical techniques. Calibrated for comprehensive data-sets, the models were used to predict an expected yield over the management regime. They are adequate for describing growth for a range of silvicultural practices and site conditions. Their relatively simple data input requirements and accuracy in predicting growth have made them the principal yield models of forest management. The scale for this type of model is very fine, it ranges from individual tree to stand level. This type of model is called the site-specific prediction of growth and yield over time. Site index is the standard measure of this model.

Along with the cognizance of reasonable and sustainable resource exploitation and management, the increase in the per capita ecological footprint as standards of living improved worldwide, the benefits derived from forests started to be considered as not only just wood production, but also their ecological values. Since then, forests had begun being managed as an ecosystem, the growth and yield models began to show their weaknesses. This approach ignores potential changes in environment, genetics, site and silviculture that might occur since there is no link to underlying causes of productivity.

Models that can connect underlying processes with productivity have in turn been launched, each meets a specific requirement, each model has its own advantages and disadvantages. The classification of forest models also depends on different aspects and different purposes to be considered, various methods of classification are possible and have been reviewed by Munro (1974), Shugart and West (1980), Shugart (1984), Dale et al. (1985), Vanclay (1994), Liu and Ashton (1995), Waring and Running (1998), Mladenoff and Baker (1999), Monserud (2003), Hope (2003), Xi et al. (2009), Kimmins et al. (2010).

In general, forest models are classified mainly base on different levels of simulated processes and different levels of scale. Typical classes of forest models include (source from http://www.forestmodels.com/):

- ***Ecological forest models*** were developed to model natural and management-induced disturbances in cultivated, semi-natural or natural forests, they model long-term ecosystem dynamics involving information on recruitment, growth and mortality of trees.

- ***Process-based models***, or also known as mechanistic models, or biogeochemical models, were developed to model key growth process(es) and fundamental causes of productivity such as: photosynthesis and respiration, carbon allocation, nutrient cycles and climate effects. They are mathematical representations of biological systems that incorporate our understanding of physiological and ecological mechanisms into predictive algorithms. They take into account at the physiological level plant responses to site factors either if they are manipulated by humans directly, such as fertility, or indirectly, such as atmospheric carbon dioxide concentrations.

- ***Hybrid forest models*** were developed from complementary merging of well understood processes and reliable tree/stand empiricism aiming to have a process model in which the shortcomings of both approaches can be overcome to some extent.

The difficulty in constructing those models lies in the ***'scale'*** at which objects and processes are simulated. One of the challenges that need to be achieved is the ***how*** of the combination between the heterogeneity of simulated objects and the ability of scale expansion (both space and time) of a model. This feature is particularly focused in the thesis.

1.2.1. Scale in forest models

The extent and detailed explanation of a model are expressed by the factor **'scale'**. Following Ratzé et al. (2007), there are three meanings of scale: (i) an observational meaning, (ii) an ontological meaning and (iii) a representational meaning. In which, the representational meaning of scale is of particular importance in modelling because modelling implies the representation of a world with some limited precision. There are two branches of approaches in ecological modelling which lead to different levels of outcomes: individual based approach and aggregated state variable approach.

The main difference between these two approaches is Individual based models (IBMs) use individuals as basic units; they deliberately include heterogeneity among individuals. Typically heterogeneity is built in for particular attributes of interest, such as body size, spatial arrangement, spatial interaction, bio-energetic or physiological parameters, behavioral characteristics, and so forth.

Aggregated state variable models (ASVMs) usually model the probabilistic behavior of individuals and average over a large number of them, in this case, the individuals are assumed to be rather homogeneous. Because of that, simulated results of ASVMs can not well explain the existence of individual variability compared to IBMs.

Over time, IBMs have demonstrated effectiveness in simulating complex processes, particularly when there are ecological interference of individuals, while models for aggregated state variables are deficient because they ignore important aspects of differentiation among individuals.

The important technical problem of IBMs is the relationship between resolution at which the model runs and landscape extent that can be simulated by the model, and the degree to which a model incorporates mechanistic detail and spatial dynamics. IBMs supply very fine

outcomes but not the spatial extent or they require large computing times. For forest ecology, the spatial arrangement and interaction of individual trees are among the factors that cause the differentiation among trees and cause the process of self-thinning. The inclusion of distance dependence adds to model complexity and computational load. Mladenoff (2004) called it the trade-offs associated between spatial resolution (the maximum area that can be simulated by the model, set by practical limits of computing resources) and the degree to which model objectives need to incorporate mechanistic detail and spatial interaction.

There have been many efforts to aggregate spatial scalability and detailed simulated results, some authors tried to simulate tree dynamics in heterogeneous stands, or forest growth models that focus on the heterogeneity of individual trees within a stand (Le Roux et al. (2001), Lischke et al. (1998), Lischke et al. (2006)). In this case, modellers generally represent an individual tree as an ensemble of growth units (height classes), or as clusters of growth units, such as leafy shoots or branches. This representation can capture essential features of the competition between trees within stands without using a complex, organbased approach.

Another trend is using IBMs to provide parameter values for the aggregated state variable model (Luan et al. (1996); Berninger and Nikinmaa (1997); Le Roux et al. (2001)). Grimm (1999) called this application a **'computer experiment'** using IBMs. In this type of aggregating, the detailed data is input into IBMs and will be summarized from IBM's outputs (statistics from many simulations of IBM). Then these outputs are used as inputs for coarser models (see Berninger and Nikinmaa (1997); Sinoquet and Le Roux (2000); Le Roux et al. (2001)).

1.2.2. Theories and methods of forest models

Ecological forest modelling follows the continuous development of forest succession theories, disturbance and non-equilibrium hypothesis of ecosystems (Xi et al., 2009). The advance of forest models can be viewed as an integrated and quantitative process of linking knowledge of forest succession, influencing factors and the non-equilibrium nature of ecosystems which can be viewed by hierarchy theory.

Hierarchy theory addresses the understanding of systems with a certain type of organized complexity (Allen and Starr (1982), Costanza and Voinov (2004), Andrew Royle and Dorazio (2008)). This theory can be used to test hypotheses related to the complexity of multilevel systems. From a scaling perspective, hierarchy theory helps to construct a partition of complex systems. It can help ecologists to understand landscape patterns and scale-dependent properties of the ecosystems (Xi et al., 2009). Ecological systems are fundamentally hierarchical systems in which we encounter hierarchies of organization and spatial and temporal scale. These scales often correspond to **'levels'** in a hierarchical model.

One of the applications of hierarchy theory in ecological modelling is the **up-scaling approach**. This is the process of translating information from small scale to large scale. There have been applications of this up-scaling procedure, representatively include Luan et al. (1996); Berninger and Nikinmaa (1997); Le Roux et al. (2001), Garman (2004) and Lischke et al. (2006). The methods for this approach range from direct evaluation which means that an equation from source scale is directly solved and then is averaged to form the target

scale equation, to implicit up-scaling, meta-modelling (Kimmins et al., 2010) and so forth. Lischke et al. (2007) described the technical approaches for the process of up-scaling as follows: (i) identify the goal for the up-scaling, (ii) understand the source scale (entities, dynamics, interactions, constraints, ...), (iii) identify the target scale, (iv) determine how the variables in the source scale can be transformed into the suitable entities of the target scale and (v) aggregate the process functions of the source scale to the target scale and check whether the aggregate model reproduces the suitable results.

Another theory which is often applied in forest modelling is the theory of **Spatial point process**. This theory originated from the origin of the study of random point sequences. Spatial point pattern data occur frequently in a wide variety of scientific disciplines, including forestry and ecology (Moller and Waagepetersen, 2007). A fundamental question of interest in this context is whether or not the points of interest are occurring at random, or do the points cluster in some manner, or perhaps the points of interest are occurring with some sort of regularity, they are located indepently or they influence each other.

One major challenge is to resolve the apparent lack of compatibility between different methods applied and between model predictions at different temporal and spatial scales. A specific procedure on how to apply the theories and methods above to build a model is thus an essential need.

1.2.3. Mangrove forest models

Mangrove have been widely studied, however, ecological models which constructed for mangrove prediction are rather few compared to other ecological forest models.

The first mangrove model may be the gap dynamics model FORMAN (Chen and Twilley, 1998), this model was applied to the mangroves in Florida and Colombia (Twilley et al., 1999). FORMAN is then embedded into a landscape based model SELVA to form the model MANGRO which is applied to the Everglades in the South of Florida.

KIWI, a spatially explicit individual based model, was developed by Berger and Hildenbrandt (2000) and was first applied to mangrove forests in North Brazil (Berger et al., 2008).

López-Hoffman et al. (2007) developed a stage and patch structured matrix model to simulate the patch dynamics of mangrove population growth, this model was applied to the mangroves in Lake Maracaibo, Venezuela.

MANHAM (Teh et al., 2008) is a spatially explicit mechanistic model which was first developed by Sternberg et al. (2007). This model simulates the plant dynamics under influences of water and salinity movement in the vadose zone caused by storm surges.

Among these models, MANGRO can simulate mangrove dynamics over a large landscape by running the IBM (FORMAN) for each discrete cell on the landscape (the driving processes are supplied by SELVA model). Basically, this model is an individual based model which applied for landscape scale. This model does not take into account the interaction between

cells (through seed dispersal for instance) and may cost time for computing.

Berger et al. (2008) analyzed in detail the three models (FORMAN, KIWI and MANGRO) and concluded that mangrove models have contributed to the understanding of critical processes in mangrove wetlands. Further study on the relationships and mechanisms, especially the regulating recruitment, productivity and forest structure, should be implemented.

In summary, ecological models can be used in forest management and for scenario simulations and those models are the essential decision-support tools for forestry practice and for policy making. All models do not however fulfill all the requirements. The development of methodologies for the integration of simulation outputs from different models and the quantification of their uncertainty is therefore in strong demand.

1.3. Objectives and presentation of the thesis

The main objective of the study is to develop an appropriate model to facilitate the assessment, monitoring and sustainable management of mangrove forest resources. It is a contribution to the understanding about the dynamics of mangroves. Results of the model provide a quantitative overview of ecosystem succession and can support decisions about natural resources management.

In this thesis, an ecological model to simulate the development of mangrove attributes under influences of environmental factors is developed and applied to the CanGio Mangrove Biosphere Reserve in Vietnam. This model includes 2 levels of scale: individual level and landscape level.

The model is developed base on the application of **up-scaling approach** which is the transformation process from IBM to Landscape based model (LBM). To achieve that, we first develop the IBM and apply the parameterization for this model by field inventory data. A procedure for parameterization is defined in which we apply the theory of **spatial point statistics** to generate artificial data to add into the data set for the parameter estimation.

The IBM is then validated to test if its predictions have matched experimental data. We apply the process of up-scaling to construct the LBM from this of validated IBM. The LBM in this thesis is used to simulate mangrove dynamics under the effects of sea level rise scenarios. The two models are developed using Matlab version 2009a. All the data are processed and analyzed using Matlab and Excel. The input data for LBM are from GIS data (shape files).

The explaination of our work starts with a general introduction about mangrove and the CanGio Mangrove Forest where we apply our simulation (Chapter 2). In this Chapter, understanding about mangrove properties is provided by analyzing the data. This is a very important step for the construction of our model structure.

Chapter 3 describes the structure of the IBM together with the process of applying hierarchy theory and spatial points distribution to estimate parameters for the model. The Chapter is

completed by the simulations of mangrove behaviors using IBM.

The landscape based model (LBM) is described in Chapter 4. The LBM which we call the CanGio Mangrove Forest model (CGMM) is then applied to simulate the scenarios of environmental changes with particularly focus on the scenarios of sea level change. This model is also validated by remotely sensed data which is described in the end of this chapter.

In the final Chapter (Chapter 5), an outlook about possible model extension by coupling remotely sensed data with the CGMM are proposed together with the conclusions.

Figure 1.1 describes the conceptual construction of our mangrove model and the order organization of the thesis.

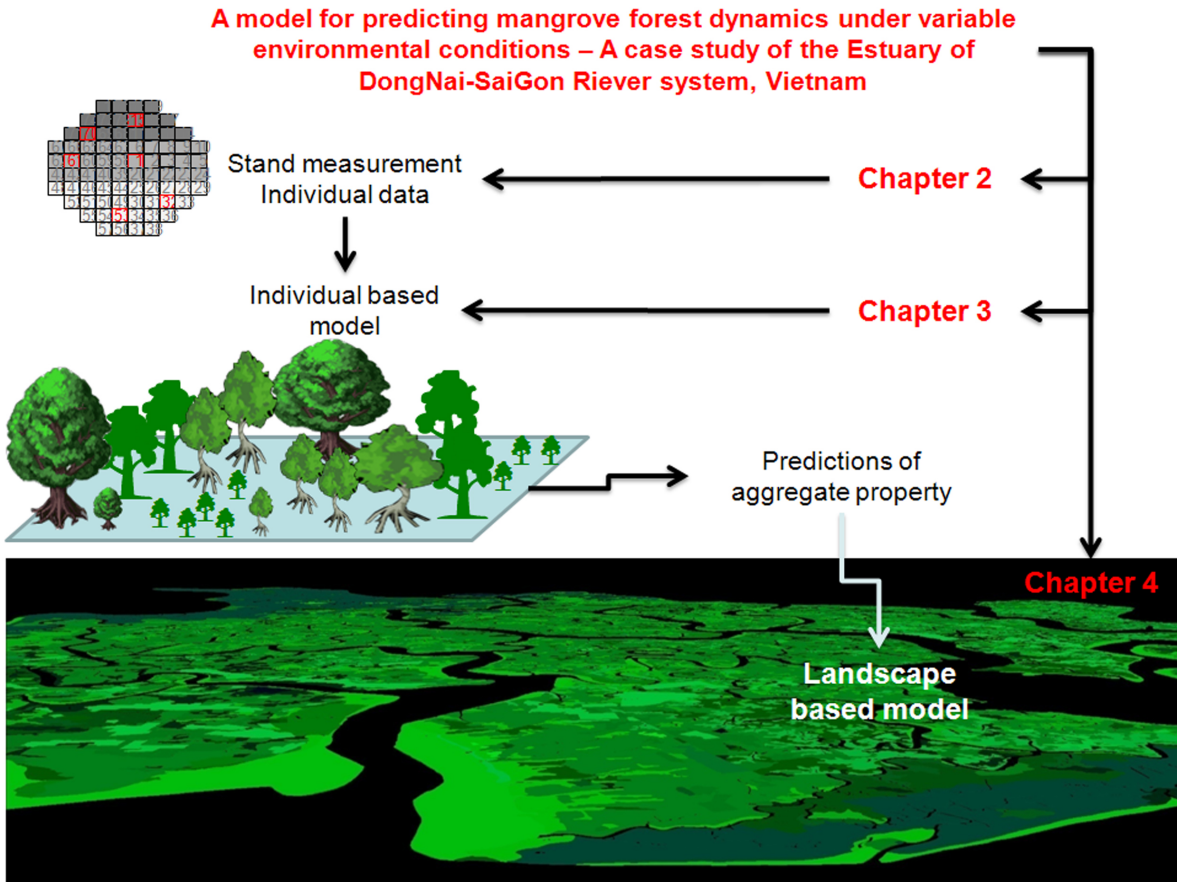

Figure 1.1.: *Conceptual structure of the ecological models in the thesis. Behaviours and interactions of individuals from data are simulated by IBM. Using IBM, these information can be aggregated to build understanding about ecosystem variables. Then, the aggregated variables are used to construct an aggregate level model.*

1.4. Data used in the thesis

This thesis has been done using the data from different sources, below are the data and sources which we used for the study

Table 1.1.: *Data used for the study*

Data	**Year**	**Sources**
Salinity data	1996 - 2006	Sourthern Regional Hydrometeorological Center (SRHC), Institute for Environment and Resources, Vietnam (IER)
Digital elevation model (DEM)	1984	IER
Map of vegetation distribution	1992	IER
Map of suitability salinity zonation for mangrove growth	2006	Anh (2007)
Mangrove mensuration data (age, diameter, height)	2005 - 2009	CanGio Protection Forest Management Board (CGProFMB), IER
Satellite data	Landsat MSS 01.01.1973, Landsat TM 06.03.1989, Landsat TM 07.01.1994, Landsat TM 03.02.1998, Landsat ETM 24.01.2003, ASTER 07.01.2006	Earth Remote Sensing Data Analysis Center (ERSDAC), IER, Earth Resources Observation and Science Center (http://eros.usgs.gov/) (EROS)

2. The Mangrove

2.1. The Mangrove

Mangroves are the characteristic intertidal plant formations of sheltered tropical and subtropical coastlines (Saenger, 2002). Worldwide, mangroves are limited between latitude 30°N and 30°S, Northern extensions of them occur in Japan (31°22′N) and Bermuda (32°20′N), Southern extensions are New Zealand (28°30′S), Australia (32°45′S) and on the east coast of South Africa (31°59′S). Temperature was said to be the factor which limits the extensions of mangroves (Tomlinson, 1986) but they have been found as far as South of New Zealand, North Japan, South Australia, South Africa and South Florida. This is explained by the warm ocean currents in East Africa and South America. Most of mangroves are found in the South East Asian countries, in which the mangroves in Indonesia account up to 23% of the world's total.

Basically, geological, climatic and biological factors determine the development and particular type of mangrove. Geological factors formed land morphology and sedimentation structure of the area, the climatic and meteological factors cause typical hydrological processes (tide, wave, coastal currents, ...). Biological factors condition the physiological adaptation of the plants (Pool et al., 1977).

Mangrove species compose a variety of morphological, physiological, biochemical and reproductive adaptations that enable them to grow in the particular kind of rather unstable, difficult environment that comprises the mangrove habitat. Approximately, there are 84 species of plants belonging to about 39 genera in 26 families which are recognized throughout the world as being mangroves (Saenger, 2002).

Mangrove species often occur in different vegetational zones parallel to the coastline and river banks (Macnae (1966), Snedaker (1982), Tomlinson (1986), Saenger (2002)). Macnae (1966) in his research on mangroves in the East and the South of Australia, he recognized the ordering of species occurring from seaward to landward as follows: *Avicennia and Sonneratia - Rhizophora - Bruguiera - Ceriops*. Bunt (1996) concluded that the diversity of sequencing of mangrove species can be explained by the presumably distinctive manner in which each mangrove species responds to environmental and biological controls.

2.1.1. Mangroves and their environment

Mangroves are special plant formations that could adapt themselves to the unstable conditions. The typical characteristics of the mangrove environment that made them are different from other terrestrial species are as follows:

Adapting to waterlogged soil conditions

As other types of vegetation, mangrove growth and productivity are influenced directly by the substrate characteristics. The type of soil and its physico-chemical states are the result of interactions of many factors: topography, climate, hydrodynamic processes, tidal regime, socio-activities, and so forth. Mangrove sediments have a unique history at any specific area, and it can provide significant insights with respect to species distribution and health (Saenger, 2002). The soil of mangrove habitats originated from sediments of recent marine alluvium, transported by the waters and are facilitated by mangrove vegetation, to aggregate and be deposited when reaching the brackish waters of estuaries. The processes of sediment transportation formed the intertidal landscapes where mangroves are located. Where deposited sediments have accumulated, the nature of the soil is primarily determined by pedogenic processes. Mangrove soils are made up of sand, silt and clay in different combinations and are rich of organic matterials. The typical character of mangrove soil is waterlogged. This is caused by the tidal flooding regime. Because of that, the soil has little aeration which decreases with depth and contain organic matters decomposing at a very slow rate. Soil condition is one of the contributing factors of zonation among different species, e.g., different species of vegetation thrive in different soil conditions, while plants like *Avicennia* prefers muddy conditions, *Sonneratia* do well in sandy areas; *Rhizophora* copes better with soft humus-rich mud while *Bruguiera* favours stiff clay containing little organic matter.

To colonize and develop on unstable soil conditions, mangroves have typical structures of root systems called aerial roots: some parts of the root system exposed to the atmosphere at low tide (Tomlinson, 1986), those parts of roots take aeration and supply for subterranean roots. The presence of aerenchymatous tissue and numerous lenticels in root systems support for those mechanisms.

Adapting to high salt concentrations

Salt is the most important and abundant characteristic of the mangrove environment. Water with high salt concentration is a factor to limit the dispersal and germination of seedlings. Soil salinity is regulated by several factors, including tidal inundation, soil type, topography, depth of impervious subsoils, amount of rainfall, freshwater discharge of rivers, run-off and evaporation. Among these, frequency and time interval of flooding are the major factors (Saenger, 2002). Thus, at a particular locality, the soil salinity along the intertidal gradient is determined more or less by the salinity of sea water and time interval between inundations.

To adapt to high salt concentration, mangroves have the special mechanisms such as secreting salt through their roots, their leaves; fruits can float in water for a period while still maintaining the ability of germinating, seeds germinate while still attached to the parent tree... Connor 1969, Downton 1982, Ball and Pidsley 1995, Khan and Aziz 2001 (cited by Saenger (2002)) suggested that mangroves can control the intake of salt and maitain a water balance which is physiologically acceptable. In dealing with salt, mangroves develop the ability to 'resist' includes salt avoidance and regulation, on the other hand is the salt 'tolerance' and 'accommodation' through their leaves and root systems (Saenger, 2002). The tolerance of mangroves to various levels of salinity has still attracted scientists interests (Tomlinson (1986), Saenger (2002)).

2.1.2. Interaction between mangroves and the environment

Mangroves occur only on certain specific conditions such as: tropical or subtropical regions where the temperature is rather stable. Temperature is the main factor that provisions processes related to energy sources inside the structure of plants, affecting growth and yield of the species.

Although mangroves are salt-resistant species, they need fresh water. Because of that, mangroves just occur on areas where the annual precipitation is higher than 1200 mm, and the dry season does not last too long during the year (Ngan and Hien, 1987).

Mangroves express their large variation from their structure on different types of geomorphology. Lugo and Snedaker (1974) classified 6 main types of mangroves and Thom (1982) classified the typical geomorphology processes from those different types of mangroves occur.

The size of the river basin and the human activities determine the types of materials that come in and out of the mangrove area. The geographical features of land and sea determine the extent of mangroves. The geological processes determine the characters of sediments and water. Those main processes affect the differentiations of mangrove on different areas.

Mangroves also contribute to the processes of the environment. Furukawa and Wolanski (1996) explained that mangroves play a role as a 'pump' to attract the fine material to input to their regions. This typical characteristic makes mangroves have the title 'The land builders'.

Mangroves stabilize river banks and shorelines, prevent the erosion by absorbing wave energy and by reducing water velocity, the effects of mangroves in protecting against the storm surges and other oceanic hazards have been widely documented (Oliver (1982), Hamzah et al. (1999), Harada and Imamura (2005), Mazda et al. (2005), Alongi (2008)).

The ecological values of mangrove ecosystems have also been discussed, including support aquatic food chains, providing habitats, spawning grounds, nurseries and nutrients for a number of animals, and so forth (Manson et al. (2005), Nagelkerken et al. (2008)).

Figure 2.1 shows the interaction between mangroves and the environment.

2.1.3. Impacts on mangroves

Mangroves are among the most threatened and vulnerable ecosystems in the world (Valiela et al., 2001). The available data as reported by FAO (2005) shows that 15.2 million hectares of mangroves are estimated to exist worldwide as of 2005, down from 18.8 million hectares in 1980. The reasons for this of mangrove reduction are mainly from the excessive exploitation for the purpose of economic development.

2.2. The Mangrove in Vietnam

Vietnam has favorable conditions for mangrove development with a long coastline of approximately 3260 km long, large river systems with rich sediment loads caused by the natural

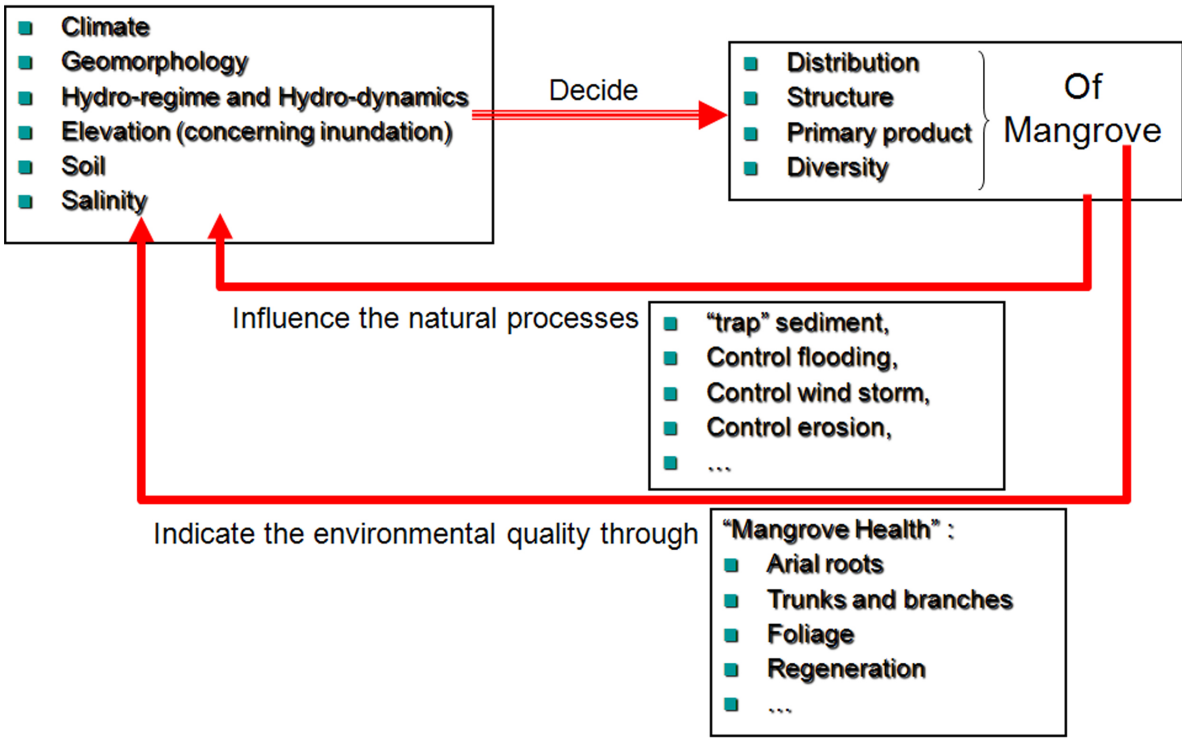

Figure 2.1.: *Interrelation between mangroves and the environment.*

processes of tropical region. Total mangrove area used to cover more than 400,000 ha in 1943 and reduced to 157,500 ha in 2000 (FAO, 2005). Various reasons for this of reduction have been discussed, major reasons include the war (more than 150,000 ha of mangroves in the South of Vietnam were destroyed during the war from 1962 to 1970), forest fire, collection of fuel wood, aquaculture and other human activities (Hong and Dao, 2003).

Vietnam had been successful with the reforestation on the destroyed forest areas. More than 52,450 ha of mangrove forests were reforested in the South of Vietnam during 1975 and 1980 (Hong and Dao, 2003). However, the new challenge to the threat of mangorves are the excessive exploitations, especially the conversion of mangrove forests to shrimp ponds which have happened from 1985 up to now.

The largest areas of mangroves are found in the Mekong Delta which is the southern part of Vietnam, approximately there are 101 species (33 true mangroves and 68 associate mangroves Hong (2004)) occur in the south. Along the central parts of Vietnam, only few areas are covered by mangroves. In the north, mangroves have developed in river deltas and estuaries and on wide tidal flats. There are fewer species in the north than in the south, possibly due to the lower temperatures. The map of mangroves distribution in Vietnam is shown in Fig. 2.2.

Figure 2.2.: *Map of mangrove distribution in Vietnam.*

2.3. The CanGio Mangrove Forest, Vietnam

CanGio located in the South of Vietnam (Fig. 2.3), from latitude 10°22′14″ to latitude 10°40′09″N, and from longitude 106°46′12″ to 107°00′59″E. It covers an area of 71,360 ha, in which the mangrove forest occupied more than 38,750 ha. CanGio is governed by the local government of HoChiMinh City.

CanGio mangrove forest has been denominated as The World Biosphere Reserve by UNESCO since 2000 and was the first Biosphere Conservation area in Vietnam. This mangrove forest is one of the most beautiful forests in Vietnam and plays a very important role in both ecological and environmental aspects for HoChiMinh City. The factors formed this typical natural formation came from the combinations of natural conditions and the efforts of human to reforestation. Since 1978, the reforestation program had been carried out. Since then, many hectares of land were covered by forest, most of *Rhizophora apiculata*. After the forest was denominated by UNESCO, local government of HoChiMinh City decided that CanGio Mangrove forest has become the Natural Conservation area, all activities affected the forest are inhibited.

2.3.1. Natural conditions

CanGio belongs to the estuary of DongNai - SaiGon River system which is the second large river system in the south of Vietnam after the Mekong Delta. The area has a very dense hydrological network where largest rivers (Long Tau, Cai Mep, Go Gia, Thi Vai, Soai Rap, Dong Tranh) connect to the sea, this area has the main waterways conecting HoChiMinh City with other regions and other countries.

Climate and meteorology

CanGio situated in tropical monsoon zone with two distintive seasons: the dry season from November to the following April, the rainy season from May to the end of October.

- Temperature: high and stable, range from 25°C to 29°C in average.
- Humidity from 73% to 85%.
- Average annual rainfall from 1000 mm to 1400 mm.
- Average rate of evaporation is 3.5 - 6.0 mm/day, highest values are in March and April (7.0 - 8.0 mm/day).
- In rainy season, the area is influenced by West - Southwest monsoon, and by North - Northeast monsoon in dry season.

Topography

Surface topography generally slopes slightly toward the Northeast - Southwest. Elevation ranges from 0.0 m to 2.5 m, except the GiongChua block is 10.1 m high. Elevation is relatively low and flat in the center and is rather higher along the coastline and river banks.

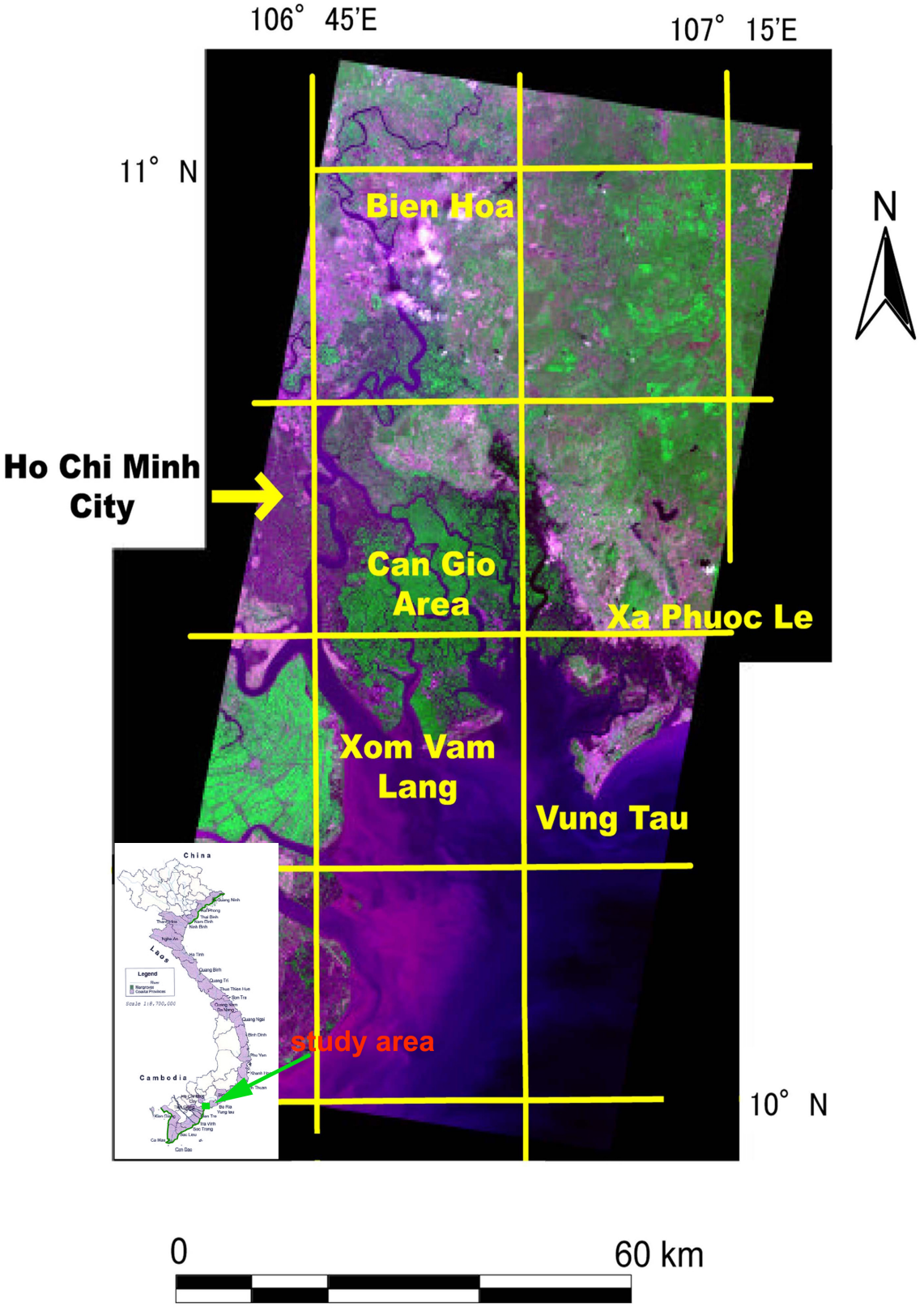

Figure 2.3.: *Map of CanGio area.*

The elevation is very important for the distribution of mangrove species. Mangrove is said to have close interaction with flooding regime, and the elevation is the key factor that influences flooding regime.

Tides

CanGio has an irregular semi-diurnal tidal regime with high amplitude (3.3 - 4.1 m). During the year, highest level of flood tide happens in November and December, ranging from 1.2 to 1.5 m high.

Tidal flooding has close relationship with elevation. The elevation in the area is divided into five levels according to flooding situation, as follows

- flooding twice a day at elevation 0.0 to 0.5 m
- flooding once a day at elevation 0.5 to 1.0 m
- flooding monthly at elevation 1.0 to 1.5 m
- flooding yearly at elevation 1.5 to 2.0 m
- periodically flooding (in several years) at elevation of more than 2.0 m.

Salinity

Salinity changes follow the seasons, highest salinity occurs in the areas located near the sea in dry season and reach the values of more than 30 *ppt* (in March and April).

Geomorphological processes and soil condition

CanGio area was formed by hundreds of meters of sediments aged from Neogene to Quaternary. Most of the surface of the area is covered by Holocene sediments, of which the thickness varies from 2 – 15 meters. They are alluvium, fluvio-marine sediments and kukersite sediments.

The soil in this area was formed from Quaternary sediments. The main pedological processes in the area are the processes of sulfuric accumulation and acidity and the process of salinization.

2.3.2. Social and economic activities

CanGio is the poorest district of HCMC, the social and economic activities in this area are mainly based on aquaculture and fishing. Agriculture poorly develops due to the lack of fresh water. Eco-tourism has developed since years, for this activity mangrove forest and its ecosystem are the main resources.

2.3.3. The CanGio Mangrove forest

Occupy more than 40% of total area, CanGio Mangrove Forest is the most important property of the area. The flora in the forest includes 72 species (30 true mangroves and 42 associate mangrove species) (Hong, 2004).

The development of CanGio Mangrove forest is devided into two stages: before 1978 and after 1978.

Mangrove status before 1978 The mangrove forest used to be managed and exploited by the Water and Forestry Burau of French Colonial Government since 1917. From 1966 to 1970, this mangrove forest was destroyed severely by bombs and herbicides (see Fig. 4.4). It was informed that many species could no longer be found since then (Hong, 2004).

The reforestation started in 1978 To meet the needs for timber supply, many efforts were undertaken to invest for this reforestation and *Rhizophora apiculata* was the main planted species in the forest. In 1991, the Government confirmed that CanGio Mangrove Forest had become the Environmental Protection Forest of HCMC. The City put into practice the policy of land and forest allocation to households, as a result, the destruction of the forest has greatly decreased.

In 2000, CanGio mangrove forest has been denominated as The World Biosphere Reserve by UNESCO. This forest became the first Biosphere Conservation area in Vietnam. Since then, all exploitation activities in the forest are inhibited. This forest is now the place for doing scientific research and for tourism activities.

Species distribution on each ecotope Hang and Anh (2002) investigated and summarized the environmental conditions which are favorable for the distribution of some typical dominant mangrove species in CanGio (as shown in Figures from 2.4 to 2.6). From their research, they created the maps of suitable environmental conditions for mangrove growth. They defined two zones of salinity that influence the growth of *Rhizophora apiculata*, in which *Rhizophora apiculata* develops well in zone I (salinity ranges from 10 *ppt* to 12.5 *ppt*) (see Fig. 2.8).

2.4. Data analysis (apply for *Rhizophora apiculata*)

Data analysis in this study is mainly based on the measured data plots of *Rhizophora apiculata*. We hope to find out the relationships between tree health and the environment, from that to design the structure for our mangrove models.

2.4.1. The data

Growth data of trees from 56 plots (include tree age, tree diameter and tree height) under different environmental conditions of salinity and elevation were analysed. The data were obtained from different institutions and were shown in Table 1.1 in Chapter 1.

Salinity data obtained from monitoring programme which had been conducted for years from 1996 to 2006 by the SRHC and the IER. Those data then were interpolated and built into a

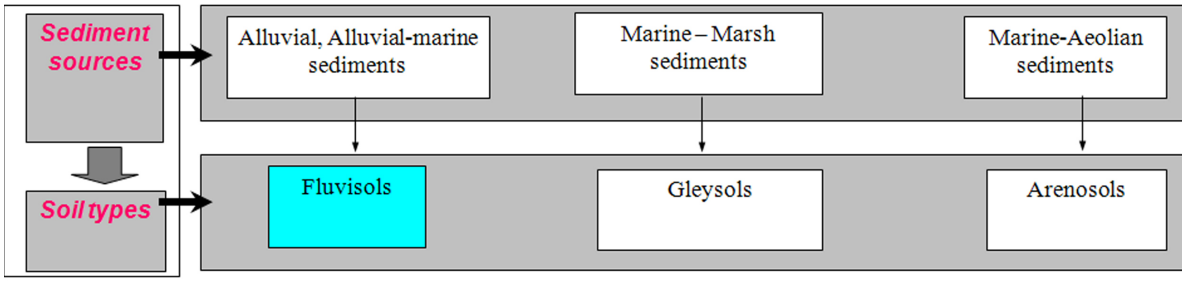

Salinity	< 4‰		4‰ – 18‰		> 18‰
Sediment types	Alluvial sediment, Alluvial-marine sediment				
Soil types	Fluvisols				
Elevation (m)					
0 – 0.5		*Nypa*			*Sonneratia*
0.5 – 1.0		Rice		*Nypa*	
1.0 – 1.5	Rice		Rice	Rice, *Acanthus*	*Rhizophora*
1.5 - >2.0	Fruit trees			Rice	

Figure 2.4.: *Species distribution: on Fluvisols (on areas with appropriate elevation and salinity, humans conduct farming activities, they destroyed mangroves for rice cultivation or planting fruit trees).*

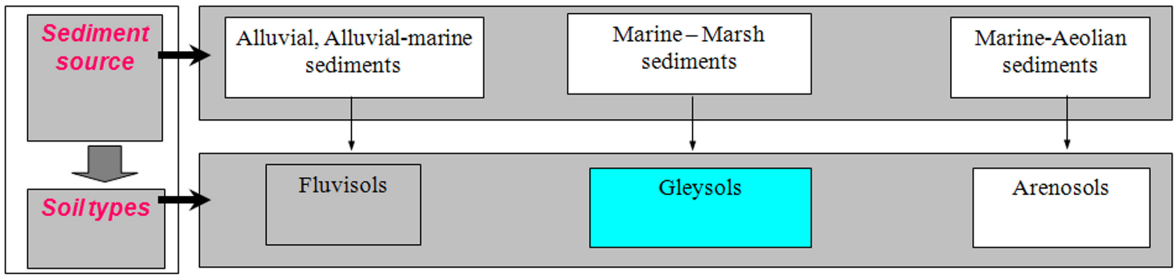

Salinity	< 4‰	4‰ – 18‰	> 18‰
Sediment types	Marsh-Marine sediment		
Soil types	Gleysols		
Elevation (m)			
0 – 0.5			*Avicennia*
0.5 – 1.0	*Nypa*	*Rhizophora*	*Avicennia, Rhizophora*
1.0 – 1.5			
1.5 - >2.0	*Acanthus*	*Phoenix, Acrostichum*	*Ceriops, Bruguiera, Phoenix*

Figure 2.5.: *Species distribution: on Gleysols.*

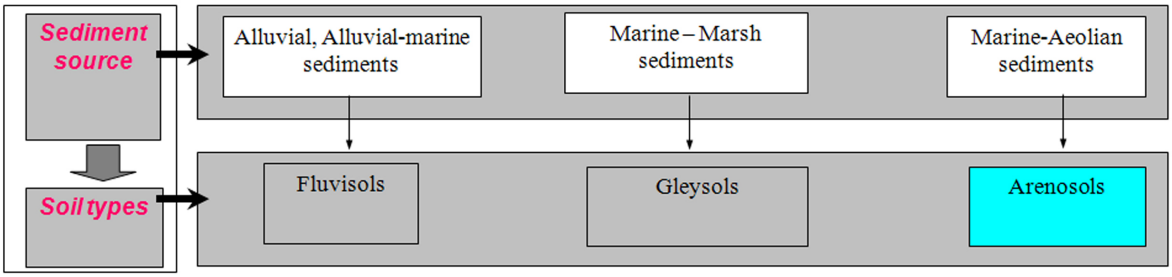

Salinity	< 4‰	4‰ – 18‰	> 18‰
Sediment types	Marine sediment		
Soil types	Arenosols		
Elevation (m)			
0 – 0.5		*Sonneratia*	*Sonneratia*
0.5 – 1.0			
1.0 – 1.5			
1.5 - >2.0			Fruit trees

Figure 2.6.: *Species distribution: on Arenosols.*

map (map of suitability salinity zones for mangrove growth) by Anh (2007), this map is used as salinity data for the analysis described below and is then used as input into the ecological model.

As discussed in Section 2.3.1, elevation is the indirect indicator for tidal flooding regime which influences tree growth. Thus, we use the Digital Elevation Model (DEM) in Fig. 2.9 as the map conditions the inundation. DEM which was created by Anh (2007) is used as the map reference for choosing the sampling positions. This map is then also used to input into the ecological model.

The maps of sampling positions, elevation and salinity are shown in Figures from 2.7 to 2.9.

The 56 sampling plots are the mensurations of different field inventory designs:

- 9 plots of 100 square meters were re-measured after one year (pink square points in Fig. 2.8), those plots are used to extract the increments of diameters of trees, the plots are distributed along a gradient of salinity, ranges from 12.5 *ppt* to 28 *ppt*

- 44 plots of 100 square meters, used to test the influence of self- thinning (pink circles in Fig. 2.8)

- 3 plots of 900 square meters (the tree age in the plots are similar) are used for calibrating remotely sensed data (green square points in Fig. 2.8)

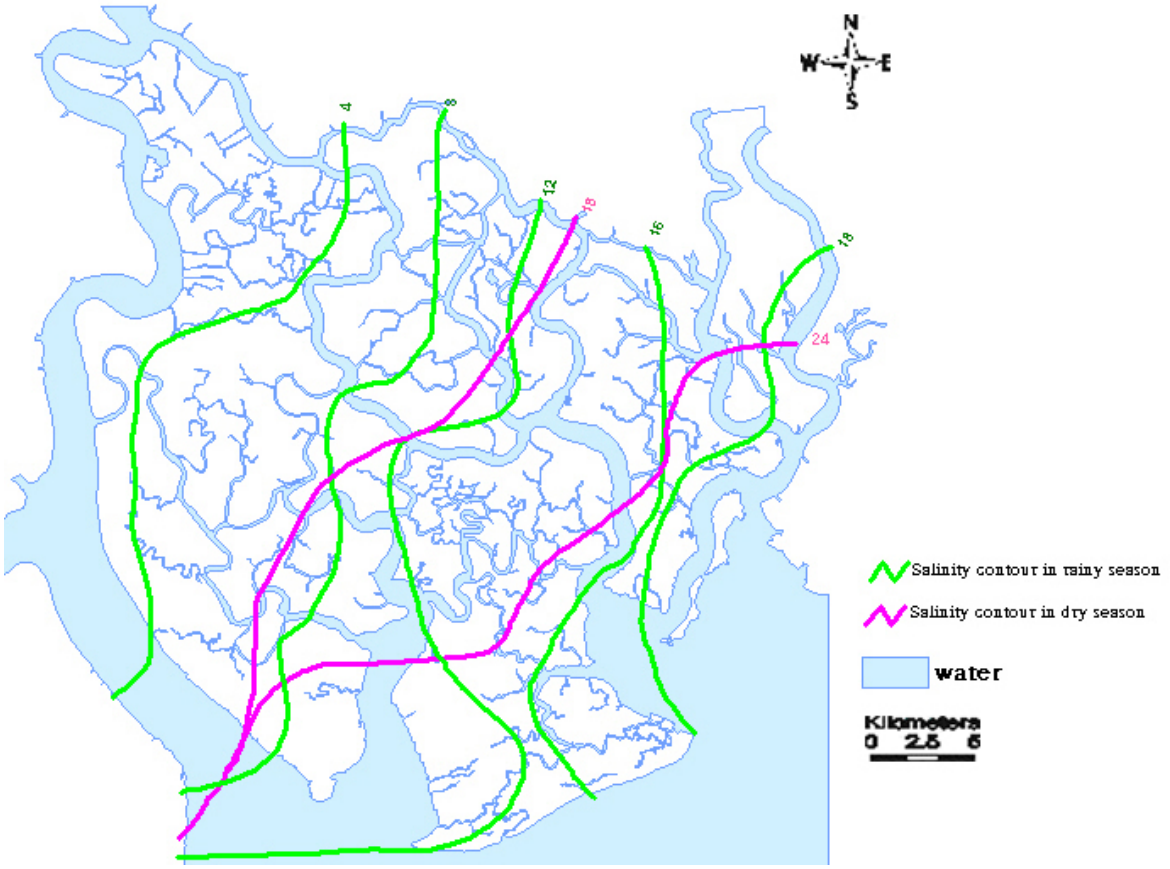

Figure 2.7.: *Salinity contour calculated from monitoring data (source: Southern Regional Hydrometeorological Center)*

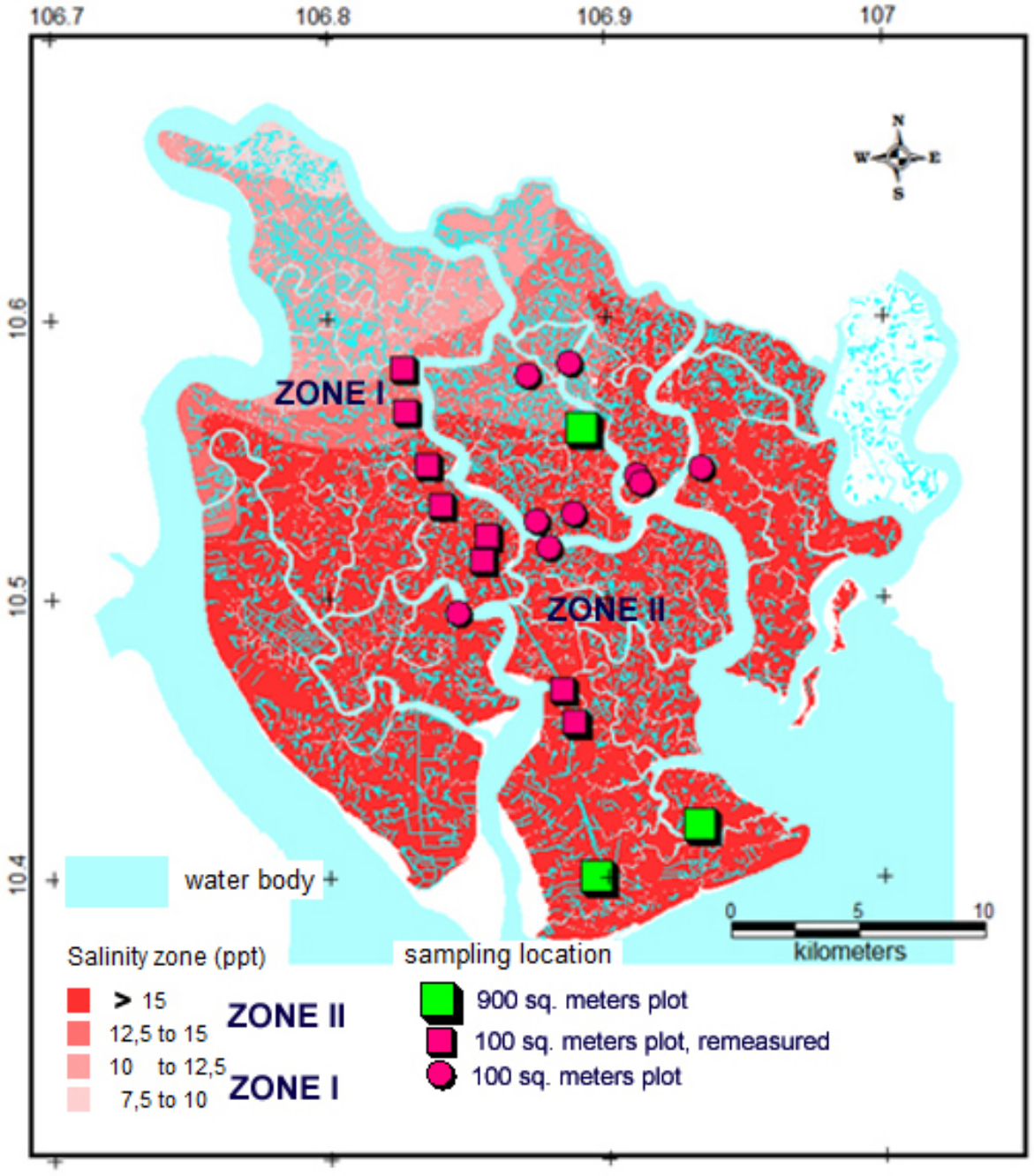

Figure 2.8.: *Positions of sampling plots (pink squares: 100 sq. meter-remeasured plots, pink circles: 100 sq. meter-temporary plots, green squares: plots of 900 sq. meters); the sampling plots located on different zones of salinity, range from 12 ppt to 30 ppt, different colours in the map show different ranges of salinity.*

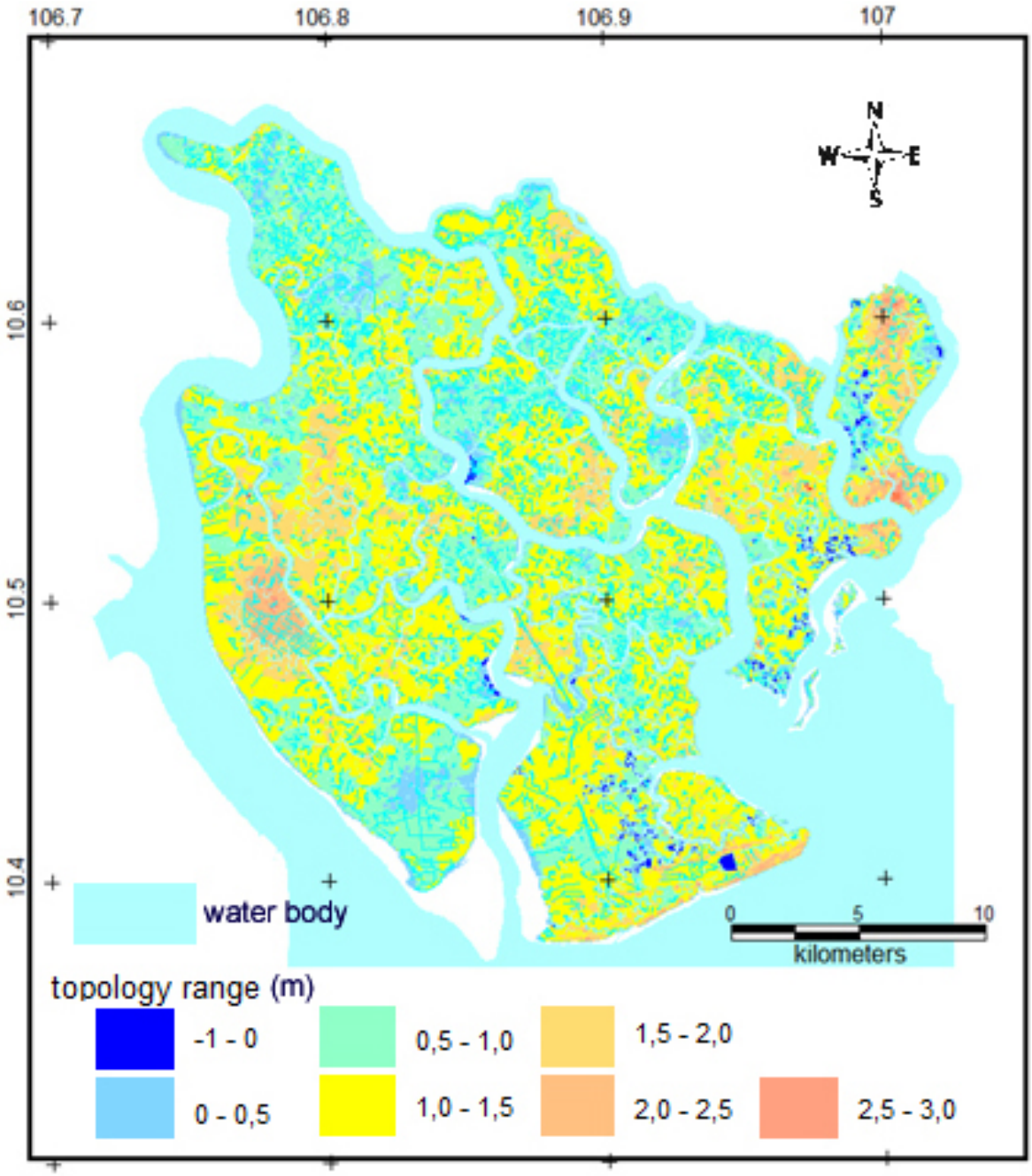

Figure 2.9.: *Digital elevation model (DEM) of the study area, the range of elevation was determined base on the correlation between elevation and flooding frequency of tidal waters.*

2.4.2. Correlation between tree size and tree density

Relationship of tree diameter and density ($dbh - N$) as in Fig. 2.10 shows high correlation ($R^2 = 0.912$). This reflects the relationship between tree size and tree number of the self-thinning effect as has been widely discussed in many studies. From this well fitted curve, we however can not confirm that the tree growth depends only on density (N).

To check this, we examine the relationship between tree growth rate (MUL) and N (MUL is considered as tree growth rate because here we just analyze and compare tree growth of the same species, thus other parameters of the first component in Eq. 2.1 are equal and can be omitted). Because growth of tree is expressed by growth rate, thus if the sizes of trees correlated with N, growth rate of trees would also correlate with N.

Driving factors influence tree growth through multipliers (MUL) which are the functions of these factors: salinity, elevation and density

$$\frac{d(dbh)}{dt} = f(dbh, H) \times MUL \tag{2.1}$$

We examine the correlation between the average values of multipliers (MUL) with the density of the stands, the results shown in Figure 2.11. There is no correlation between MUL and N when we test the entire data ($R^2 = 0.372$) without considering other differentiations inside the data.

In Figure 2.11, the data inside the circle are from the plots of trees of more than 20 years old, the remains are trees of less than 20 years old. It could be shown that, if omitted the data inside the circle, the correlation between MUL and N may be better. This suggests that tree age also affects tree growth rate. In addition, other driving factors is also important in influencing the growth of trees.

The value of MUL plays a very important role for the process of parameterization for the ecological model which we constructed as will be discussed in the next chapters. Therefore, finding a correlation between MUL of trees and other driving factors (salinity, elevation and density) will be helpful for the process of designing the ecological model and parameter estimation for the model.

To find out the relationship between tree growth rate (MUL) and the driving factors (here we just examine salinity and density), we conduct these analyses:

- Compare tree sizes along a gradient of salinity
- Compare tree sizes at the same zone of salinity. In which we examine two cases. The first case we check the plots that have: different tree age, same salinity zone, same density (N) . The second case we check the plots that have: same tree age, same salinity zone and different tree number N.
- Analyze tree sizes and tree growth rate in different zones of salinity. In which we consider the plots of same-age trees in each zone. There are two series of plots, one series are the plots of 13-year-old trees located in salinity zone I, another series are the plots of

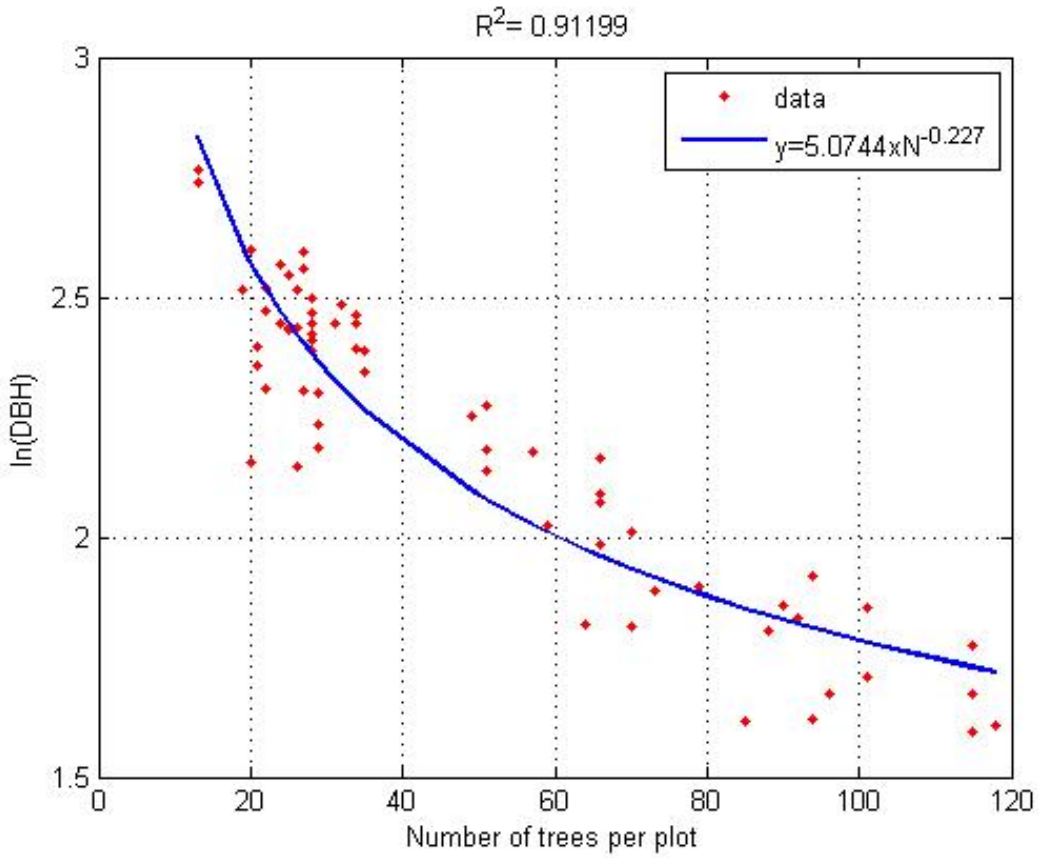

Figure 2.10.: *Self-thinning effect of R. apiculata.*

25-year-old trees located in salinity zone II. All the plots have different number of trees from each other.

- Analyze the relationship between tree size (dbh) and salinity and between tree growth rate (MUL) and salinity. To do this, the plots of same-age trees and same number of trees located along salinity gradient are tested.

2.4.3. Tree size along a gradient of salinity

9 plots distributed along salinity gradient were examined as shown in Fig. 2.12. The first two plots which have small values of age, N and salinity are the most healthy plots among those 9 plots (high dbh values).

When we look at the two plots number 1 and number 9. They have nearly same density (N=22 in plot 1 and N=21 in plot 9), the age of trees in plot 9 is older than this in plot 1 (26 compares to 12) but mean dbh of plot 1 is higher. It should be noted the difference in salinity values between plot 1 and plot 9, salinity at the position of plot 1 is lower than this value at the position of plot 9.

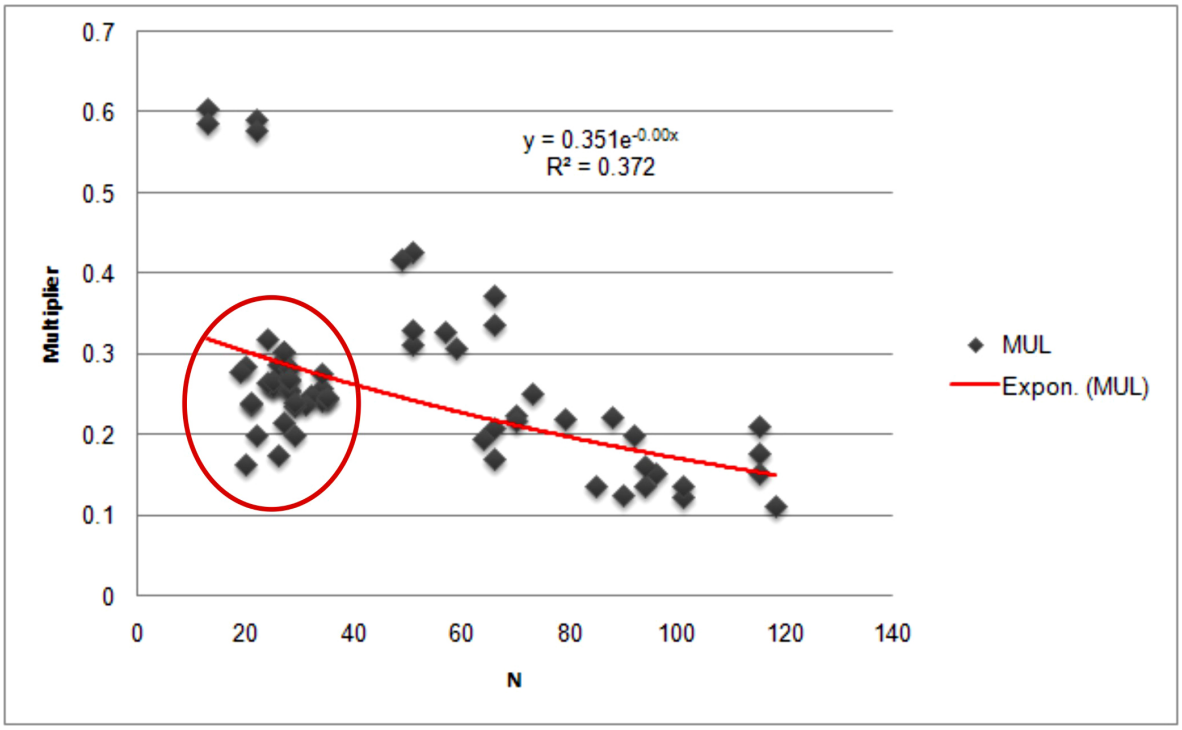

Figure 2.11.: *Growth multiplier (MUL) and density (N) relationship of R. apiculata. Result shows very weak correlation between growth rate and density. All the data inside the circle are the trees which are more than 20 years old, the rest are the data of trees which are less than 20 years old.*

The plots which have same density (N) also show the variation in mean *dbh* along salinity gradient (plot 3, 4, 6, 7). The plots that have same tree age also express similarly (3, 6, 9). All the mean *dbh* values along salinity gradient decline.

2.4.4. Tree size at the same zone of salinity

Case: plots of different tree age, same salinity zone, same density (N) We test the plots located at the same range of salinity (salinity $\cong 20ppt$). Two series of plots are used. The first series include the plots of 15-year-old trees (the first 4 plots in Fig. 2.13), the next series are the plots of 25-year-old trees (the next 4 plots in Fig. 2.13). It is interesting when we could see that even the age-distance is 10-year, all the plots have not much differences in tree size. The slightly difference happens between plot number 4 ($N = 64$) and plot number 6 ($N = 66$), all other plots which have very large number of trees have rather similar sizes. This indicates that, tree does not grow well when there are very dense density of trees or we can say that growth rate (MUL) of trees in this case is closed to 0.

Case: plots of same-age trees, same salinity zone and different tree number N Similarly, we test two other series of plots in the same range of salinity, this time the plots have: same age (each plot has trees of same age), same salinity range (salinity $\cong 20ppt$), different N. We can see from Fig. 2.14, the size of trees in the plots which have small number of trees are

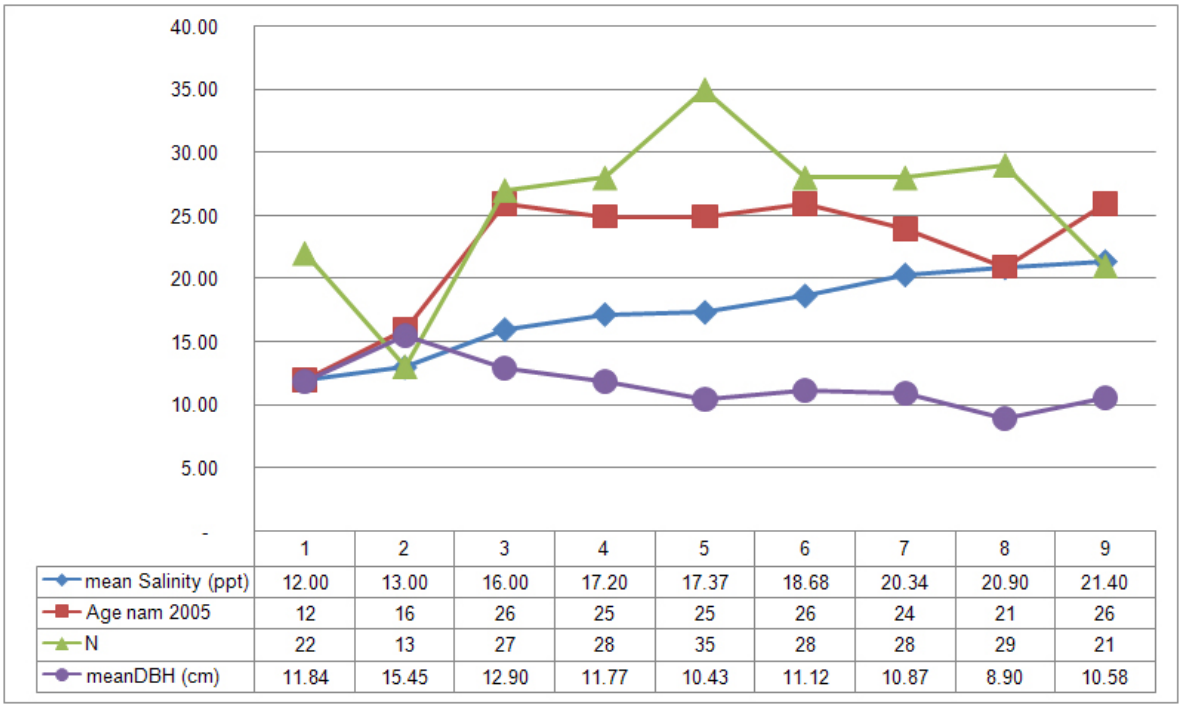

	1	2	3	4	5	6	7	8	9
mean Salinity (ppt)	12.00	13.00	16.00	17.20	17.37	18.68	20.34	20.90	21.40
Age nam 2005	12	16	26	25	25	26	24	21	26
N	22	13	27	28	35	28	28	29	21
meanDBH (cm)	11.84	15.45	12.90	11.77	10.43	11.12	10.87	8.90	10.58

Figure 2.12.: *Tree health (as expressed by dbh value) along salinity gradient.*

higher than the size of trees which have high density. This means that growth rate of trees are influenced by density.

2.4.5. Tree size and tree growth rate in different zones of salinity

The relationships of $dbh - N$ and $MUL - N$ are examined. We consider the plots of same-age trees in each zone. There are two series of plots, one series are the plots of 13-year-old trees located in salinity zone I, another series are the plots of 25-year-old trees located in salinity zone II. All the plots have different number of trees from each other.

The relationship of $dbh - N$ as shown in Fig. 2.15 shows that trees located at salinity zone I will reach the size of trees which are located at salinity zone II even they are younger than the trees in salinity zone II (13 compares to 25) if the density (N) is small. The size of trees in zone I (13 years old) is also not much different compared to the size of trees in zone II (25 years old) when N is large ($N > 100$). It proves that, growth rate of trees is dependent on salinity and N.

The relationship of $MUL - N$ as shown in Fig. 2.16 shows that, growth rate of younger trees in zone I is much higher than this of older trees in zone II when N is small and this value of growth rate will be not much different between trees of different zones of salinity and age when N is high.

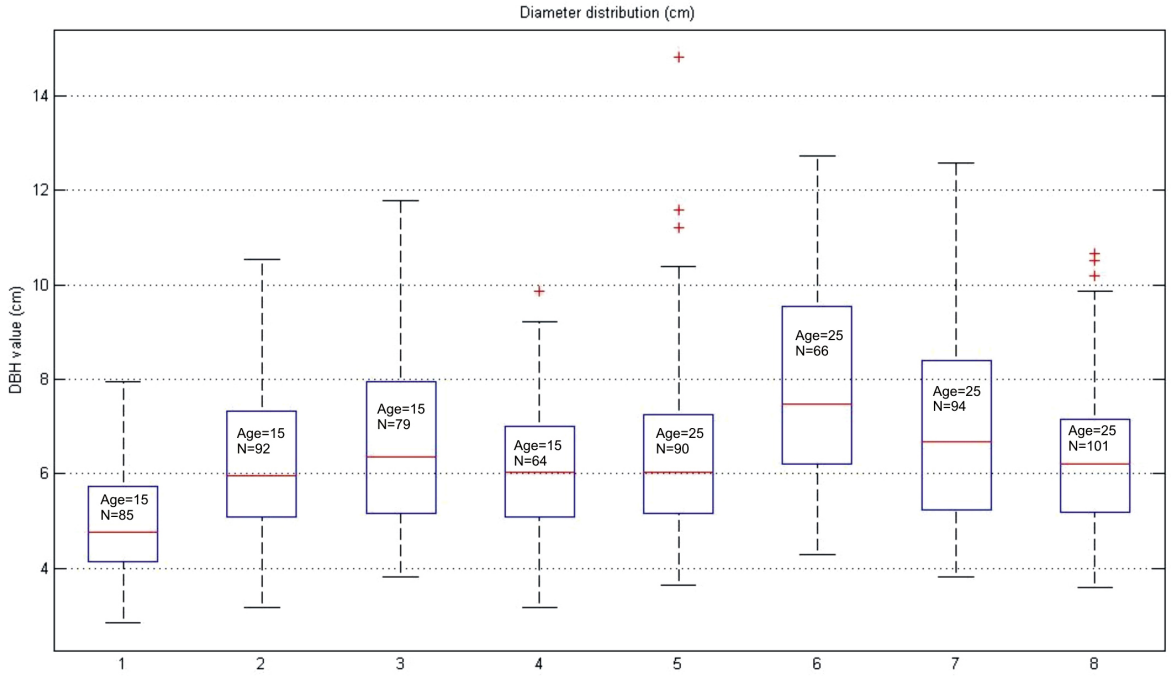

Figure 2.13.: *Tree sizes at the same zone of salinity. Case: plots of different tree age, same salinity zone, same density (N). The influence of N on tree growth is strong. The sizes of trees in the plots are not much different even the first series of 4 plots are 10 years younger than the second series (the next 4 plots).*

2.4.6. Tree size and tree growth rate along gradient of salinity

The relationships between tree size (dbh) and salinity and between tree growth rate (MUL) and salinity are examined. To do this, the plots of same-age trees and same number of trees located along salinity gradient are used. It is shown that tree size is dependent on salinity and also tree growth rate is dependent on salinity (Fig. 2.17 and Fig. 2.18).

2.5. Conclusion

Mangrove ecosystem with the ability to survive on the changing environmental conditions has become a particular ecosystem. Zonation characteristics of mangrove species have been mentioned widely. We test this feature base on data from mangrove plants in CanGio by analyzing tree size and tree growth rate on different environmental conditions. Growth data of *Rhizophora apiculata* is analyzed and the relationships between the growth of *R. apiculata* with environmental conditions and density are determined. The results show a close correlation between the growth of the mangrove species and their environmental conditions as well as their density.

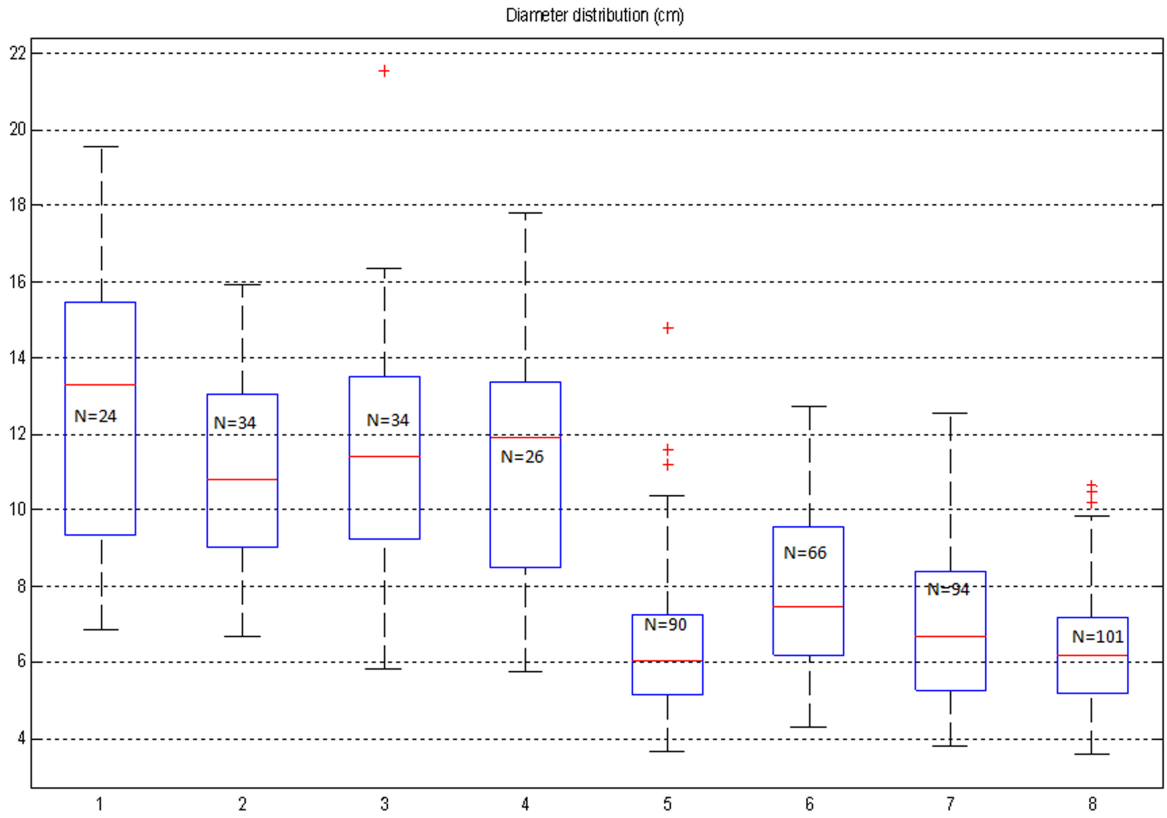

Figure 2.14.: *Tree sizes at the same zone of salinity. Case: plots of same-age trees, same salinity zone and different tree number N. The first series (the first 4 plots) of plots have higher dbh values than the others even they have same-age trees. This is because of the differences in density (N)*

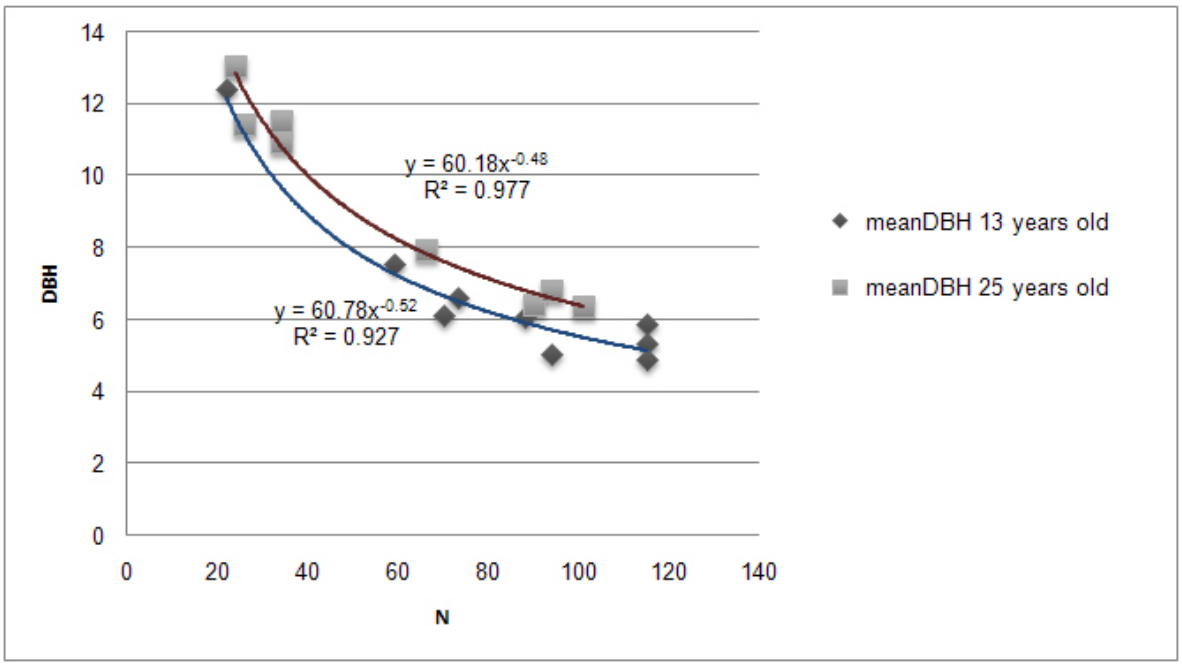

Figure 2.15.: *dbh and salinity relationship of R. apiculata.*

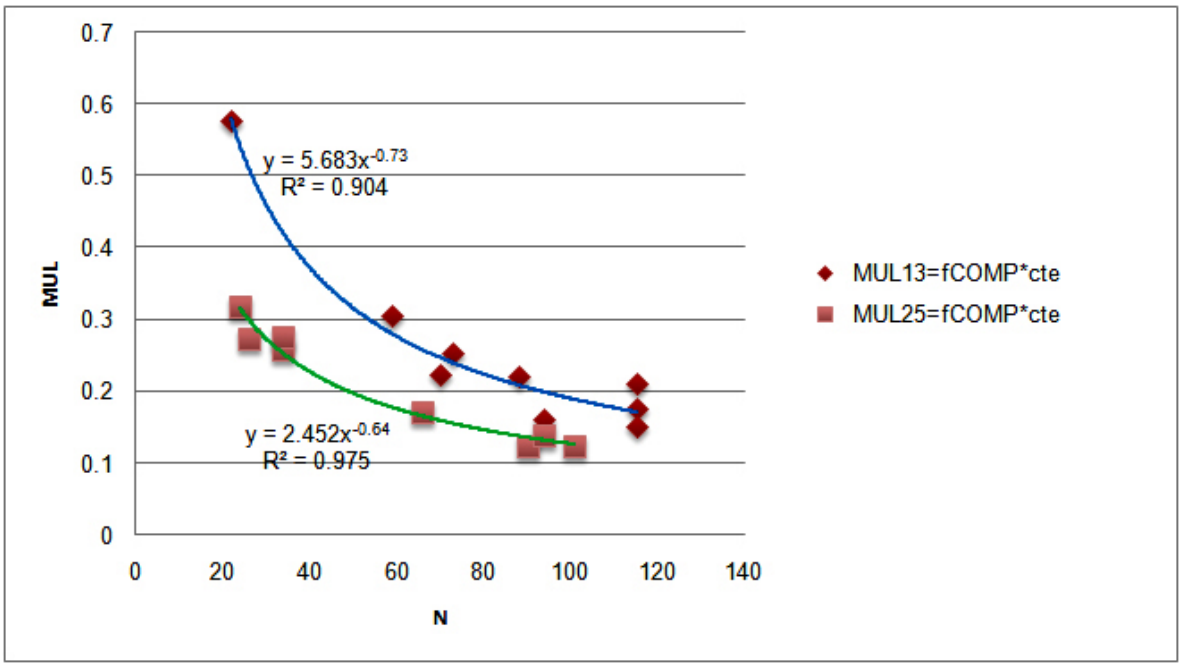

Figure 2.16.: *Growth rate (MUL) and density (N) relationship of R. apiculata, result shows very good relationship between growth rate and N.*

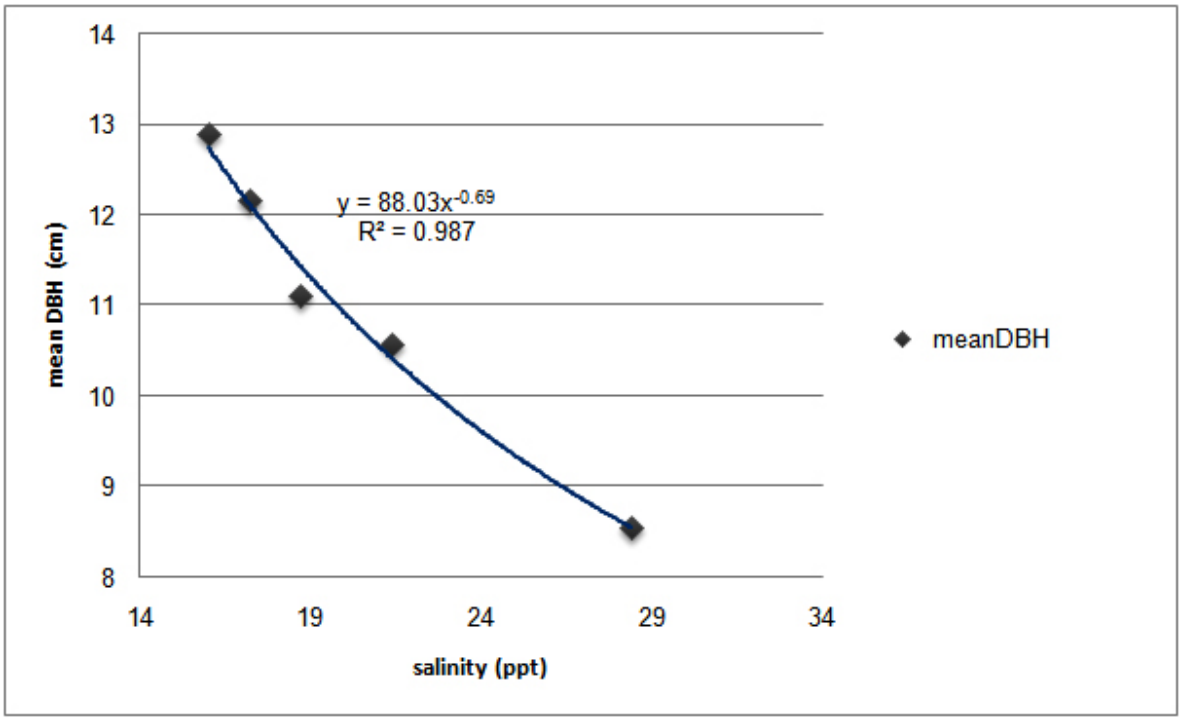

Figure 2.17.: *Mean dbh of R. apiculata along salinity gradient.*

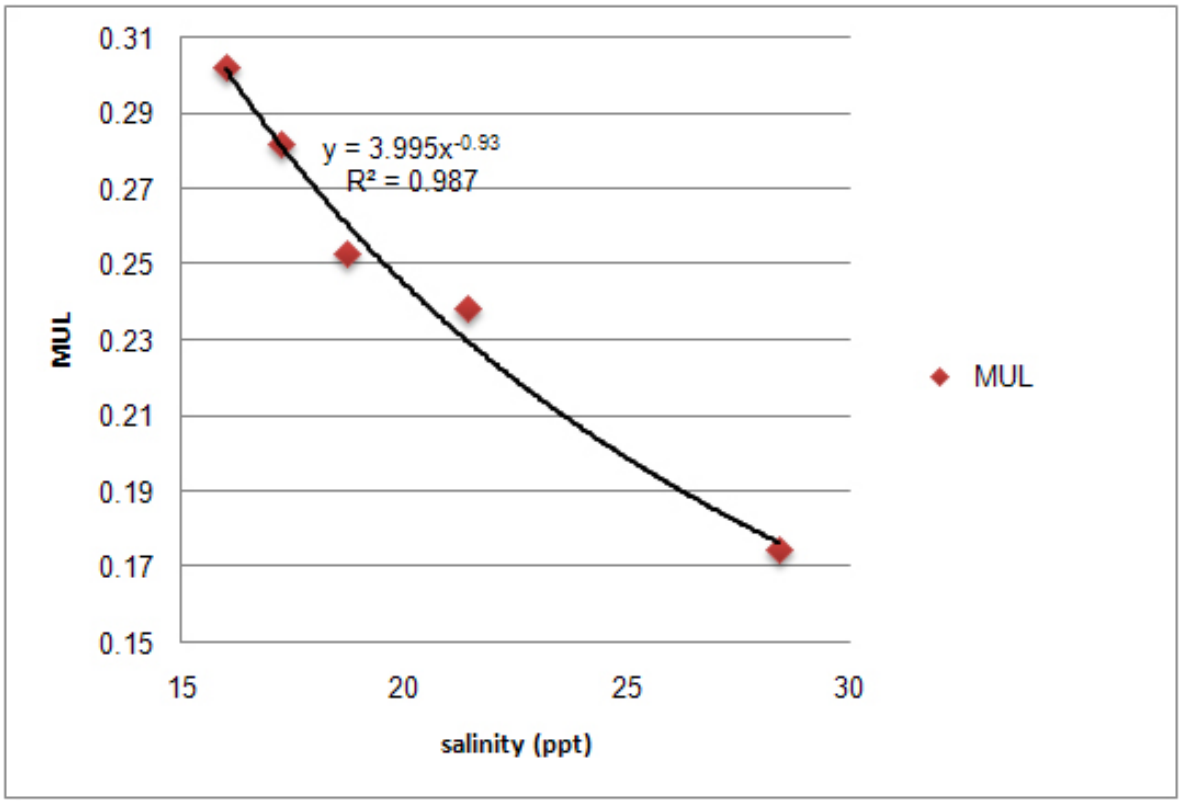

Figure 2.18.: *Growth rate of R. apiculata along salinity gradient.*

Part II.

Modelling the dynamics of CanGio Mangrove forest

3. Understanding Mangrove Dynamics using IBM

As discussed in Chapter 1, the aim of this thesis is to develop a model to simulate the dynamics of mangrove in CanGio area. The model is designed so as it is possible to simulate mangrove dynamics from a fine scale (individual level) to a coarser scale (landscape level). To achieve this, the IBM was developed and was parameterized firstly. This IBM is applied to ***examine*** the behaviours of individual trees under different circumtances because IBM can be used for ***experiment by computer simulations***. Then, we apply the ***up-scaling*** approach to construct a landscape model (the model CGMM in Chapter 4) from this of IBM.

In this chapter, dynamics as well as interactions of mangrove vegetation will be explained and simulated by the individual based model (IBM) and data fixed to this model. Following that, a process for parameterization is conducted.

Parameter estimation is sometimes difficult because of the incompleteness of the data. In this chapter, we introduce a procedure to deal with this problem, it is to create artificial data by simulating the situations that can happen in reality, then combine these artificial data and real data for the parameterization.

Typical interests in this chapter include:

- Mangrove dynamics models and IBM construction
- Procedure for parameter estimation for the IBM
- Creating artificial data for the parameter estimation
- IBM's simulations for testing behaviours and dynamics of mangroves under aggregated conditions (influenced by environment and competition).

3.1. Individual Based Model for simulating the CanGio Mangrove forest dynamics

The Individual-based model is developed for simulating the CanGio Mangrove Forest dynamics under influences of environmental settings (salinity and elevation) and competition. The tree species simulated include *Rhizophora apiculata*, *Avicennia alba* and *Phoenix paludosa*. The dynamics are embedded in this of IBM are ***'Establishment - Growth - Competition - Reproduction - Mortality'***. In which, the processes of ***Growth*** and ***Competition*** are parameterized.

The structure of the IBM is expressed in Figure 3.1 and the submodels are in Figure 3.2. The IBM implements 5 submodels, in which the submodel ***'Competition Factor'*** is actually a component process of ***tree growth***.

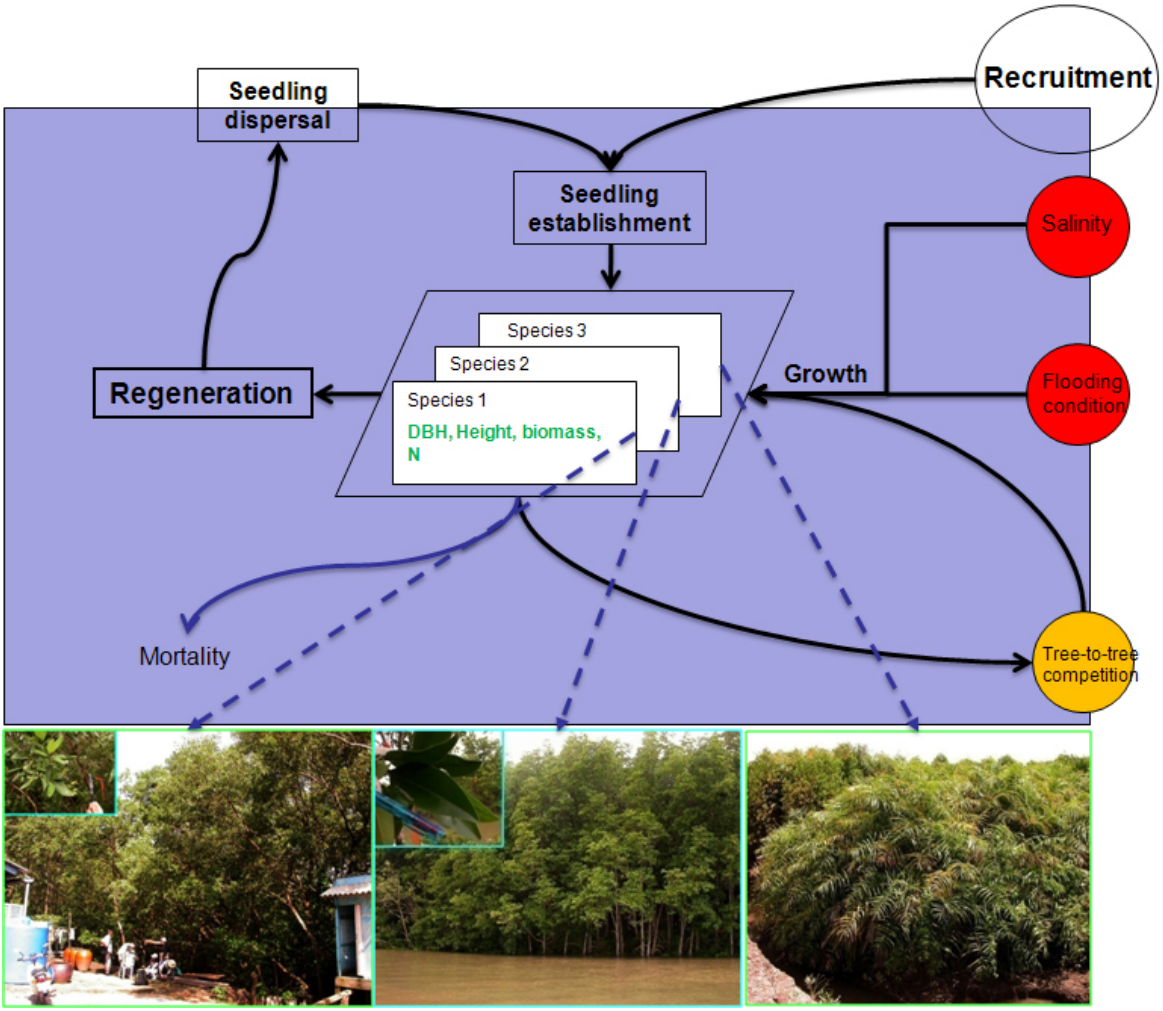

Figure 3.1.: *Conceptual structure of the IBM. Three species are simulated. Species 1 is Avicennia alba which occurs on the front of the sea side, species 2 is Rhizophora apiculata located on the intermediate area and the last one Phoenix paludosa is shrub species which occurs on the higher land on landward side.*

3.2. Mangrove dynamics models

3.2.1. Growth model

It is possible to say that the main differences between mangroves and other terrestrial forests lie in the factors of salinity and periodic tidal flooding in mangrove habitat. Therefore, these two elements are prerequisite to mention among factors that influence the growth of mangrove trees. We explore tree growth under influences of salinity and elevation, in which elevation is a factor that reflects the tidal flooding frequency (see Section 2.3.1 of Chapter 2). Spatial

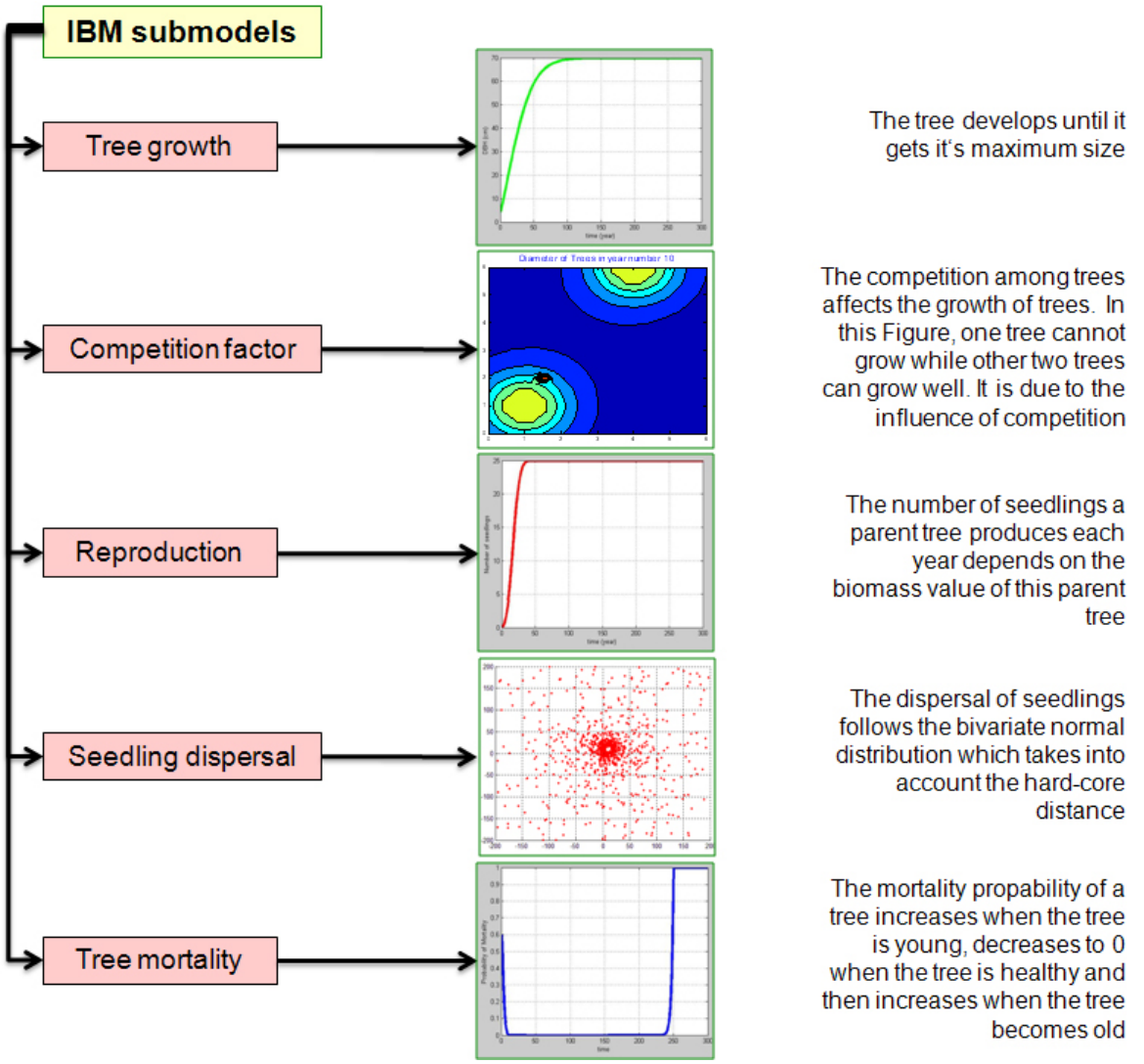

Figure 3.2.: *The IBM submodels.*

competition among trees is also included because it influences tree health (self-thinning effect in Fig. 2.10).

The choice of structure and conceptual basis of the growth model are based on the works of Botkin (1993), Chen and Twilley (1998), Berger and Hildenbrandt (2000). Their models are applied with some modifications.

The growth model is parameterized for two species *Rhizophora apiculata* and *Avicennia alba*. We describe the process of parameterization for *Rhizophora apiculata* because this species is distributed most frequently in the forest (they were planted). For *Avicennia alba*, parameters for growth equation are estimated using data from Nam (2003).

Tree growth equations:

$$\frac{d(dbh)}{dt} = \frac{G_{opt} \cdot dbh \cdot (1 - dbh \cdot H/D_{max}/H_{max})}{2b_1 + 3b_2 \cdot dbh - 4b_3 \cdot dbh^2} \times MUL \tag{3.1}$$

$$H = b_1 + b_2 \cdot dbh - b_3 \cdot dbh^2 \tag{3.2}$$

$$MUL = f_s \times f_{el} \times f_c \tag{3.3}$$

where: dbh is diameter at height b_1,
G_{opt} is species specific growth rate under optimal environmental condition,
H is tree height,
H_{max} and D_{max} are maximum values of tree height and tree diameter,
b_1, b_2, b_3 are species specific growth constants,
MUL is growth multiplier and
f_c, f_{el}, f_s are multipliers of competition factor, elevation factor and salinity factor. They are normalized to 1.

The parameter G_{opt} expresses the growth rate of a tree, it determines how early a tree achieves most of its growth. The larger the value of G_{opt}, the earlier a tree will reach one-half of its maximum size. However, G_{opt} just can be valid at optimal growth conditions, the actual tree's growth rate also depends on other factors (MUL in Equation (3.1)).

Equation (3.1) can be re-written as follow:

$$\frac{d(dbh)}{dt} = \frac{G \cdot dbh \cdot (1 - dbh \cdot H/D_{max}/H_{max})}{2b_1 + 3b_2 \cdot dbh - 4b_3 \cdot dbh^2} \tag{3.4}$$

where: $G = G_{opt} \times MUL$ is the growth rate under envinronmental settings. By integration, G can be expressed as follow:

$$G = \frac{2H_{max} \times \left[\int \frac{b_1 + a(3e^x - 2e^{2x})}{a + b_1 - e^x(b_1 + a(2e^x - e^{2x}))} dx - C\right]}{t} \tag{3.5}$$

in which, $a = H_{max} - b_1$, $x = ln(dbh/D_{max})$ and C is an integration constant. Equation (3.5) shows that we can calculate G given tree age (t), tree diameter (dbh) and tree maximum diameter (D_{max}). From that, we can calculate the value of growth multiplier MUL that influences the growth of tree at time t given G_{opt}. This is a very important step for the parameter estimation. From the values of MUL, it is feasible to extract the parameters of a single factor (f_c or f_s, see below). The MUL value extraction is given in Appendix A.

Growth multiplier of salinity

The growth multiplier of salinity proposed by Chen and Twilley (1998) is modified as follow:

$$f_s = \frac{1 - a_{0s}}{1 + e^{d(x_{1s} - s)}} + a_{0s} \tag{3.6}$$

where:
a_{0s} is the minimum value of the salinity factor multiplier, d is a constant describing the steep-

ness of the salinity multiplier, x_{1s} is the salinity threshold and s is salinity in *ppt*.

We assume that mangroves can adjust themselves to adapt to saline conditions. They may still survive, although very limited in the extreme conditions. The parameter a_{0s} in Eq. (3.6) takes into account that mangroves still can endure under extreme salinity condition (salinity multiplier curves for three different species are given in Figure 3.3 (b)).

Elevation factor multiplier

Frequency and duration of tidal flooding influence species distribution and health, some species can adapt well with longer flooding duration (for instance *Avicennia alba*) and some can not (*Phoenix paludosa*), some can stay in the area of medium flooding duration (*Rhizophora apiculata*). Elevation can be considered as the indirect factor that reflects the frequency and duration of tidal flooding, thus, instead of considering two factors that influence tree health (tidal frequency and duration) we integrated both into only one factor (elevation). Effect of elevation factor on mangrove's growth is expressed by Equation (3.7) and it's curve is shown in Figure 3.3 (a).

$$f_{el} = \left\{(a_{maxe} - a_{1e})\left[1 - e^{-(el/el_1)^{\alpha}}\right] + a_{1e}\right\} e^{-(el/el_2)^{\beta}} + a_{2e}\left[1 - e^{-(el/el_2)^{\beta}}\right] \tag{3.7}$$

where: a_{maxe} is the maximum value of the elevation factor multiplier,
a_{1e} and a_{2e} are minimum values of elevation factor multiplier,
el is elevation in meter,
el_1 and el_2 define the optimal elevation range,
α and β are form parameters determine the steepness of elevation multiplier curve.

Growth multiplier for tree competition

The result of data analysis in Chapter 2 shows the effect of spatial competition on tree's health through tree density. Many researchers (Adler (1996), Li et al. (2000), Nakajima et al. (2011)) have developed models to explain the mechanisms for this process (self-thinning effect). In our growth model, we apply the assumption of '***Field Of Neighbourhood***' from Berger and Hildenbrandt (2000).

Berger and Hildenbrandt (2000) assumed that the size of a focused tree is influenced by other neighbouring trees, this process is taken into account by the competition factor FA. This factor is the proportion of the strength of competition of the focused tree which is overlapped by the competition's strength of it's neighbours. The higher the value of FA, the lower the growth rate of this focused tree. Equations (3.8 to 3.10) describe for this process:

$$FA_i = \frac{1}{FON_i} \times \sum_{j=1;j\neq i}^{Nn} \int_O FON_{o,ij} \tag{3.8}$$

$$FON = \begin{cases} F_{max} & 0 \leq r \leq rbh \\ \exp\left[-\frac{|log(F_{min})|}{R-rbh}(r - rbh)\right] & rbh < r \leq R \\ 0 & r > R \end{cases} \tag{3.9}$$

$$R = a_2 \times rbh^{c_2} \tag{3.10}$$

where: FA_i is the proportion of the competition strength of focused tree i which is overlapped by it's neighbours,
FON_i is the field of neighbourhood of the focused tree i,
Nn is the number of neighbouring trees of the focused tree,
$\int_O FON_{o,ij}$ is the overlapped value of FON_i of the focused tree which is overlapped by neighboring tree j,
O is the overlapped area,
R is radius of zone of influence (Berger and Hildenbrandt, 2000),
a_2 and c_2 are scaling parameters.

The growth multiplier of competition is given by (see Figure 3.3 (c) and (d)):

$$f_c = (a_{maxc} - a_{0c}) \exp\left[-(FA/FA_{thr})\right] + a_{0c} \tag{3.11}$$

a_{maxc} and a_{0c} are maximum and minimum values for competition effect on growth and FA_{thr} is the threshold value of FA.

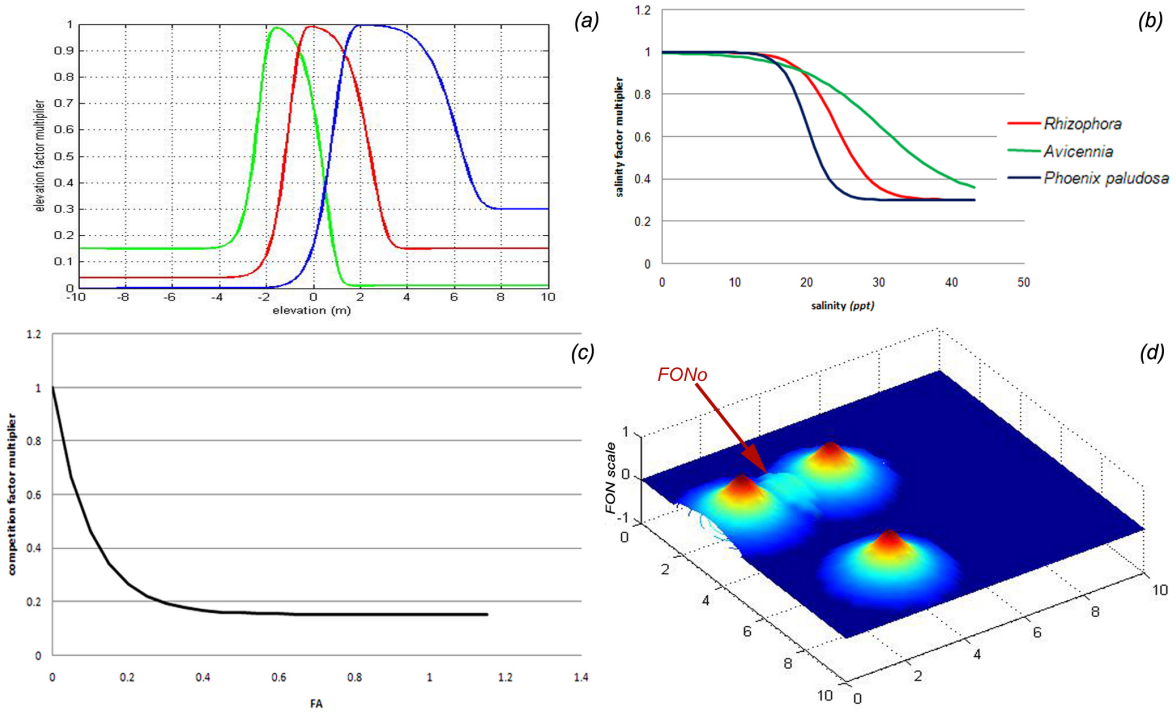

Figure 3.3.: *The curves of multipliers which affecting tree growth. The multipliers for elevation and salinity are species specific (Fig. (a) and (b)), the multiplier for competition (Fig.(c)) is homogeneous for the three species. Fig.(d) shows the strength of competition of trees (FON) which is equal to 1 at the stem and decreases exponentially until the distance R.*

3.2.2. Reproduction and seedling dispersal

The number of seedlings a tree produces depends on it's biomass

$$\frac{dN2}{dt} = r_2 \cdot fRep \cdot Biom \cdot (1 - \frac{N2}{N2_{max}}) \tag{3.12}$$

$$fRep = 1 - exp\left[-(Biom/Ec)^{\gamma 2}\right] \tag{3.13}$$

$$Biom = a_1 \cdot dbh^{c_1} \tag{3.14}$$

$N2$ is the number of seedlings a tree produces at time t (we use the symbol $N1$ for the seedlings which are recruited by planted as will be described in Chaper 4),
r_2 is the rate of reproduction,
$Biom$ in Eq. (3.14) denotes tree's biomass,
$N2_{max}$ denotes maximum number of seedlings a tree can produce,
$fRep$ is switching function which is a function of biomass and takes into account the period a tree will produce seedlings,
a_1, c_1 and $\gamma 2$ are scaling parameters.

A seedling dispersed from a parent tree (which is located at position (μ_1, μ_2)) to a location (x, y) is determined by a spatial stochastic process with probability density function $h(x, y)$. This probability density function takes into account the ***Hard-core process*** (detailed explaination of this spatial point process is in Appendix B) with fixed number of points $N2$. The ***Hard-core*** distance is the half diameter of tree, it means a tree cannot grow inside another tree.

$$h(r) = \left\{ \begin{array}{cc} 0 & r \leq rbh \\ k_s(x, y|\mu_1, \mu_2) & r > rbh \end{array} \right\} \tag{3.15}$$

where

$$r = \sqrt{(x - \mu_1)^2 + (y - \mu_2)^2} \tag{3.16}$$

For the kernel $k_s(x, y|\mu_1, \mu_2)$, a bivariate normal density function is taken, which also allows to simulate nonisotropic distribution.

$$k_s(x, y|\mu_1, \mu_2) = \frac{1}{2\pi \cdot \sigma_1 \cdot \sigma_2 \sqrt{1 - \rho^2}} exp\left[-\frac{1}{2(1 - \rho^2)} \cdot \left(\frac{(x - \mu_1)^2}{\sigma_1^2} - \frac{2\rho(x - \mu_1)(y - \mu_2)}{\sigma_1 \cdot \sigma_2} + \frac{(y - \mu_2)^2}{\sigma_2^2}\right)\right] \tag{3.17}$$

where r is the distance between parent tree and seedling, x and y are coordinates of a seedling. The form of $h(x, y)$ guarantees that a seedling cannot grow inside another tree.

3.2.3. Tree mortality

The mortality probability of a tree is dependent on it's energy. We assume that a tree during it's life time, it accumulates energy. This energy is defined as the proportion of biomass increment minus the amount of consumption energy for respiration and reproduction (Eq.

3.18). When biomass stops increasing, this reserved energy decreases following time because the tree has to spend energy for respiration and reproduction, it causes the increasing of probability of mortality (Eq. 3.20).

$$\frac{dE}{dt} = r_1 \cdot \frac{dBiom}{dt} - r_3 \cdot N2 - \mu \cdot Biom \tag{3.18}$$

$$\mu = \mu 0 \times exp[-(\frac{t}{t_{thr}})^{\alpha_\mu}] \tag{3.19}$$

$$P_m = P0 \times exp(-r_4 \cdot E) \tag{3.20}$$

where E is the energy reserve of a tree,
r_1 is the rate of increasing energy reserve,
$Biom$ is biomass of tree,
$N2$ as in Eq. (3.12) is the number of seedlings a tree produces,
$r_3 \cdot N2$ and $\mu \cdot Biom$ are the amount of energy a tree consumes for reproduction and respiration,
μ as in Eq. (3.19) is time dependent function that takes into account the period a tree consumes more energy for respiration,
α_μ is form parameter for the curve of μ,
P_m is the probability of mortality,
$P0$ is the mortality probability at zero growth and
r_4 the decay rate of the function.

3.3. Parameter estimation for growth model (apply for *Rhizophora apiculata*)

Parameter estimation in ecology is a difficult task, since in ecology it is not feasible to employ experimental designs for the purpose of parameter estimation as is the case in agricultural field trials involving the systematic variation of fertilizer input, plant protection or variety. In ecology, one has to look at the natural variation occurring in the field and hopefully find an inherent data structure somehow equivalent to a well planned experimental design.

3.3.1. General statement of the problem

The underlying differential equation of the growth model for mangroves (3.1) has the following form:

$$\frac{dz}{dt} = f(z, \psi) \prod_{i=1}^{n} g_i(z, e_i, \theta_i) \tag{3.21}$$

where $f(z, \psi)$ denotes the growth rate under optimal condition and z the breast height diameter (dbh). The multipliers g_i denote the influence of environmental variables e_i on the growth rate. They are normalized to one. The parameter vector ψ refers to the growth term and the parameter vectors θ_i refer to the multipliers.

3.3.2. Estimation strategy

Preliminary remark: Although included in the model, parameters for the elevation multiplier have not been estimated. Instead, we assume plausible parameters for the elevation multiplier (Eq. 3.7) in our growth model based on our experience. The process of parameter estimation for other factors (salinity, competition) is based on data that are located on the same level of elevation.

Growth data obtained from plots with different environmental conditions concerning salinity and mutual competition as quantified by the number of trees in a plot yield suitable data structures. In the first step, the parameters of the optimal growth term (first factor of Eq. 3.21) are estimated on the basis of a data set obtained under (quasi) optimal environmental conditions. Data choosing for this step are time series data that are located in zone I in Figure 2.8, including data of breast height diameters and height of the trees. Trees of largest *dbh* values in plots that have smallest tree numbers are chosen for this estimation.

In the second step the parameters of the multipliers are estimated from *dbh* data from plots with non optimal environmental conditions (zone II in Figure 2.8). Under the assumption that the parameters of the growth factors are also valid under different environmental conditions (this assumption is already implied from the formulation of the general model equation), parameters of the multipliers are estimated. For estimating the parameters of growth multiplier of salinity, the choice of the data is as follows: (i) plots of trees that have same age, (ii) plots of trees that have same number of trees and (iii) plots that are located along a salinity gradient. In the case of the competition multiplier, a special method has to be employed, because only the number of trees and not their exact positions are known. These will be obtained by models of spatial point processes which generate possible sets of tree positions.

Process and data used for each step of estimating parameters are illustrated in Figure 3.4. Choice of parameter values after various regression diagnostic procedures is based on high correlation coefficient, R, and low residual sum of squares, SE.

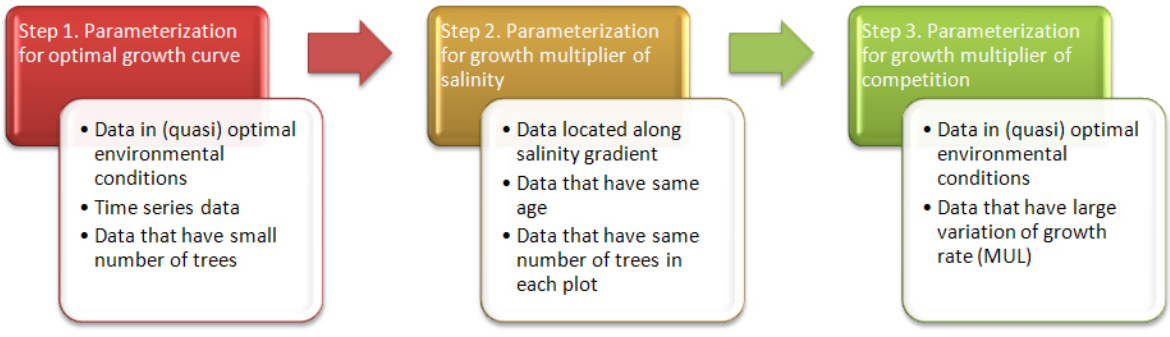

Figure 3.4.: *Order and data choosing for the process of parameter estimation.*

3.3.3. Parameterization using real data

Parameterization for optimal growth

Under optimal condition, Eq.(3.21) has form:

$$\frac{dz}{dt} = f(z, \psi) \tag{3.22}$$

Since the model is defined by a differential equation, the parameter estimation problem involves the solution of the differential equations either in analytical form or as a numerical approximation. For the problem of time series of dbh and H, the method of least squares was applied, the least square function is given as

$$SQ(\psi) = \sum_{i=1}^{n} (dbh_i - z(t_i, \psi))^2 + (h_i - h(z(t_i, \psi)))^2 \tag{3.23}$$

where dbh_i and h_i are diameter and height values from data; $h(z)$ as in Eq. (3.2) is tree height.

The above regression problems were solved with Matlab version 2009a. Figure 3.5 shows the optimal growth curves obtained together with the data. The limitation of this parameterization is we don't have enough time series data. Thus, some parameters have to be fixed (D_{max} and H_{max}) based on our knowledge on the trees in this forest and based on the reference from other publication (Chen and Twilley (1998)), then we apply the sensitivity analysis. In the sensitivity analysis, we change both maximum diameter and maximum height of tree to see how is the sensitivity of different fitted curves compared to the data (Figure 3.6), the final result we choose based on highest value of correlation coefficient and lowest value of sum of squared error.

Parameterization for salinity factor multiplier

In order to estimate the parameters for the multiplier of salinity, it is necessary to separate the competition effect. We choose the data in the plots which are distributed along salinity gradient, those plots must have trees of same age and numbers (see Table 3.1). In this case, we assumed that trees that have same age and same numbers are distributed rather regularly in the plots (they were planted), thus the effect of competition is equally in each plot and thus the variations of tree sizes are caused by salinity factor.

Table 3.1.: *Data used for estimating parameters for salinity factor multiplier*

Plot ID	**Number of trees**	**Age**	**Mean diameter**	**Salinity** (*ppt*)	MUL
49	27	26	12.904	16	0.338168605
37	28	26	12.16	17.2	0.310465116
35	28	26	11.118	18.68	60.275613372
41	21	26	10.58	21.4	0.25677907
64	26	26	8.5496	28.4	0.174748287

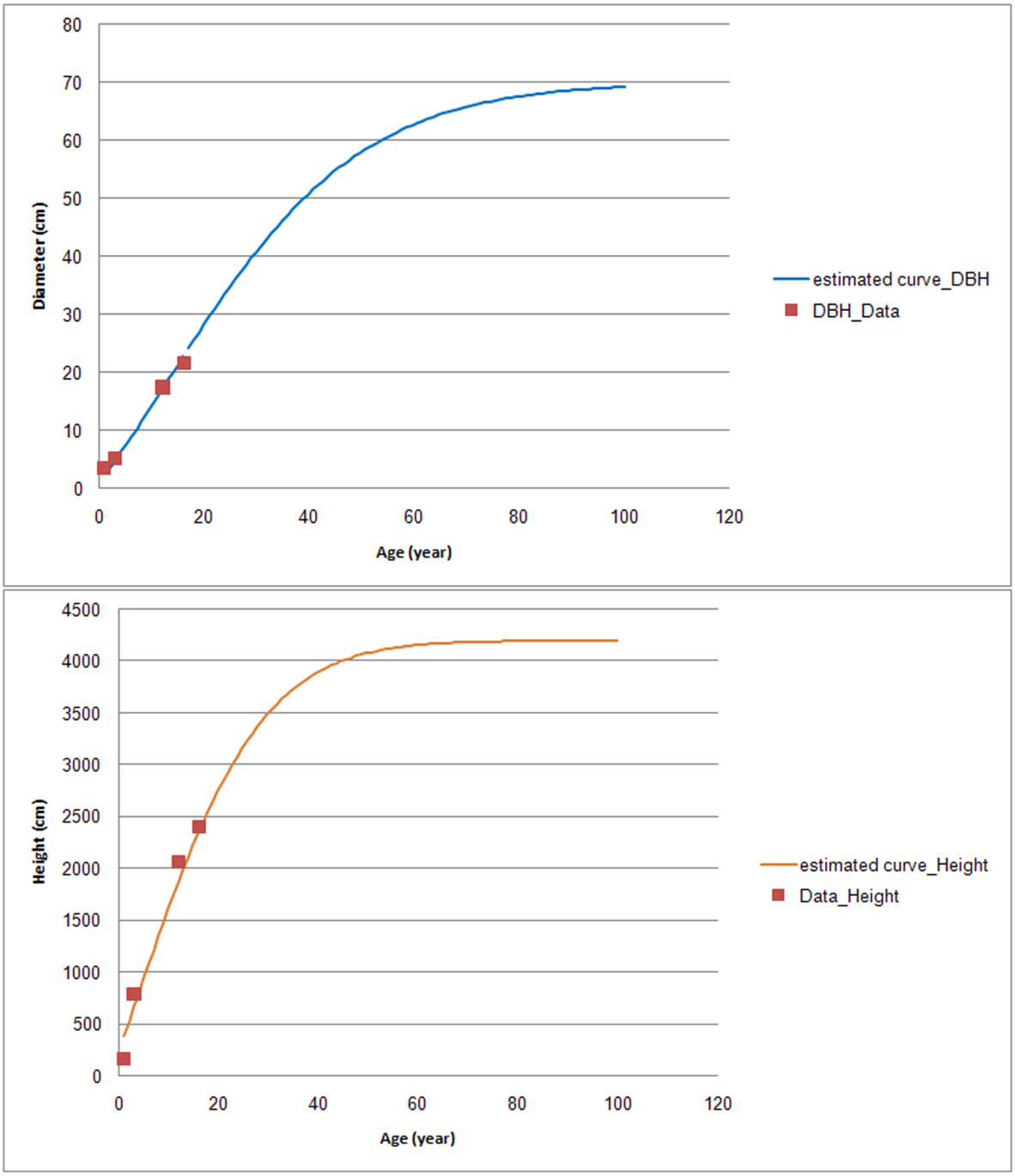

Figure 3.5.: *Fitted diameter and height curves under optimal environmental conditions, square points are the data.*

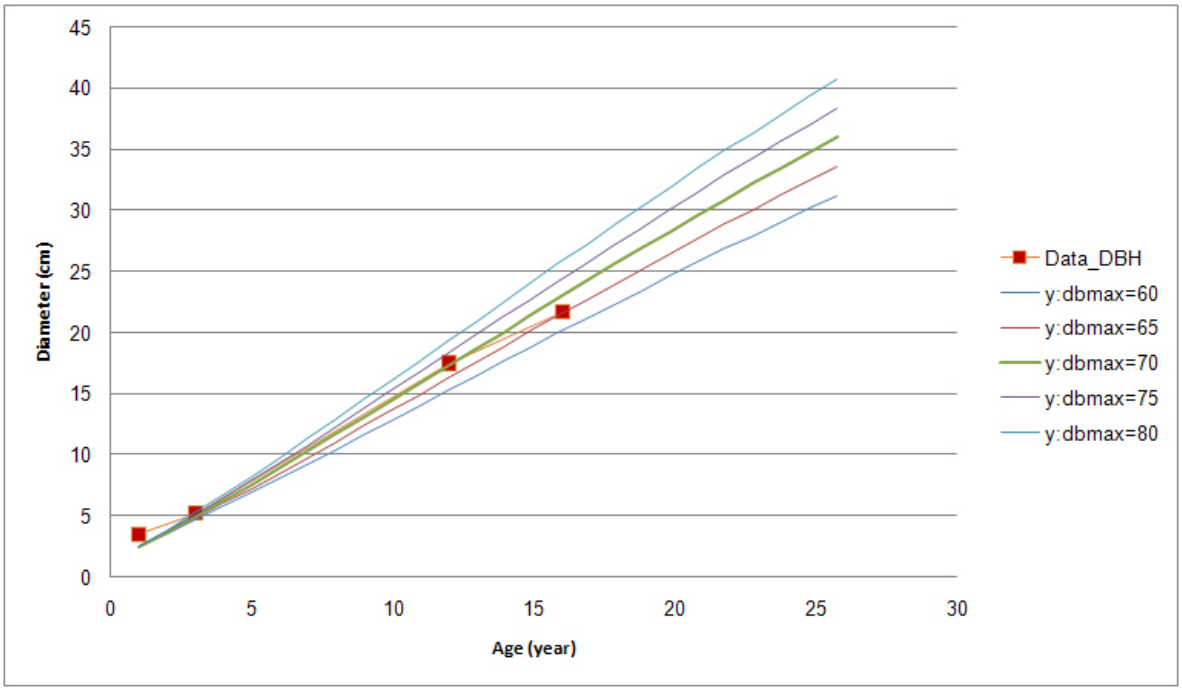

Figure 3.6.: *Sensitivity analysis of optimal growth curve.*

Nonlinear least square method was used to estimate the parameters of the following equation:

$$MUL = f_c(\frac{1 - a_{0s}}{1 + e^{d(x_{1s} - s)}} + a_{0s}) \tag{3.24}$$

f_c is assumed to be equal (a constant) for all plots that have same-age trees and same number of trees, the values of a_{0s} and x_{1s} are fixed during the estimation. After running the estimation for some values of a_{0s} and x_{1s}, we get the fitted curve as in Figure 3.7 with $SE = 0.0036$ and $R^2 = 0.947$.

3.3.4. Parameterization for competition factor multiplier by combining real data and artificial data

The main objective is to estimate parameters for the Equation (3.11). To accomplish this task, we need to determine the values of $y-$axis (f_c) and $x-$axis (FA) from data. Data used for this estimation are located on the optimal environmental conditions (f_s equals 1).

Values for f_c ($y-$axis) are the values of MULs from the data (extracted from Eq. (3.3) with $f_s = 1$ ignoring the factor of elevation). MULs were extracted by $MUL = G/G_{opt}$ when G_{opt} was estimated (see Appendix A).

Values for FA ($x-$axis) are extracted by Equations (3.8 to 3.10). To get these values, it is necessary to estimate the parameters in reverse order (from 3.10 up to 3.8). Problem encountered here is the calculation for the value of FON_o. In order to extract values for this parameter, distances among trees in the data must be known (see Figure 3.3 (d)) but we have only the number of trees in each plot. Thus, we try to reconstruct the position of each

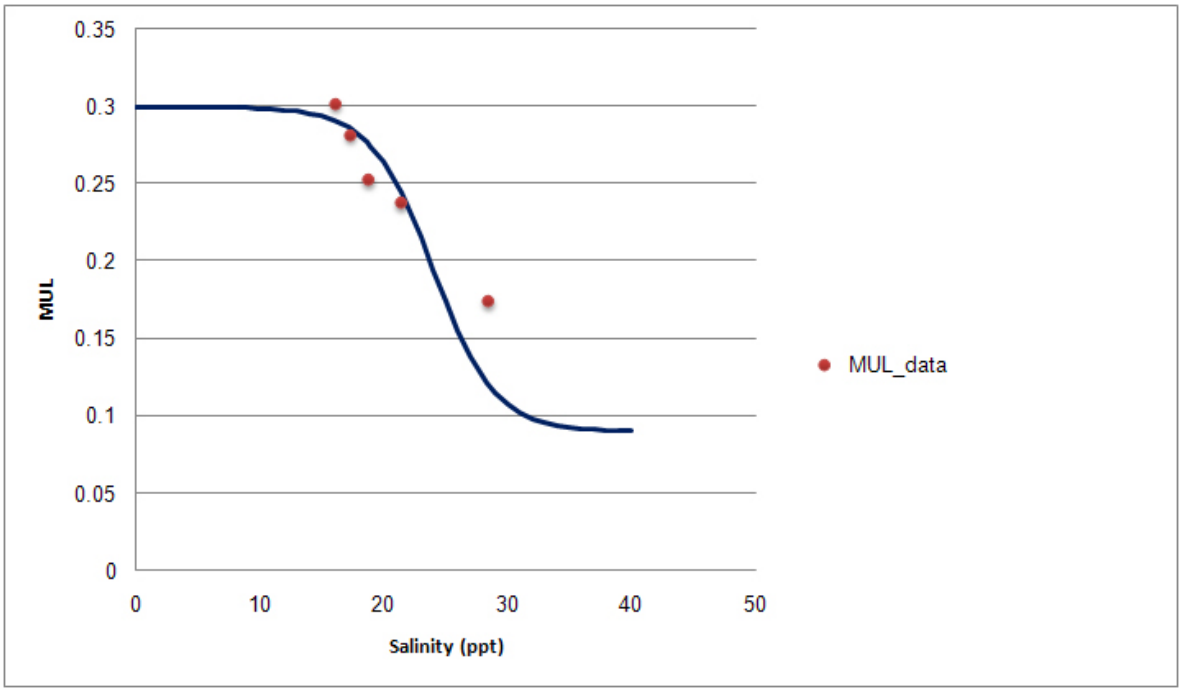

Figure 3.7.: *Fitted multiplier curve with data.*

tree in each plot by simulating spatial point process. We test several types of spatial point distribution. The distribution that could explain our data best is the ***'Hard-core Strauss'*** point distribution (Illian et al., 2008).

Hard-core Strauss point pattern denotes that there are no pairs of points that are closer than the distance r_o and just a specified fraction of points is allowed (with a probability) within a certain distance of any given point (see Figure 3.8 and Equations from 3.25 to 3.26).

The location density function f_n (Illian et al., 2008)

$$f_n(x_1, ..., x_n) = exp\left[-\sum_{i=1}^{n-1}\sum_{j=i+1}^{n}\phi(\|x_i - x_j\|)\right]/Z_n \tag{3.25}$$

is a multivariate probability density function which defines a point process with exactly n points. $r = \|x_i - x_j\|$ is the distance between two ponits (trees) and $\phi(r)$ is pair potential function, it measures the *'potential energy'* caused by the interaction among pairs of points (x_i, x_j) as a function of their distance r

$$\phi(r) = \left\{ \begin{array}{cc} \infty & r < dbh/2 \\ \beta & dbh/2 < r \leq R \\ 0 & r > R \end{array} \right\} \tag{3.26}$$

To generate this type of pattern so that it best explains the data, the first certain number of bigger trees in the plot (75% of total trees with higher *dbh* values) are generated uniformly,

then the other smaller trees (the remain 25%) are generated sequentially. If there are existing events within the distance of $dbh/2$ of each event (hard-cord distance), then they are rejected. A certain number of smaller trees can be located within a radius $dbh/2 < r \leq R$ of the bigger tree's location (Eq. 3.26). Detailed explaination of this type of point pattern is in Appendix B.

In summary, the order for parameter estimation for competition multiplier is as follows: (i) estimate parameters a_2 and c_2 (in Eq. 3.10) to extract the radius of zone of influence (R) of each tree, (ii) simulate samples of tree positions for each plot in the data, (iii) extract FAs of trees in each simulated sample and (iv) estimate parameters for the competition multiplier in Eq. (3.11).

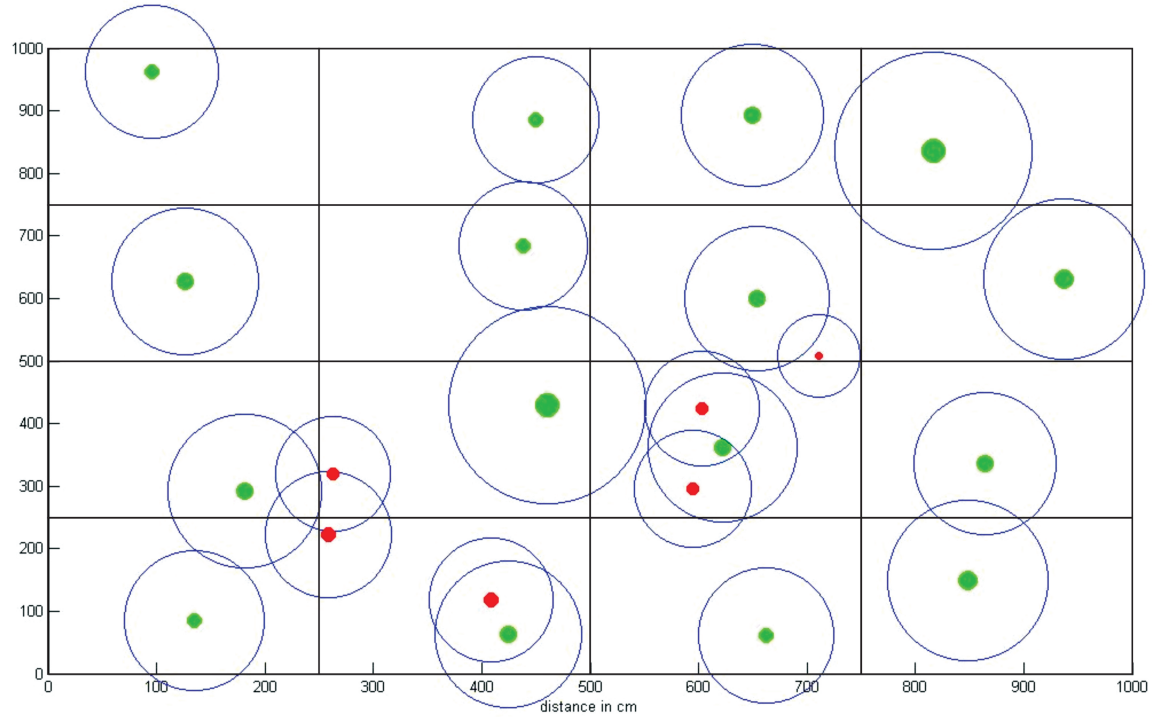

Figure 3.8.: *A sample of a realisation of a* ***'Hard-core Strauss'*** *process. The larger trees (green circles) are located rather regularly, the smaller trees (red circles) are distributed within a certain radius (determined by a probability) of the larger trees, the blue circles are the R of the trees. This sampling process will be conducted many times, each time the trees located at different positions in the plot.*

Estimation of the parameters a_2 and c_2

Parameters a_2 and c_2 are scaling parameters for calculating the zone of influence of trees (Eq. 3.10). To estimate these two parameters, we make the following assumptions: (i) trees are located on optimal conditions, (ii) trees are distributed regularly within each plot and (iii) trees are influenced by the effect of self-thinning (when tree size increases, tree numbers will be decreased as in Fig. 2.10). The procedure for this estimation:

- Simulate time series of *dbh* values under optimal condition by submodel **Growth model** from the IBM (the parameters for the optimal growth were estimated before)

- Calculate number of trees in the plot at each time step according to $N = (ln(dbh)/5.0744)^{-4.40529}$ (self-thinning effect, the relationship between N and dbh was discussed in Section 2.4.2 of Chapter 2, this relationship was shown in Figure 2.10)
- Calculate area of zone of influence (ZOI) by $Scell/N$, where $Scell$ is the area of the measured plot
- Calculate R by $R = \sqrt{ZOI/\pi}$
- Estimate a_2 and c_2

Result of this parameter estimation is shown in Figure 3.9 with $a_2 = 21.99$ and $c_2 = 0.876$.

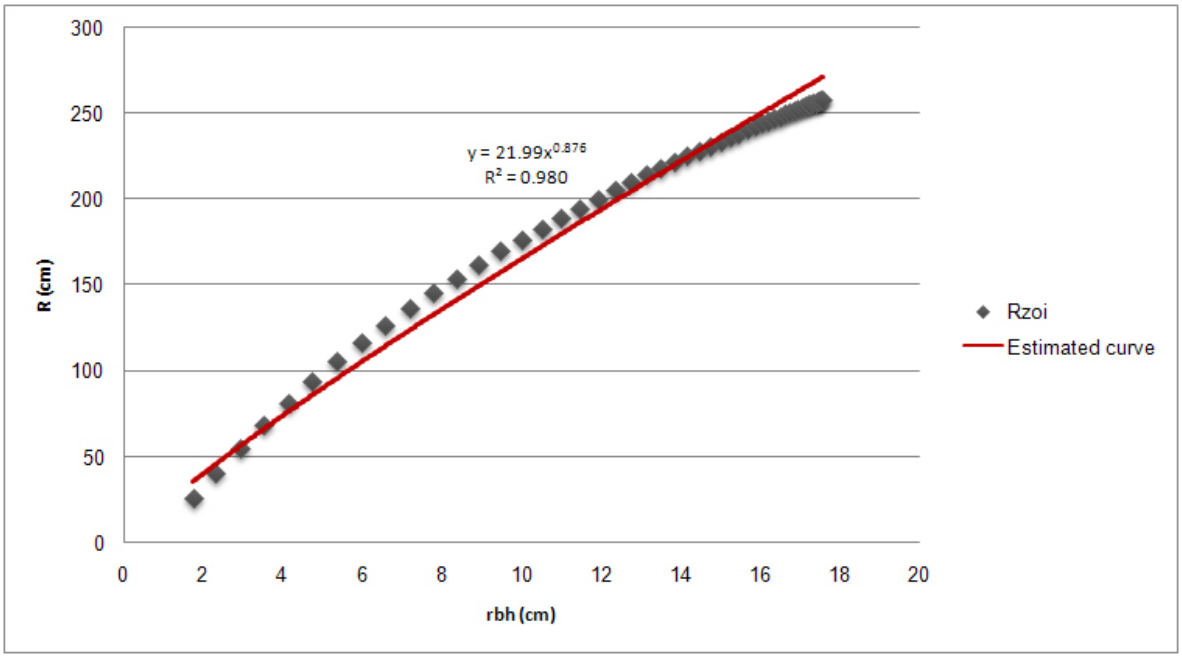

Figure 3.9.: *Fitted R's curve with simulated data (square points).*

Parameterization for growth multiplier of competition

When the parameters a_2 and c_2 are known, the spatial configuration of each plot is generated many times (100,000) by the *'Hard-core Strauss'* process. Then, FAs will be extracted by running one module of IBM (the module Competition factor).

The data plots that are used for reconstructing tree locations must satisfy the following conditions: (i) the plots are located along a salinity gradient and (ii) the number of trees in the plots are different from each other. We choose the plots that have number of trees range from very small (13 $trees/100m^2$) to very large (115 $trees/100m^2$).

Totally there are 5 plots were re-sampled, of which 2 plots belong to the optimal salinity zone (zone I in Figure 2.8). These two plots are used for the estimation to exclude the influences from other environmental factors, the other plots are used to test the parameterization results

in the context of including influences from environmental factors. All of these 5 plots are assummed to have non-zero FA values because their MUL values (from data, calculated following the formulae expressed in the Appendix A) are smaller than one.

Result

The results of parameterization from 2 representative plots on optimal salinity zone are as follows:

- Representative plot 1 (number of trees = 13, age = 16): In 100,000 samples; there are 5290 samples have non-zero FA values. Estimating parameters for these 5290 samples (used nonlinear least square method), only 160 samples give the results that satisfy: $0.8 \leq R^2 \leq 1$ and $res \leq 0.5$, where res is the residual sum of squares
- Representative plot 2 (number of trees = 22, age = 13): There are 1650 samples (in 100,000) have non-zero FA values. After parameterization step for these 1650 samples, 118 samples have given the following results: $0.65 \leq R^2 \leq 1$ and $res \leq 1.5$.

We choose the final parameter values base on the following criteria:

- Values that have largest R^2 (0.91 for the first representative plot and 0.7 for the second plot)
- Values that have smallest sum of square error ($res = 0.25$ for the first plot and 1.0 for the second plot).

Figure (3.10) shows some samples of fitted curves together with the reconstructed data and the estimated parameter values are shown in Table C.5 in the Appendix C.

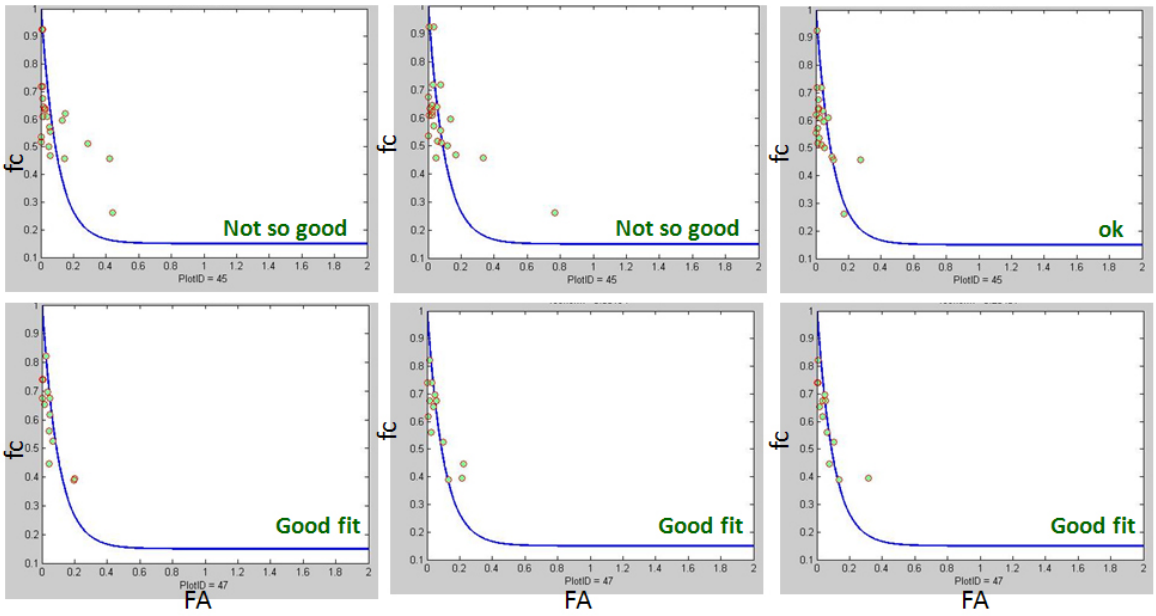

Figure 3.10.: *Examples of fitted curves for the relationship between f_c and FA.*

3.3.5. Test of the estimated parameters

The step of estimating parameters for the multiplier curve of competition factor was based on the simulated positions of the trees in the plots. Because of that, uncertainties of the results might occur.

To test the reliability of the results, we conduct a procedure for testing the result quality. Firstly we apply these estimated parameters for testing the correlation between the data and the estimated curve using the other 3 representative simulated plots (totally there are 300,000 re-sampled plots) to check if there would be any plot that fix the curve. Secondly, we simulate the whole picture of the data plots (IBM validation) by running many times the IBM for some other selected data plots, to check if there would be a simulated sample that is close to the real data.

Test the estimated parameters with other re-sampled plots

Three resampled plots that located on non-optimal environmental conditions (along salinity gradient) are examined. After excluding the factor of salinity for these plots (using parameters estimated before for salinity multiplier curve), we examine the correlation of the non-zero FA plots with the estimated parameters of f_c's curve (see Figure 3.11) and the results are as follows:

- plotID 41: there are 9 samples that have non-zero FA values, in which just only 1 sample that rather correlates with f_c's curve: $R^2 = 0.545$ and $res = 4$ (Fig. 3.11)
- plotID 35: 7846 samples that have non-zero FA values, in which 6 samples have $R^2 > 0.6$ and $res \leq 4$
- plotID 37: there are 30036 samples of non-zero FA values and 36 samples have $R^2 > 0.6$ and $res \leq 2.5$.

These results show that, at least there is one plot can suite the estimated curve in total 100,000 configurations of data plots (plot ID41). This proves that the reliability of the estimated parameters are possible.

Reconstructing the data plots by IBM simulations

We apply the parameters that have been estimated for the module ***tree growth*** in IBM (including parameters for the multipliers of salinity factor and competition factor) and run this module of IBM to simulate again some data plots. The purpose of this work is to check if we could obtain the samples that are close to mean dbh values of the data (in the interval $\left[\bar{dbh} - 0.5, \bar{dbh} + 0.5\right]$). The data we try to reconstruct are shown in Table 3.2, each data plot is reconstructed 500 times, at each time the positions of the trees in the plot are re-allocated following the ***Hard-core Strauss pattern***.
In 7 reconstructed data plots, there are 4 plots can achieve the mean values of dbh of the real data. In 500 runs for every representative data plot, the results are as follows (see Figure 3.12):

- Plot ID04: 69 simulated plots have same mean dbh values as the observed data (Fig. 3.12 (a))

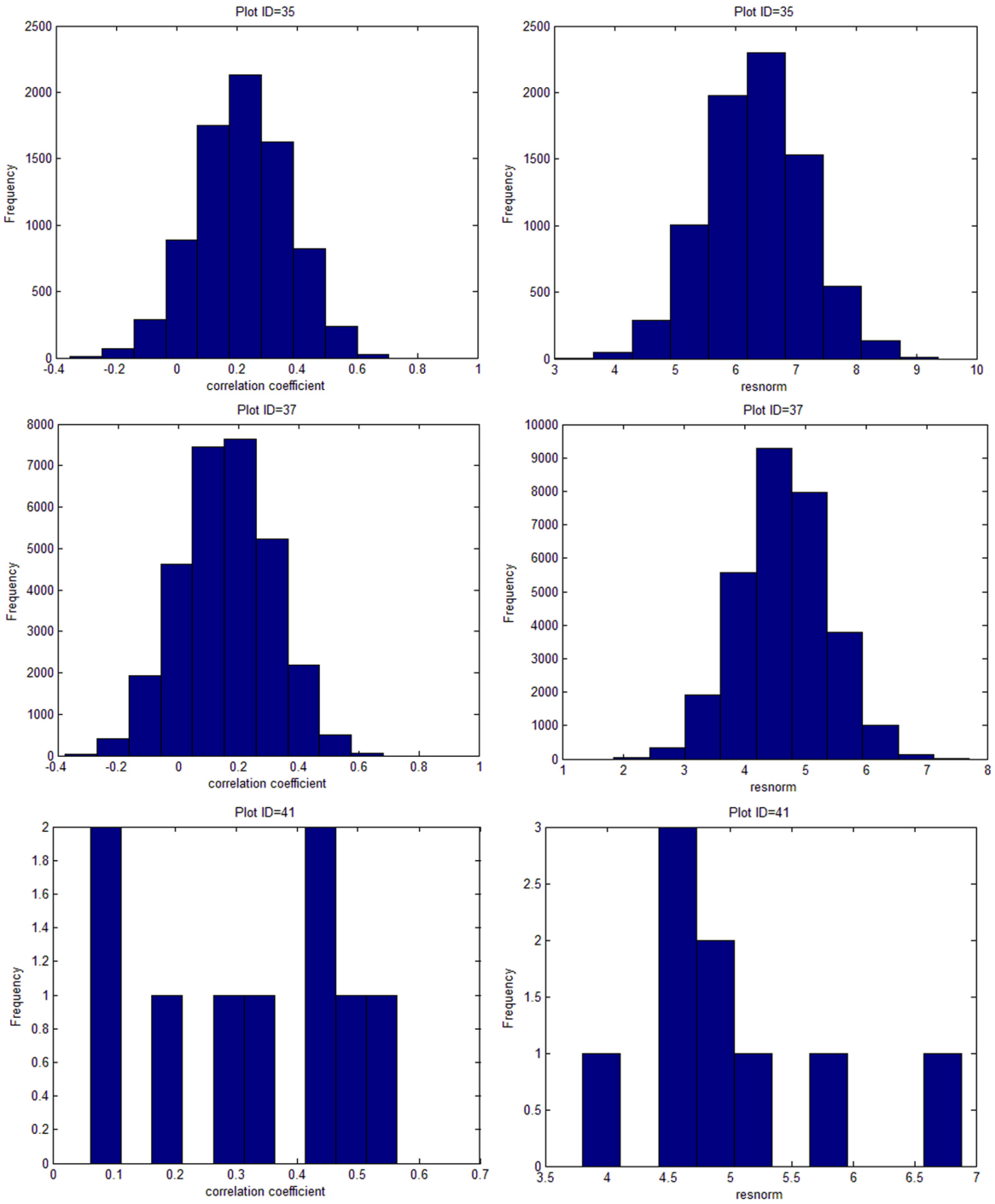

Figure 3.11.: *Correlation and sum of square of residual between f_c and FA from 3 examined plots (ID35, ID37 and ID41).*

Table 3.2.: *Data used to test the estimated parameters*

Plot ID	**Number of trees**	**Age**	**Mean diameter (cm)**	**salinity (*ppt*)**
45	22	13	12.42	12
47	13	16	15.45	13
49	27	26	13.06	16
35	28	26	11.118	18.68
41	21	26	10.58	21.4
04	59	13	7.559	14.6
02	115	13	5.335	14.6

- Plot ID47: 67 simulated plots have same mean *dbh* values as the observed data (Fig. 3.12 (b))
- Plot ID45: 20 simulated plots have same mean *dbh* values as the observed data (Fig. 3.12 (c))
- Plot ID41: no result can explain the observed data (Fig. 3.12 (d))
- Plot ID49: 4 simulated plots have same mean *dbh* values as the observed data (Fig. 3.12 (e))
- Plot ID35: no result can explain the observed data (Fig. 3.12 (f))
- Plot ID02: no result can explain the observed data (Fig. 3.12 (g))

Figure 3.13 shows the examples of diameter distribution from simulated plots compare to observed plots.

3.4. Simulating mangorve dynamics using IBM

Dynamics of mangroves is simulated base on life cycle of trees (Initialize - Grow - Regenerate - Die). We simulate three representative species as mentioned at the beginning of the Chapter, each adapts well on a particular environmental condition. Two scenarios are considered, the first scenario is the stable environmental condition where we let mangroves grow and examine the behaviours of each species; the second scenario is the changes of environmental conditions over time, particularly focuses on sea level rise due to the effect of global climate change.

Figures from 3.14 to 3.16 illustrate simulation study from IBM. Figure 3.14 (uper) describes the succession of mangrove species: *Avicennia alba* occupies the near-shore zone where the frequency and duration of tidal inundation are high, *Rhizophora apiculata* occupies the intermediate zone and *Phoenix paludosa* occupies on higher land. Figure 3.14 (below) shows the salinity and elevation from 'landward' (at distance 0 cm) to 'seaward' (to distance 2000 cm). Figure 3.15 describes the scenarios of changes of salinity and elevation following time (300 years) caused by global warming effect. Figures (3.16 (a1) to (e1)) and (3.16 (a2) to (e2)) are

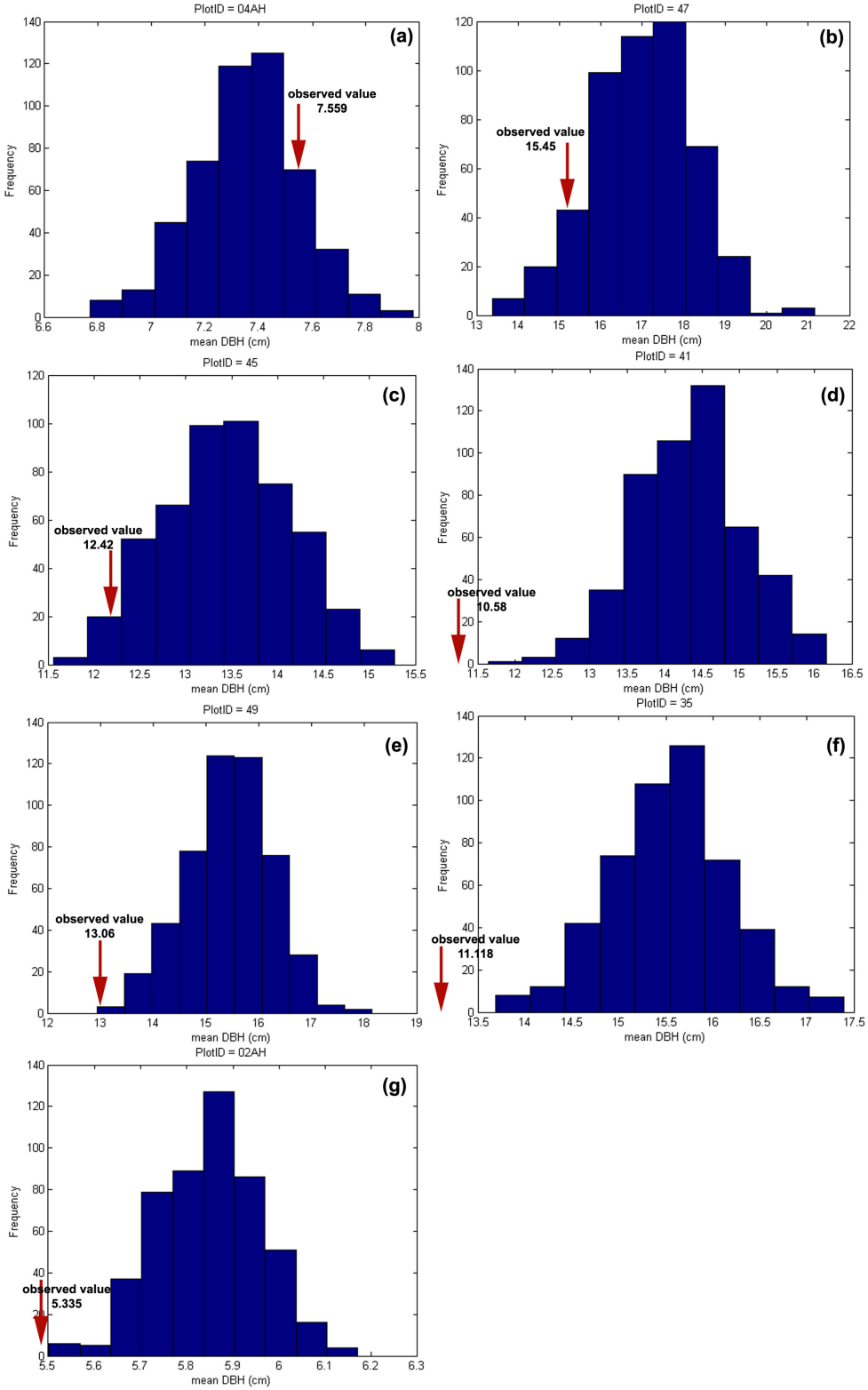

Figure 3.12.: *Frequency of mean diameters from 500 simulations, there are 4 plots give the results which close to the data.*

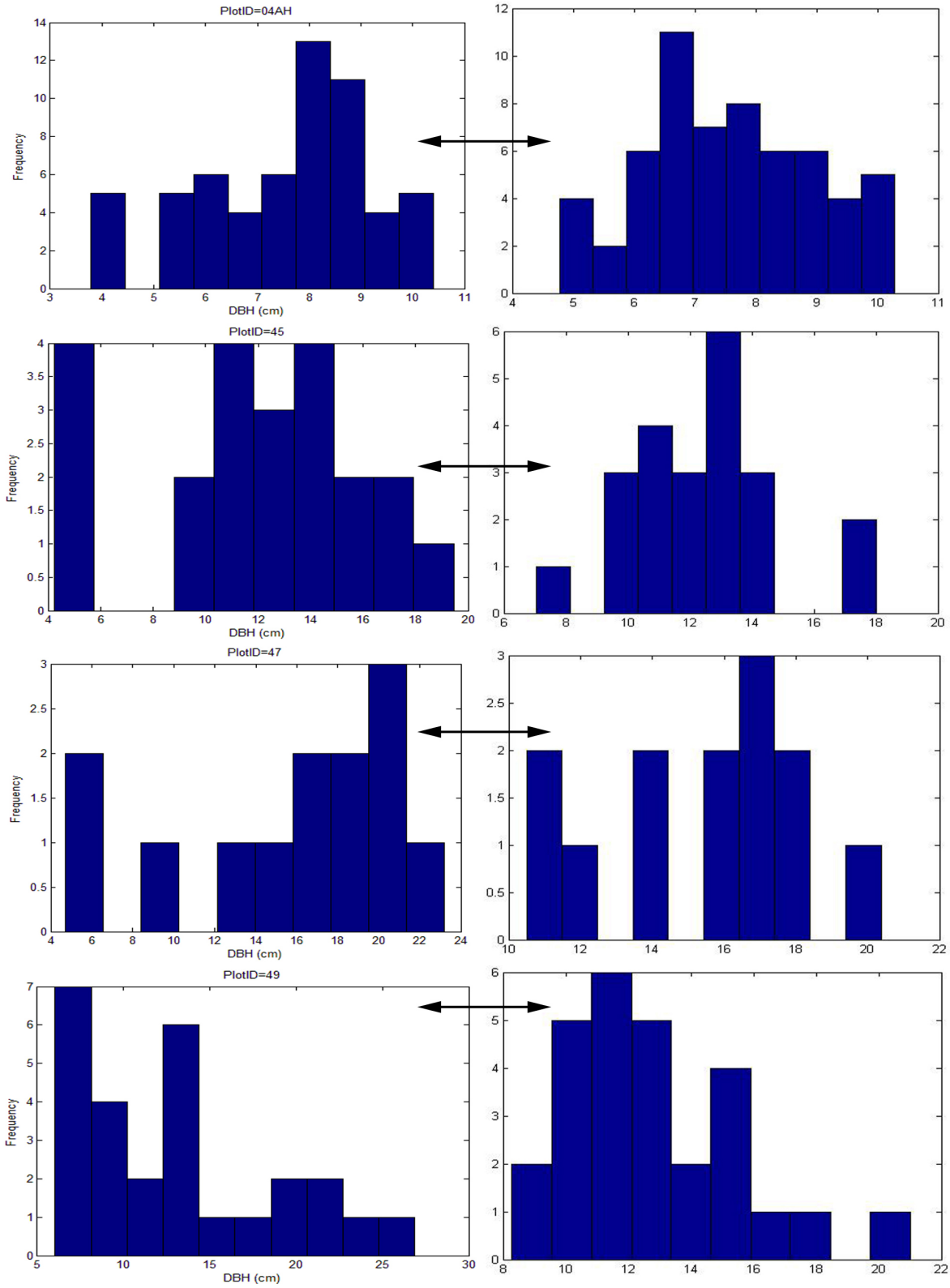

Figure 3.13.: *Example of frequency of tree diameters of each plot in one of 500 simulations from IBM. On the left side are simulated plots and on the right side are the data of equivalent plots.*

the results from IBM simulations for two scenarios: stable conditions (on the left side) and changing conditions (on the right side).

Results from the simulations of stable environmental conditions show that the species distributed in three zones. For the long term of succession, the shrub trees (*Phoenix paludosa*) cannot survive. The reason might because we just look at a closed area and the trees do not have any exchange with other areas via seedlings. Result of this stable condition shows that in the long term, in a closed situation without seedling exchanging, the wood tree will be dominant.

For the scenario of sea level increases, the behaviors of three species are different. *Phoenix paludosa* disapears first due to the high frequency of inundation. *Avicennia alba* actually can due with high frequency of inundation, but it also cannot remain. It is because *Avicennia alba* cannot deal with the changing situation. *Rhizophora apiculata* shows it ability to adapt to changeability. *Rhizophora apiculata* moves landward and still remain.

Figures 3.17 and 3.18 show time course of biomass resulted from two scenarios. The tendency of total biomass resulted from the stable condition scenario is continuously increasing while another is not. It is because of the high level of water inundation and saninity increment which are not favorable for tree growth.

Figures 3.19 and 3.20 are simulated results of species composition following time.

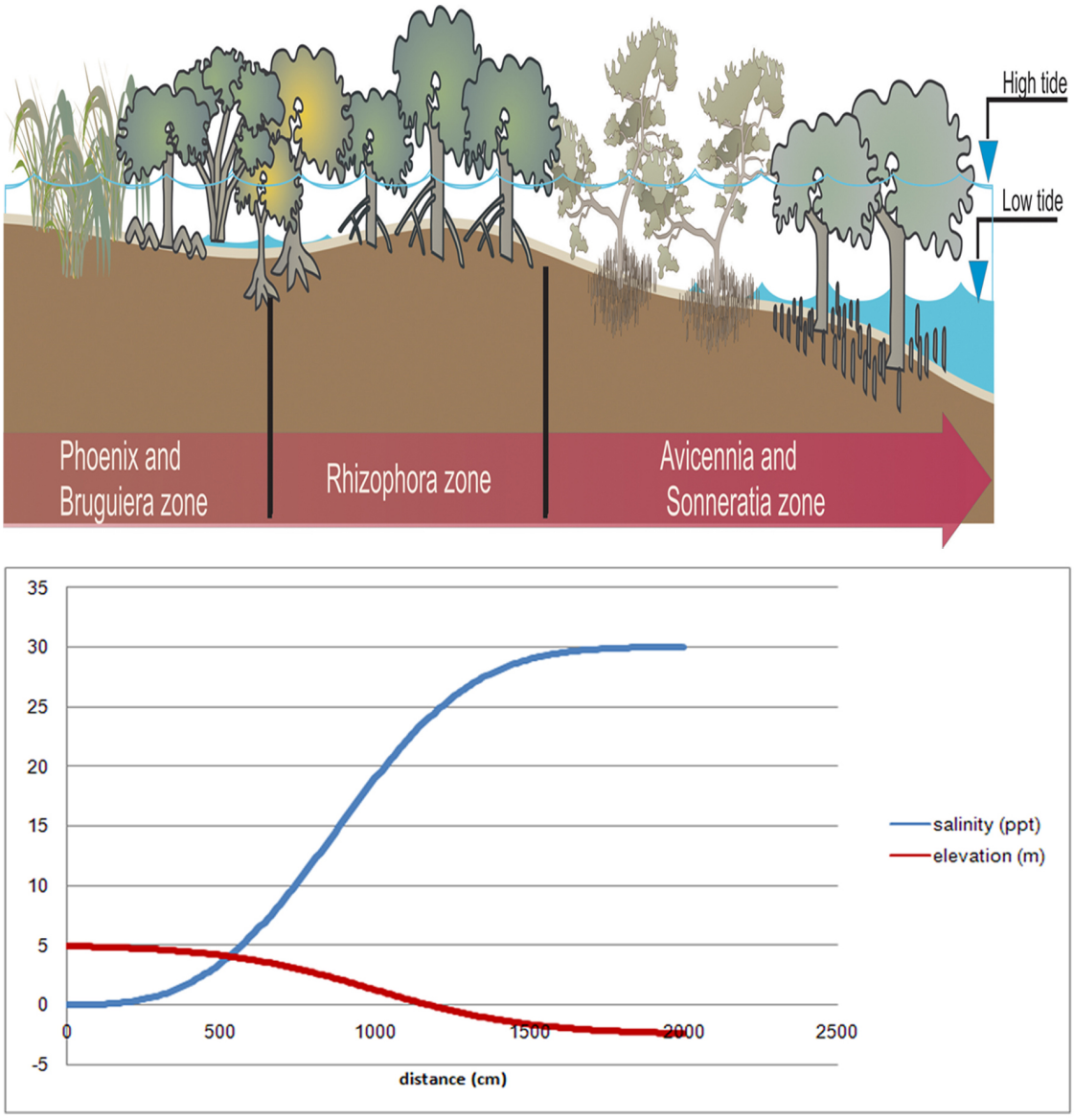

Figure 3.14.: *Simulated stable environmental conditions. The above figure describes the zonation of representative mangrove species and the below shows the elevation and salinity from landward to seaward.*

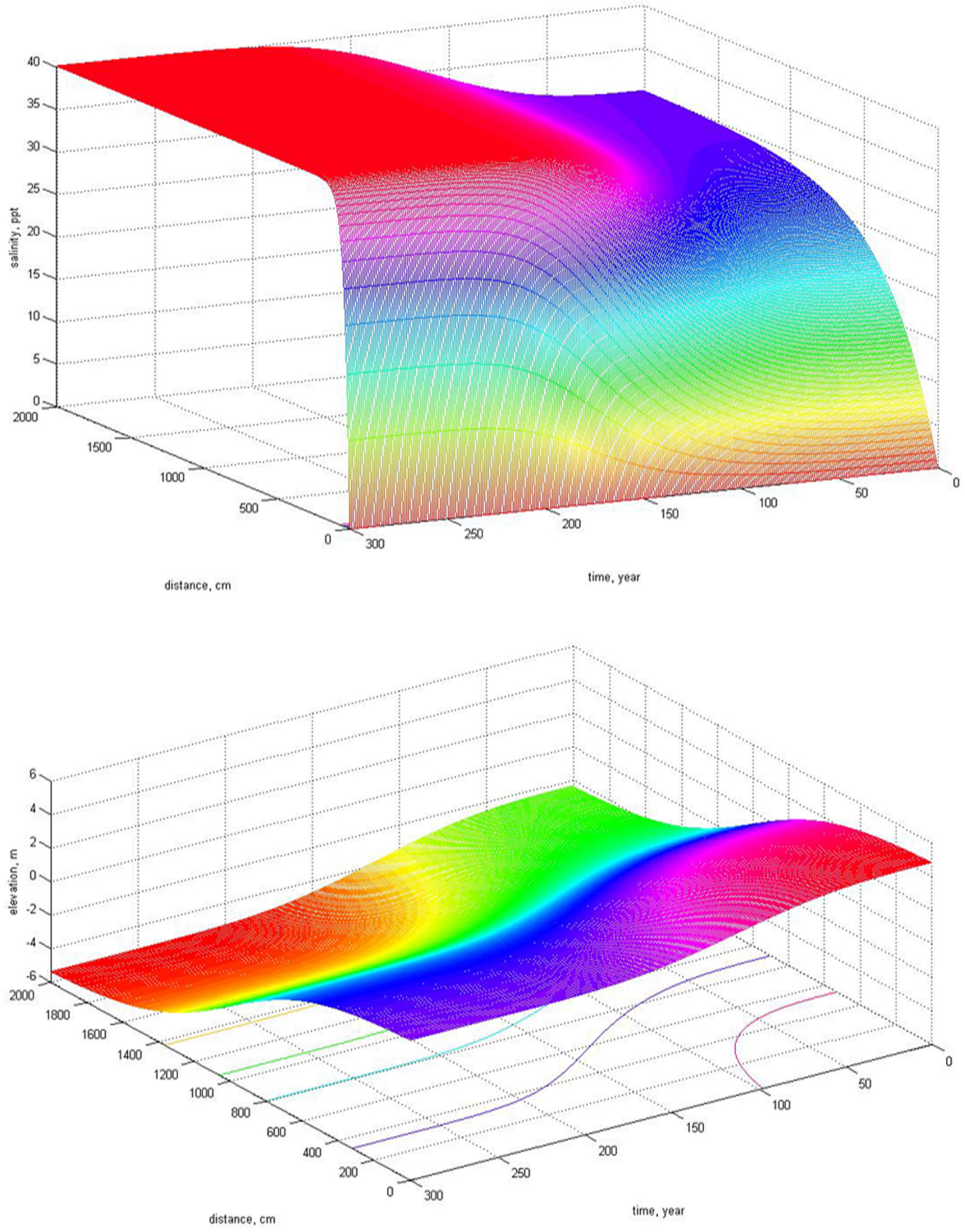

Figure 3.15.: *Simulated environmental conditions (salinity and elevation) for sea level change scenario following time (year).*

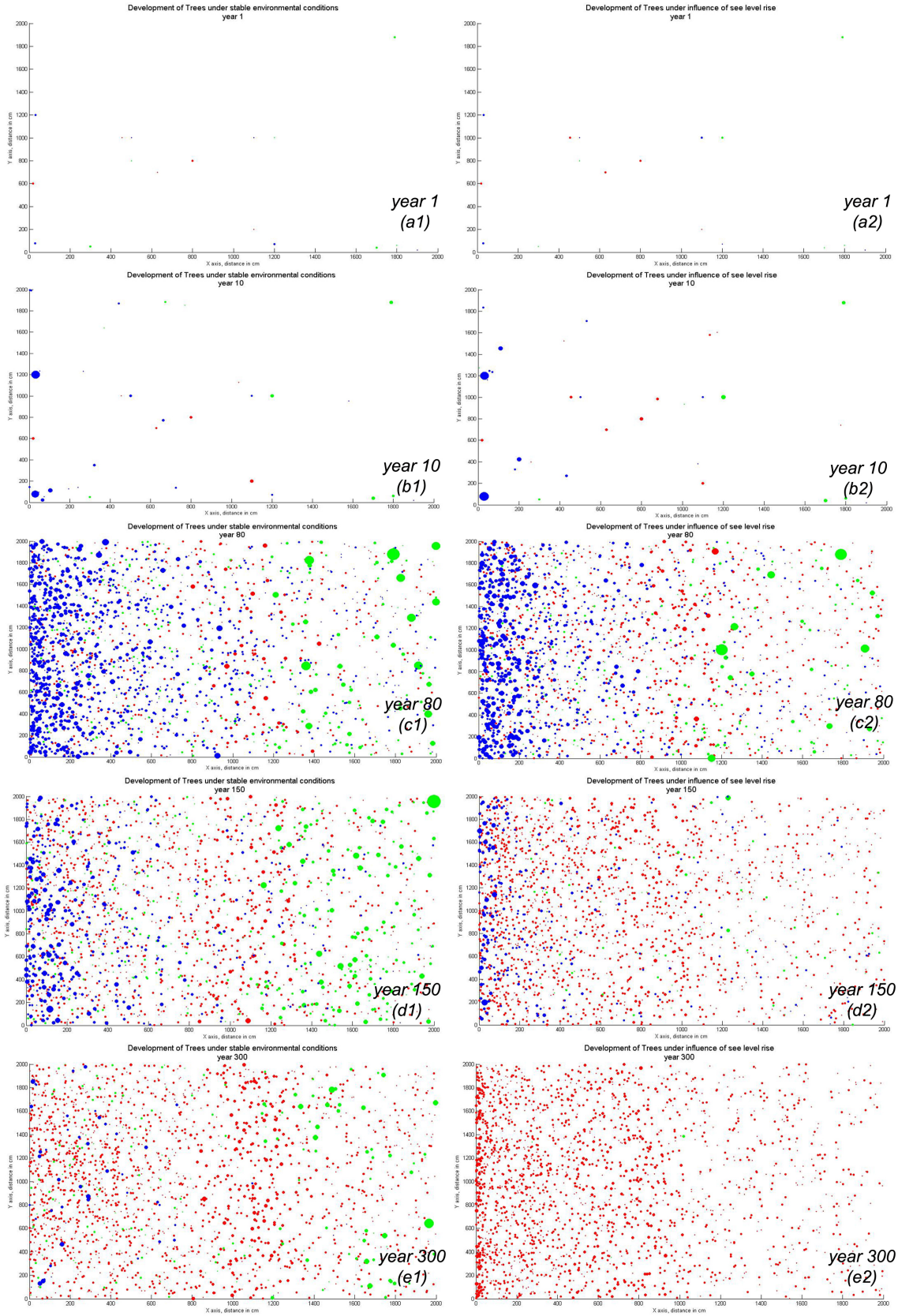

Figure 3.16.: *Mangrove growth and distribution under two scenarios: stable environmental conditions (on the left side) and sea level rise (on the right side). Green filled circles are Avicennia alba, red filled circles are Rhizophora apiculata, blue filled circles are Phoenix paludosa.*

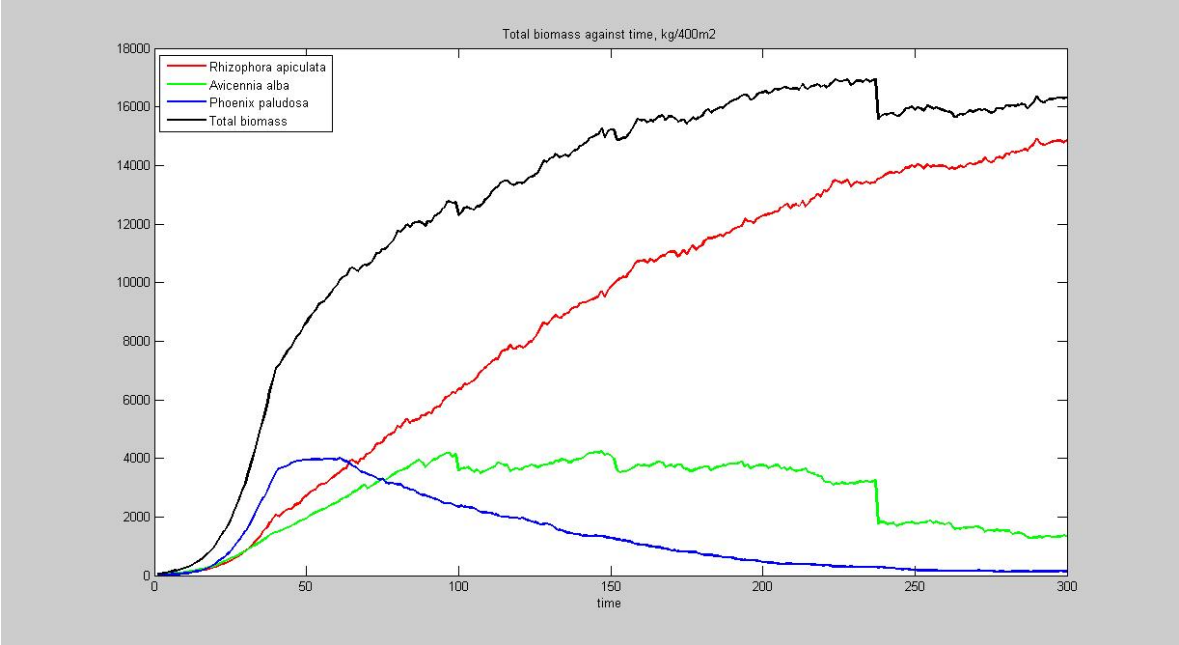

Figure 3.17.: *Time course of total biomass of each species under stable environmental conditions.*

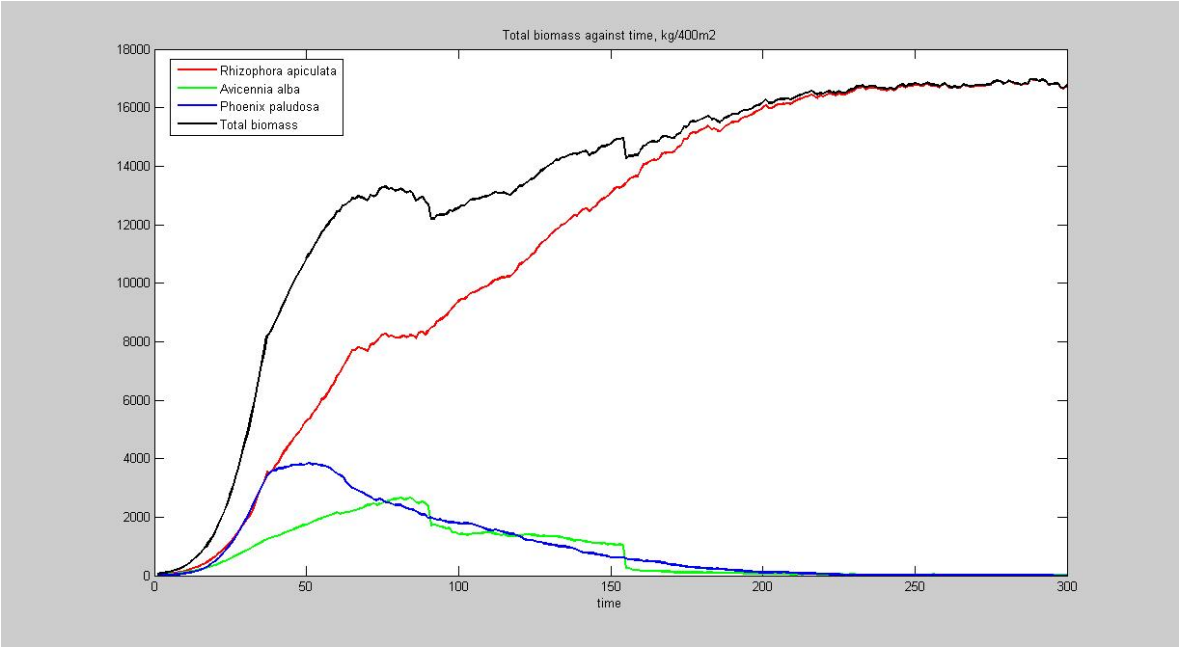

Figure 3.18.: *Time course of total biomass of each species under influence of sea level rise.*

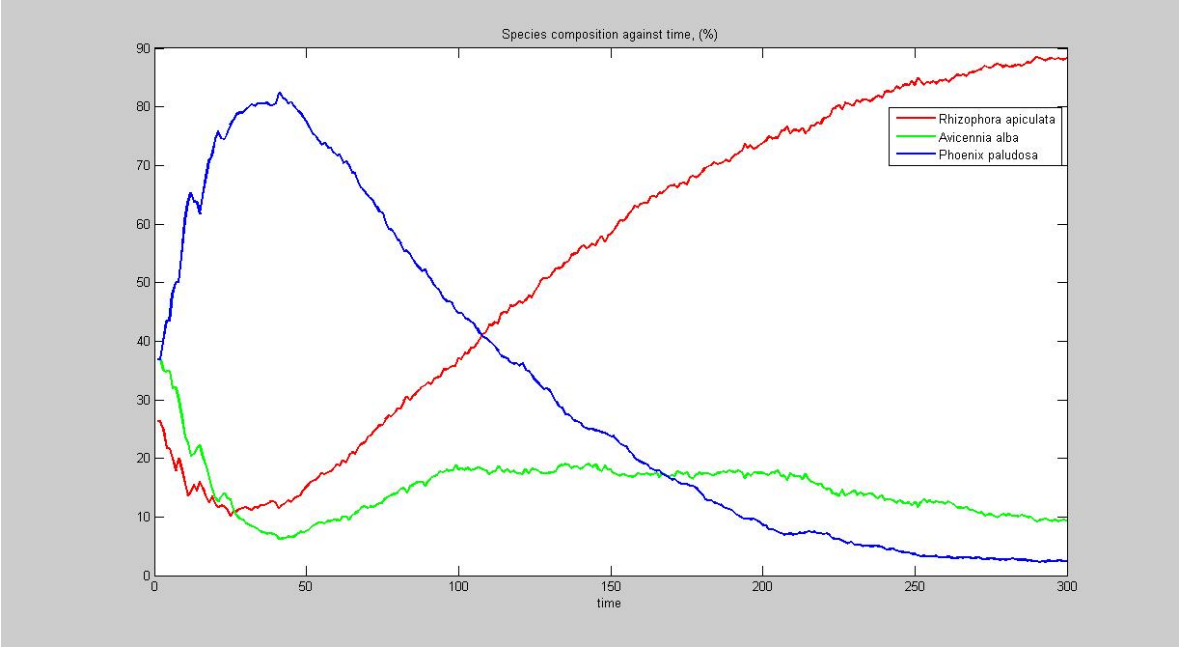

Figure 3.19.: *Species composition (%) following time under stable environmental conditions.*

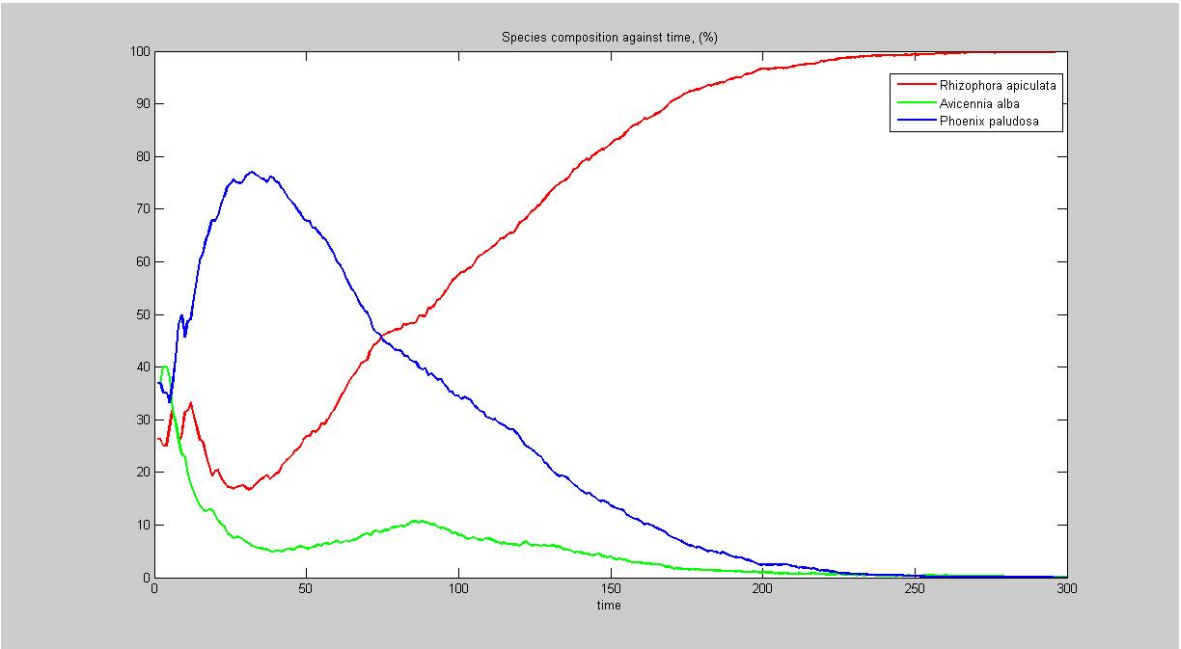

Figure 3.20.: *Species composition (%) following time under influence of sea level rise.*

4. CanGio Mangrove Forest Model (CGMM)

The CanGio Mangrove Forest Model (CGMM) is an up-scaled model from the IBM in Chapter 3. IBM in our work is applied as a basic model for constructing the model at larger scale (CGMM). We use the modules built for IBM to construct the CGMM. For our opinion, model construction and test at smaller scale (like IBM) and then develop this model to a larger scale model will be easier than directly construct a large scale model and test it.

CGMM simulates mangrove dynamics on a large landscape, it has the advantages compare to the IBM are those: (i) it is computationally much more efficient at only slightly reduced precision and (ii) it still includes the heterogeneity of the simulated individuals while (iii) it has capability of extending to a large area.

In this chapter, we present the model CGMM in association with the IBM. Firstly, generalization of the conceptual design of the model is presented following the ODD protocol from Grimm et al. (2010). Next, methods and procedures for the ***'up-scaling'*** from IBM to CGMM will be described. Then, we present the basic structure of CGMM. Detailed descriptions of the equations, variables and parameters of both models (CGMM and IBM) will be expressed and also presented in Appendix C. Finally, the results of CGMM simulations based on scenarios of changing the environmental conditions will be discussed.

4.1. The CanGio Mangrove Forest Model

4.1.1. Purpose

The CanGio Mangrove Forest Model (CGMM) is designed for simulating the dynamics of mangroves in CanGio, Vietnam. This model is developed in order to meet the need of a model that can simulate and forecast the succession of mangrove species in the context of changes of environmental conditions. Results of simulation from the model will support the decision makers to have a further vision and from that to make appropriate decisions.

4.1.2. Design concept of CGMM

CGMM is a model of multi-species population dynamics. It describes dynamical processes of forest (initiate, grow, interact, reproduce, die) over large spatial and temporal scales. The model is up-scaled from the IBM in Chapter 3. We apply the connection from the individual level to the aggregate level: by simulating many times the behavior of individual objects (trees) using IBM, and averaging over a large number of them, then derives functional responses for the entired levels.

CGMM includes two levels of scales: stand level and landscape level. At stand level, the model simulates the interactions between each *dbh* class of trees, the interaction between

trees and underlying environment (salinity, flooding situation). At landscape level, the model simulates the interaction among stands by seed dispersal.

The model is able to adapt to new applications with their specific biotic and abiotic conditions by adjusting the drivers, parameters or single process functions, while the model structure remains. CGMM receives input data directly from GIS layers (salinity data, elevation data, initial species located, ...) and it's outputs can be visualised by GIS softwares.

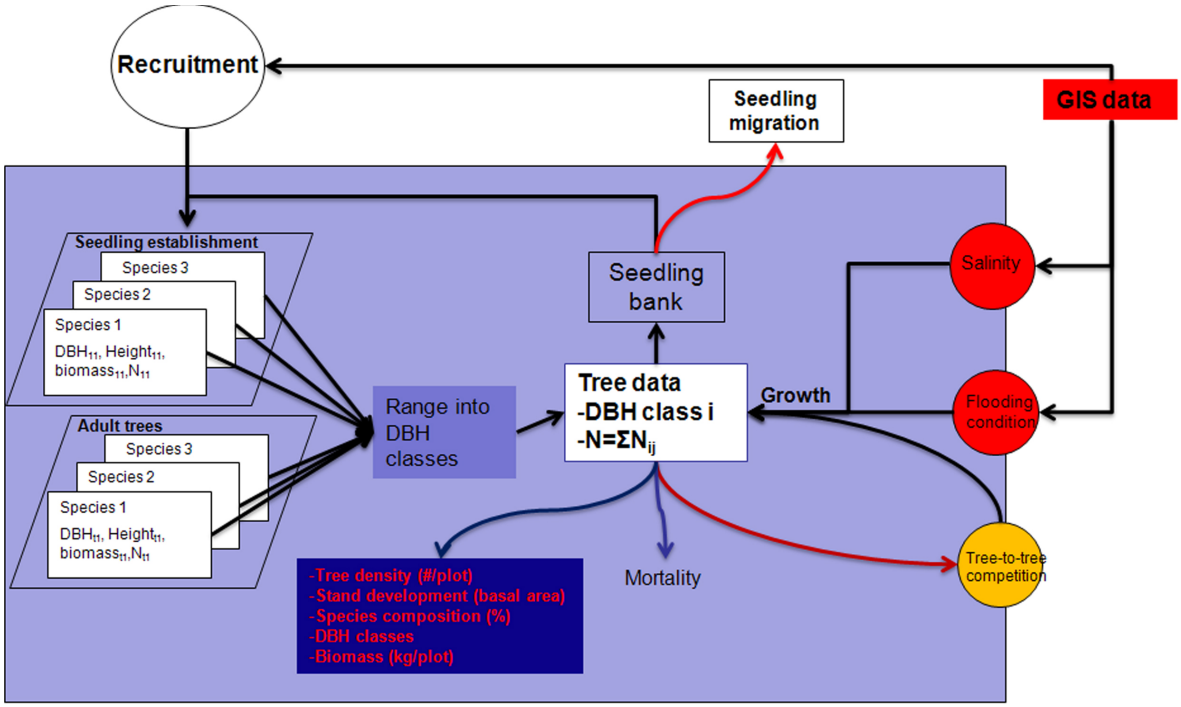

Figure 4.1.: *Conceptual structure of CGMM. Dbhs of each species are classified into dbh classes. Each dbh class is then calculated its increment under the influences of environmental factors and competition factor.*

4.1.3. Entities, variables and scales

CGMM is structured as a landscape of cells, each cell plays a role of a forest stand, the size of the cell can be varied. Simulated attributes of forest structure and composition are stored in attribute data structures associated with each cell. The heterogeneity within a stand (cell) includes different *dbh* classes and different species.

Environmental factors (salinity and elevation) are imported to the model directly from GIS layers. Within stand, environmental factors are assumed to be homogeneous.

Two levels of scales with different types of interaction are accounted for in CGMM. At stand level, growth rate of each *dbh* class of trees is determined by tree-to-tree interaction (based on the assumption of Field of Neighbourhood) and environmental conditions. At landscape

scale, the stands interact with each other by the spread of seedlings (see Table 4.1).

Table 4.1.: *Description of components and variables of different scales of CGMM.*

	Landscape level	**Stand level**
Components	GIS-based	Individual *dbh* class
	Spatial explicitness	Spatial statistics
	Habitat specific	Species specific
Variables	Salinity, elevation, recruitment	Total tree number, growth (*dbh*, height), biomass, basal area
	Regeneration	Reproduction
		Mortality

4.1.4. Process overview and scheduling

At stand level, the tree life cycle (establishment, growth, reproduction, mortality) is updated at each time step (one year) by solving a set of coupled different equations. At landscape level, the environmental variables and the coordinates of survived seedlings are calculated at each time step.

The followings are simulated at each time step:

- Tree stem and height increment
- Biomass increment
- Number of seedlings (produced by trees of *dbh* class k)
- Seedling dispersal
- Tree mortality and seedling mortality
- Updated environmental conditions (if there are changes)

These processes are incorporated as sub-models in a general model scheme in Figure 4.2, more details about sub-models will be discussed.

4.1.5. Interaction

CGMM implements two levels of interactions:

- Landscape level: the stand-to-stand interaction through seedling dispersal
- Local level: the competition among trees. This competition is phenomenological described using the Field of Neighborhood (FON) approach (Berger and Hildenbrandt, 2000).

4.1.6. Initialization and input data

Initially, maps of *'number of trees'* of species are imported into the model. Each seedling is planted with the initial values of $dbh = 2 - 3.15cm$ and $H = 100cm$ (these are estimated as discussed in Chapter 3). The seedlings are added each year are from two sources: one from the regeneration of adult trees and one from the recruitment (if they were planted).

The input abiotic factors for the model are from GIS data, including map of salinity and map of elevation. The number of seedlings recruited into each stand in the model is also from GIS layer. The changes of environmental factors (if happened) are updated at each time step (one year).

4.1.7. Submodels

CGMM is the up-scaled model from the IBM. The structure of CGMM's submodels is based on IBM and CGMM implements some submodels from IBM. Below is the description of CGMM's submodels (Fig. 4.2).

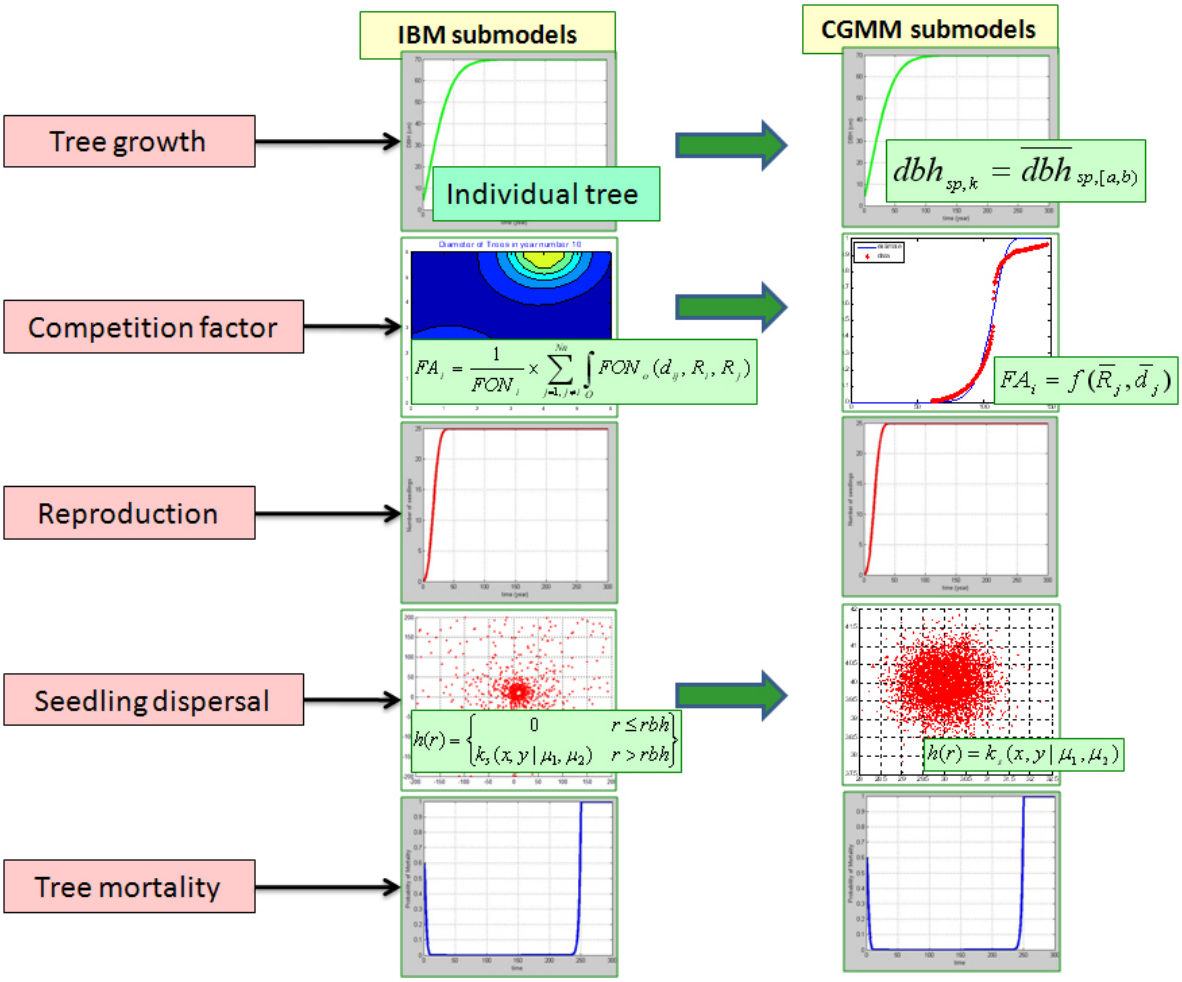

Figure 4.2.: *Submodels of CGMM, they are developed from the submodels of IBM.*

CGMM implements 3 submodels from IBM (growth, reproduction and mortality). The differences here are the granularity of the entities being simulated. Instead of applying for individual tree as in IBM, in CGMM it is applied for each *dbh* class. From the spatial aspect, if the trees in IBM are expressed by the plane coordinates, in CGMM they are the populations in the cells (stands) which belong to the geographic coordination system.

The module *'Competition factor'* in CGMM is constructed base on a derived function from average summarization over many replicates of IBM (it will be discussed in section 4.2). The module seedling dispersal in CGMM does not take into account the Hard-core process as in IBM (Fig. 4.2).

4.2. The up-scaling approach from IBM to construct CGMM

Up-scaling from lower scales can corroborate existing models, yield reliable forcast models and enhance ecological understanding by identifying relevant source scale processes and explaining how target scale phenomena are constituted from source scale mechanisms (Lischke et al., 2007). Model up-scaling techniques are usually based on hierarchy theory which consists of these processes: (i) aggregating source scale variables to target scale variables and (ii) deriving the target scale model functions

$$Y_s(\Xi) = M\left[\Xi(y_s(x), y_d(x))\right] + \Delta \tag{4.1}$$

$Y_s(\Xi)$ is the target scale function of the state variable s of one specific realization Ξ, M is the aggregated function which describes the ideal up-scaled model (in practice, M is the statistical model extracted from many simulations from a source scale model), $y_s(x)$ and $y_d(x)$ are the state and driving variables from the source scale model, x is the scaling variable and Δ is the mathematically tractable error during the up-scaling process.

The Equation (4.1) shows that at source scale, the specific realization Ξ depends on state and driving variables and also depends on scaling variable x (i.e. coordinates). The target scale function $Y_s(\Xi)$ is extracted by the process of transformation to get the aggregated function M.

The ***scale*** that we mention here are grain (or resolution) and extent (or size). The purpose of the up-scaling is to yield a simplified model in a controlled way in order to decrease simulation times or to decrease the complexity of the model. The source scale for the aggregation is the IBM. In IBM, spatial interactions and species structures are taken into account by stochastically simulating establishment, growth, competition and death of individual trees of different species in a stand. The outputs are the summation of the state variables of the simulated individuals (density, *dbh*, height, biomass). The derived functions for CGMM are obtained by the process of averaging summarization over many replicates of IBM (see Table 4.2).

The following transferring processes are applied

- Aggregating the size (*dbh*) of individuals to structured populations (*dbh* classes)
- Aggregating the spatially explicit state varialbe of competition factor (FA) to the target scale function (as will be discussed below)

Table 4.2.: *Processes implemented in IBM and CGMM.*

Process	**Symmbol**	**IBM**	**CGMM (LBM)**
Growth	dbh, H	Individual tree	Individual dbh class
Factor of tree-to-tree competition	FA	Spatial explicitness, competition between individual trees	Spatial statistics, competition between focused dbh class and other classes
Reproduction	Ns	Total number of seedlings are given by a species specific parent tree	Total number of seedlings of tree species sp at dbh class k in the cell (x, y)
Seedling dispersal	k_s	By a kernel k_s which is the bivariate normal probability density function, the seedlings are dispersed from the position of the parent tree. This process takes into account the hard-core process, a seedling can not grow inside the hard-core distance $dbh/2$ from other trees	By a kernel k_s which is the bivariate normal probability distribution, the seedlings are dispersed from the source cell to target cells
Mortality	Pm	The individual tree will die if it's mortality probability increases beyond a threshold	When the mortality probability of dbh class k increases beyond a threshold, a random number (from 1 to Nc) of trees in dbh class k of species sp will die
Level of interaction		Spatially explicit interaction among trees and between trees and the environment	Two levels of interaction: the local interaction within cell (through growth, competition, reproduction, mortality) and the spatial interaction between cells through seedling dispersal
Abiotic factors		The salinity and elevation values are the functions which are dependent on the coordinates (x, y) in the stand	The salinity and elevation are input from GIS data

- Aggregating the seedling dispersal kernel from spatially explicit positions of parent trees in IBM to the spatially explicit positions of the source cells.

4.2.1. Aggregation of individual sizes to size structured populations

In CGMM, dynamics of population densities per species and *dbh* class are implemented instead of dynamics of each individual

$$z_{sp,k} = \bar{z}_{sp,[a,b)} \tag{4.2}$$

$z_{sp,k}$ is the *dbh* class k of species sp and $\bar{z}_{sp,[a,b)}$ is the mean value of all *dbh* values that range from a to b of species sp. After each time step, the new *dbh* values will be re-classified into new *dbh* classes. This process produces a purely deterministic description of the dynamics and still reflects the size variability in the forest.

4.2.2. Process to extract the aggregated function of competition factor FA

From the Equation (3.8) in Chapter 3:

$$FA_i = \frac{1}{FON_i} \times \sum_{j=1;j\neq i}^{N_n} \int_O FON_o(d_{ij}, R_i, R_j) \tag{4.3}$$

The factor FA reflects the strength of competition of each individual tree. It is extracted by calculating the overlapped proportion $FON_o(d_{ij}, R_i, R_j)$ of focused tree i by a neighbouring tree j (the integral part $\int_O$ in the Eq. 4.3) and sum over all those values for many neighbouring trees (the summation ($\sum$) part in the Eq. 4.3). To achieve the value for this factor, these parameters must be known: (i) the distance d_{ij} between pairs of trees and (ii) the number of neighbouring trees N_n.

The purpose of up-scaling approach we apply here is to extract a simpler function for calculating FA because the integral part in Eq. (4.3) consumes computing time and especially for an aggregate model we do not have the exact positions of trees.

To do that, first, consider the case a focused tree has just one neighbour (case of one neighbouring tree), thus, the summation $\sum$ in Eq. 4.3 is omitted. The spatial distance among individual trees can be extracted by means of spatial point statistics in which we assume the trees distributed uniformly in the stand and the distance among nearest trees is the mean distance $\bar{d}$. Equation 4.3 becomes:

$$FA_i = \frac{1}{FON_i} \times \int_O FON_o(\bar{d}, R_i, R_j) \tag{4.4}$$

The value of FA of focused tree i is now dependent on the size of zone of influence (R) of itself and of the neighbouring tree j. We measure the values of FA of focused tree i in turn with each other neighbouring tree R_j in the plot and doing that many times for all trees in the plot: keep the focused tree and change R_j of the neighbouring tree. Then values of FA of the focused tree is the sequence of dissimilarities for different R_j values of the neighbouring

tree. The sub-model *'Competition factor'* of IBM is employed to do this job. The followings are conducted (under the assumption that trees are located uniformly):

- Choose some data plots, each plot must have different number of trees from other plots
- Calculate the average distance among trees by $dist = 0.5 \times \sqrt{\frac{Scell}{N}}$, where $Scell$ is the area of the plot (stand) and N is the total number of trees in the plot
- Choose a focused tree (we choose three representative focused trees in each plot: the smallest tree, the medium size tree and the largest tree) to calculate FA in turn with each R of other trees in the plot (by sub-module of IBM) as in Eq. (4.4)
- Plot the distribution of FAs of this focused tree against the range of R's values of other neighbouring trees (Fig. 4.3 from (a) to (d))
- Extract the curve for this distribution (the results are shown in Equations from 4.8 to 4.11)

Equation (4.4) now has form (case of a focused tree has only one neighbour):

$$FA_i = f(R_j, \bar{d}) \tag{4.5}$$

The next step is considering the number of neighbouring trees (the summation part in Eq. (4.3)). For the aggregate model, we cannot know this value N_n. Thus, we apply the **mean-field approach** which means applying the model to the average variables. Instead of calculating FA value of a focused tree base on the number of neighbouring trees as in IBM, we calculate FA of a *dbh* class by averaging other *dbh* classes. It means that the summation (in Eq. (4.3)) from N_n neighbouring trees now becomes one neighbouring tree with the averaged size

$$FA_i = f(\bar{R}_j, \bar{d}) \tag{4.6}$$

where $\bar{R}_j$ is the mean value of R_j of all other *dbh* classes ($j \neq k$) and is expressed as follow:

$$\bar{R}_j = \frac{\sum_{N_n} R_j}{N_n} \tag{4.7}$$

Figure 4.3 shows the step-by-step results of the order of this up-scaling approach. Figures from 4.3 (a) to 4.3 (d) are the examples of distributions of FA values of a focused *dbh* class against different neighbouring *dbh* class. The extracted equations have the forms as in Equations from 4.8 to 4.11.

Figures from 4.3 (e) and 4.3 (f) are the fitted curves for R_{thr} and $\gamma 1$. After each estimation for the curve of FA, we plot the value of R_{thr} against the mean distance $\bar{d}$ and the value of $\gamma 1$ against $\bar{R}_i$, then we extract the forms of the curves as shown in Eq. (4.9) and Eq. (4.11).

Result

$$FA_i = 1 - exp\left[-(\frac{\bar{R}_j}{R_{thr}})^{\gamma 1}\right] \tag{4.8}$$

$$R_{thr} = a_3 + c_3 \cdot dist \tag{4.9}$$

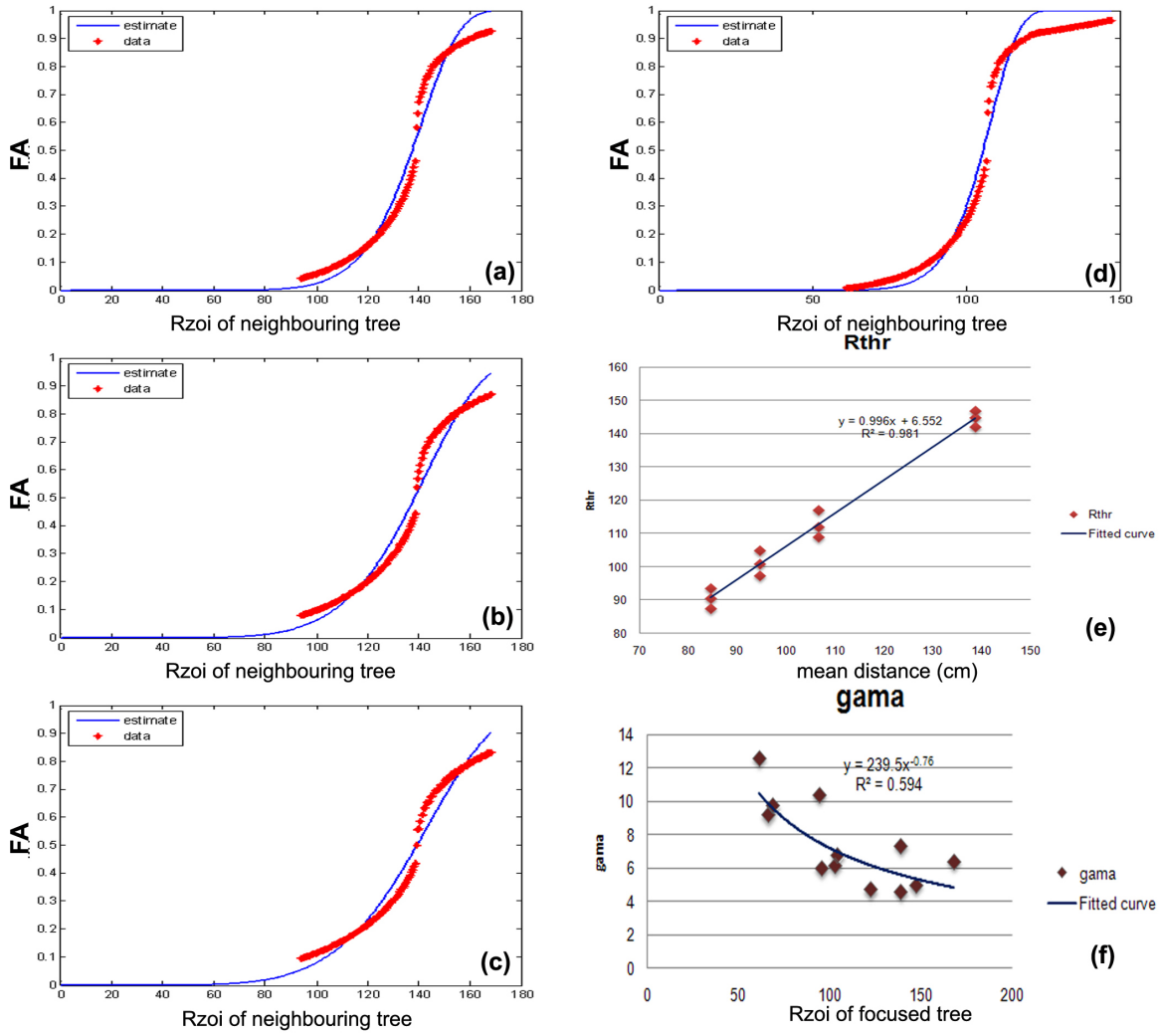

Figure 4.3.: *Examples of fitted curves of simulated FA from focused trees against different neighbouring trees.*

where a_3 and c_3 are extracted as shown in Fig. 4.3 (e).

$$dist = 0.5 \times \sqrt{\frac{Scell}{N}} \tag{4.10}$$

$$\gamma 1 = a_4 \cdot R_i^{c_4} \tag{4.11}$$

The values of parameters of Equations (4.8 to 4.11) are shown in Fig. 4.3 (e) and 4.3 (f) and in Table C.6 in the Appendix C.

4.2.3. Seedling dispersal

In the up-scaled model CGMM, the dispersal of seedlings are not from each parent tree but from each source cell (stand). The 'Hard-core' distance which was applied for seedling dispersal in IBM is not applied for this of up-scaled model.

The number of seedlings an individual tree produces in IBM: (from Eq. (3.12)):

$$\frac{dN2}{dt} = r_2 \cdot fRep \cdot Biom \cdot (1 - \frac{N2}{N2_{max}}) \tag{4.12}$$

In CGMM, $N2$ in a source cell (x, y) is the summation of seedlings produced by *dbh* class k of species *sp*:

$$\frac{dN2_{sp,(x,y)}}{dt} = \sum_k r_2 \cdot fRep \cdot Biom_{k,sp,(x,y)} \cdot (1 - \frac{N2_{k,sp,(x,y)}}{N2_{max,sp}}) \tag{4.13}$$

(x, y) is the element cell of a matrix of cells, each cell in the matrix has an attribute data of geographic coordinates (lat, lon),
$fRep$ is switching function for reproduction and is given by Eq. (3.13),
$Biom_{k,sp,(x,y)}$ is biomass values of species *sp* at *dbh* class k and is given by Eq. (3.14),
$N2_{k,sp,(x,y)}$ is the number of seedlings produced by *dbh* class k of species *sp* in the cell (x, y) and
$N2_{max,sp}$ is the maximum number of seedlings a species can produce.

The number of seedlings $N2_{sp,(x,y)}$ produces by the source cell (x, y) with coordinates (lat, lon) will disperse. Considering the target cell (x', y'), seedlings of species *sp* are dispersed into target cell (x', y') from source cell (x, y) at time t:

$$Ns_{sp,(x',y'),t} = \sum_{(x,y)} N2_{sp,(x,y),t} \times P(x', y'|x, y) \tag{4.14}$$

where $P(x', y'|x, y)$ is the probability, that a seedling produced at source cell (x, y) will enter the target cell (x', y'). This probability is derived from a bivariate normal distribution dispersal kernel $k_s(x', y'|x, y)$

$$k_s(x', y'|x, y) = \frac{1}{2\pi \cdot \sigma_1 \cdot \sigma_2 \sqrt{1 - \rho^2}} exp\left[-\frac{1}{2(1-\rho^2)} \cdot \left(\frac{(x'-x)^2}{\sigma_1^2} - \frac{2\rho(x'-x)(y'-y)}{\sigma_1 \cdot \sigma_2} + \frac{(y'-y)^2}{\sigma_2^2}\right)\right] \tag{4.15}$$

4.3. Dynamic processes implemented in CGMM

4.3.1. Tree life cycle

CGMM consists of a set of coupled different equations that describe the tree life cycle: initilization - growth - reproduction - mortality.
At the beginning, the first number of initialized seedlings in cell (x, y) is

$$N_{(x,y),t=1} = \sum_{sp}(N1_{sp,(x,y),t} + Ns_{sp,(x,y),t} - Nd_{sp,(x,y),t}) \tag{4.16}$$

where
N is total number of seedlings added to the stand (x, y),
$N1$ is the number of seedlings that come from the recruitment and is input from GIS data,
Ns as in Eq. (4.14) is the number of seedlings that come from reproduction,
Nd as in Eq. (4.19) is the number of seedlings that die,
x and y are the coordinates of the cell in the matrix,
sp is the species and
t is time.

Growth

$$\frac{dz_{sp,k,(x,y)}}{dt} = f(z_{sp,k,(x,y)}) \prod_i g_i(z_{sp,k,(x,y)}, e_{i,(x,y)}) \tag{4.17}$$

where
$f(z_{sp,k,(x,y)})$ denotes the growth rate under optimal condition and $z_{sp,k,(x,y)}$ the breast height diameter (dbh) of species sp at dbh class k in the cell (x, y). The multipliers g_i denote the influence of driving variables $e_{i,(x,y)}$ on the growth rate. They are normalized to one.

Reproduction

The number of seedlings that are produced by trees of dbh class k of species sp depends on the biomass of tree at that dbh level (Eq. 4.13)

$$\frac{dN2_{sp,(x,y)}}{dt} = \sum_k f(N2_{sp,k,(x,y)}, Biom_{sp,k,(x,y)}) \tag{4.18}$$

where $Biom_{sp,k,(x,y)} = a_1 \cdot dbh^{c_1}$ as in Eq. (3.14) is biomass value of tree of dbh class k of species sp in the cell (x, y).

Mortality

The total number of fatalities (adult trees or seedlings) $Nd_{sp,(x,y),t}$ of species sp in the cell (x, y) at time t is defined as the number of *'inflow'* of trees of species sp at dbh class k in the cell (x, y) multiplied by the mortality probability $Pm_{sp,k,(x,y),t}$

$$Nd_{sp,(x,y),t} = \sum_k (N1_{sp,k,(x,y),t} + Ns_{sp,k,(x,y),t}) \times Pm_{sp,k,(x,y),t} \tag{4.19}$$

where $Pm_{sp,k,(x,y),t}$ was shown in Eq.(3.20).

4.3.2. Local interaction

CGMM takes into account within-cell (x, y) heterogeneity through the local interaction includes (we omit the indices (x, y) in the below equations):

Different *dbh* classes in one stand The accrued diameter increment is updated each time step (one year). When the averaged accrued and computed diameter increment exceeds the size-class interval, the new size-class is determined, the stems are transferred to the new size class.

The competition among trees The competition among trees is expressed by the competition factor FA:

$$FA_{k,t} = 1 - exp\left[-(\bar{R}_{j\neq k,t}/X_{thr})^{\gamma}\right] \tag{4.20}$$

$$X_{thr} = f(dist) \tag{4.21}$$

$$\gamma = f(R_{k,t}) \tag{4.22}$$

$\bar{R}_{j\neq k,t}$ is the mean value of the zone of influence of the *dbh* class $j \neq k$ and k is the focused *dbh* class,
X_{thr} is the threshold value of $\bar{R}_{j\neq k,t}$ and is dependent on the mean distance among trees $dist$ which is the function of total number of trees in the cell and the area of the cell $(dist = 0.5 \times \sqrt{\frac{Scell}{N_t}})$,
γ is the form value that determines the steepness of the curve of $FA_{k,t}$ and is dependent on the zone of influence $R_{k,t}$ of the focused *dbh* class k.

The equations (4.20 to 4.22) are extracted from the simulations of IBM. We try to take into account the spatial interaction among trees through a statistical based method and summerize into the equations.

4.3.3. Spatial interaction

The cells in the model interact through seed dispersal. The number of seedlings $Ns_{(x,y),t}$ enter the cell (x, y) at time t is the summation of all seedlings from cell (x, y) and from other cells multiplied by the probability $P(x, y)$ as described by Equation (4.14).

4.4. Modelling CanGio Mangrove Forest Dynamics using CGMM

We apply the model to simulate some scenarios to test the model's ability to form the patterns in different situations. The area that we apply the simulation is located in the South-West of CanGio District (Fig. 4.4 (d)). The starting time for our simulation was in 1970, this is a gap time when nearly all the trees in this forest were destroyed (see the NDVI map in 1973 in Fig. 4.4 (a)). The Normalized Difference Vegetation Index (NDVI) as will be described in the next chapter is an index that expresses the "greenness", values of NDVI in a dense vegetation canopy will tend to positive values (around 0.3 to 1). NDVI map in 1973 in this

area (Fig. 4.4 (a)) shows that vegetation this year was poorly covered.

Topography (Fig. 4.4 (b)) is rather flat, ranges from 0 to 1.8 m. Mean salinity during the year ranges from 24 *ppt* to 30 *ppt* (Fig. 4.4 (c)).

Dominant species in this area are *Avicennia alba* and *Rhizophora apiculata* in which *Avicennia alba* was naturally regenerated (we assume they started to be regenerated in 1973 because from the image in 1973, this area still had very little green cover). *Rhizophora apiculata* was planted in 1982 in this area, *Phoenix paludosa* occupied naturally on the land which has elevation is higher than 1.5 m.

We apply three scenarios for our simulations. The first scenario is the stable environmental conditions and the next two scenarios are sea level changes. Following Nguyen (2009), climate would significantly change over all regions in Vietnam, especially in the South of Vietnam. By the end of the 21^{th} century, sea level is expected about 65 to 100 cm higher compared to the average 1980 - 1999. We apply the two scenarios of sea level changes in the simulations, one is 65 cm and one is 100 cm (see Fig. 4.5).

The simulations are run for 131 years (from 1970 to 2100) on a grid consisting 342×141 cells of 30 m length. Totally there are 4384 ha of forest are simulated.

Figure 4.6 shows the distribution of mangrove species. Series (a) are the simulated results from the scenario of stable condition. Series (b) are the simulated results from the scenario of sea level increases 65 cm. Series (c) are the simulated results from the scenario of sea level increases 100 cm.

Figure 4.7 shows the distribution of total biomass in the simulated area. Series (a) are the simulated results from the scenario of stable condition. Series (b) are the simulated results from the scenario of sea level increases 65 cm. Series (c) are the simulated results from the scenario of sea level increases 100 cm.

Figures 4.8 and 4.9 show the biomass values and species composition following time, they are the results from the simulations of the stable environment.

Figures 4.10 and 4.11 show the biomass values and species composition following time, they are the results from the simulations of the scenario of sea level increases 65 cm.

Figures 4.12 and 4.13 show the biomass values and species composition following time, they are the results from the simulations of the scenario of sea level increases 100 cm.

Result For the stable condition scenario, *R.apiculata* shows the trend of increasing biomass but decreasing composition, *A.alba* shows the trend of increasing biomass and increasing composition, *P.paludosa* shows the decreasing trend in both factors.

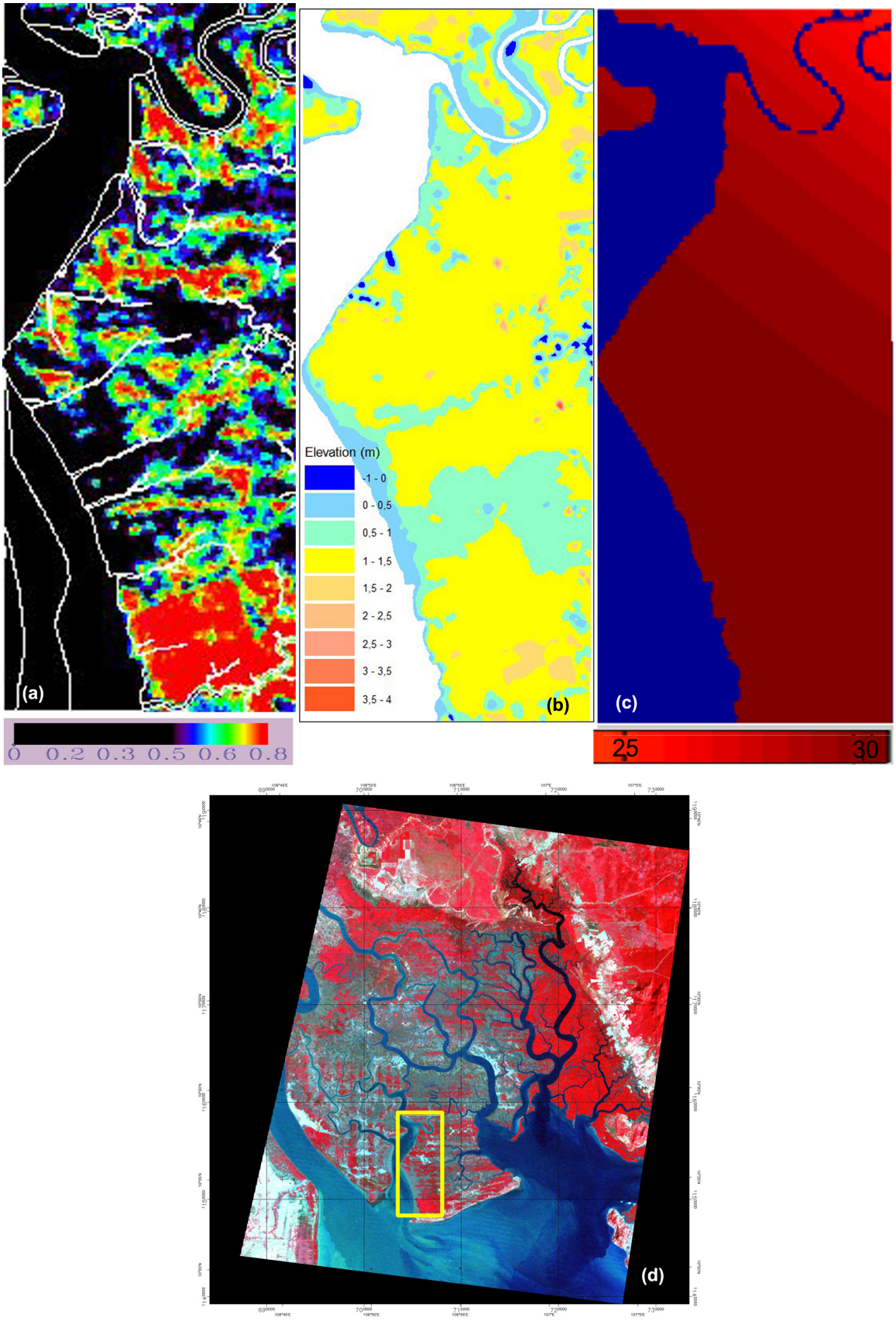

Figure 4.4.: *Maps of simulated area. Fig. (a) is NDVI map from Landsat MSS imagery. Salinity and elevation maps are in Fig. (b) and Fig. (c). Salinity in the simulated area ranges from 25 to 30 (ppt), elevation is rather flat and ranges from 0 to 1.5 (m). Fig. (d) is Landsat MSS image in 1973, the red color denotes the vegetation cover.*

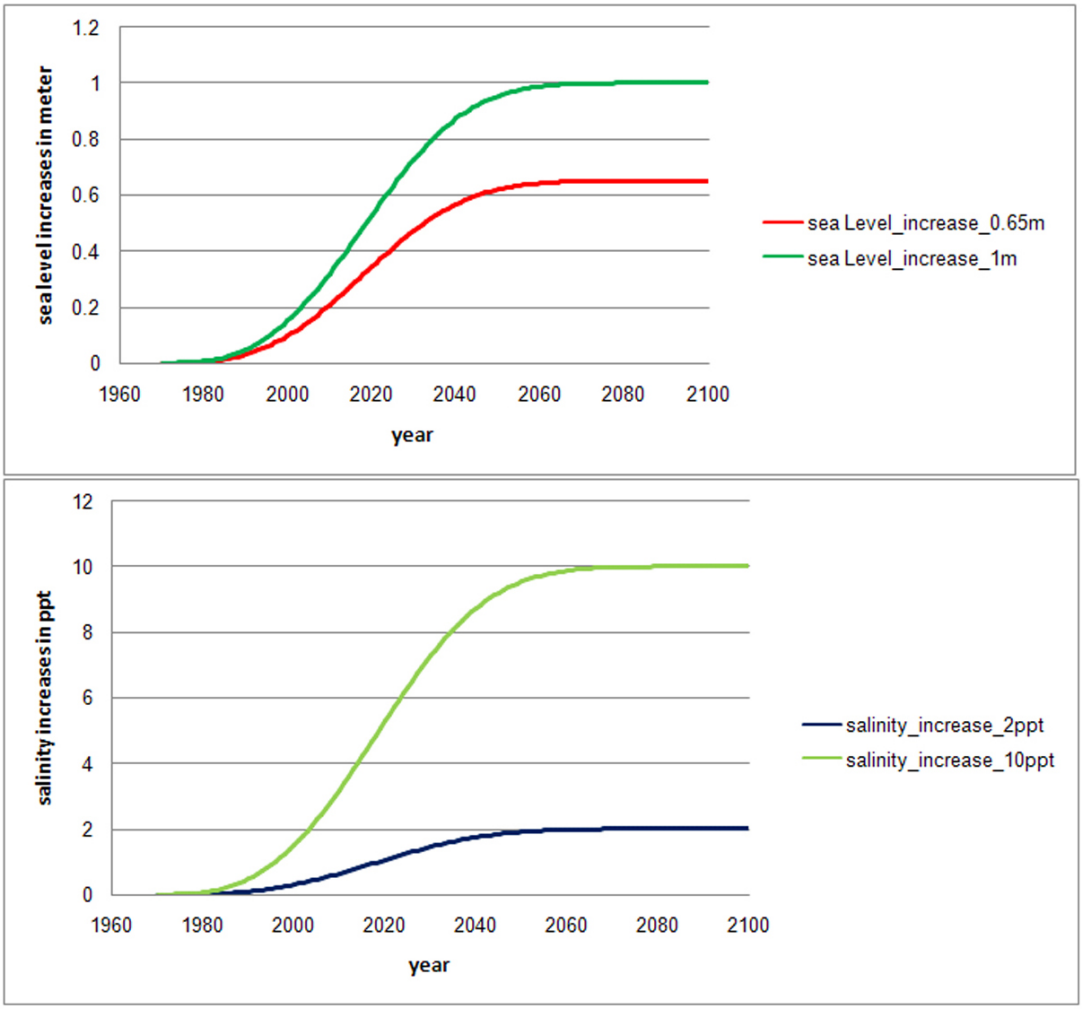

Figure 4.5.: *Two scenarios of sea level rise and salinity rise. The first scenario is sea level increases 65 cm and salinity increases 2 ppt by the end of 2100. The second is 100 cm of sea level increasing and 10 ppt of salinity increasing.*

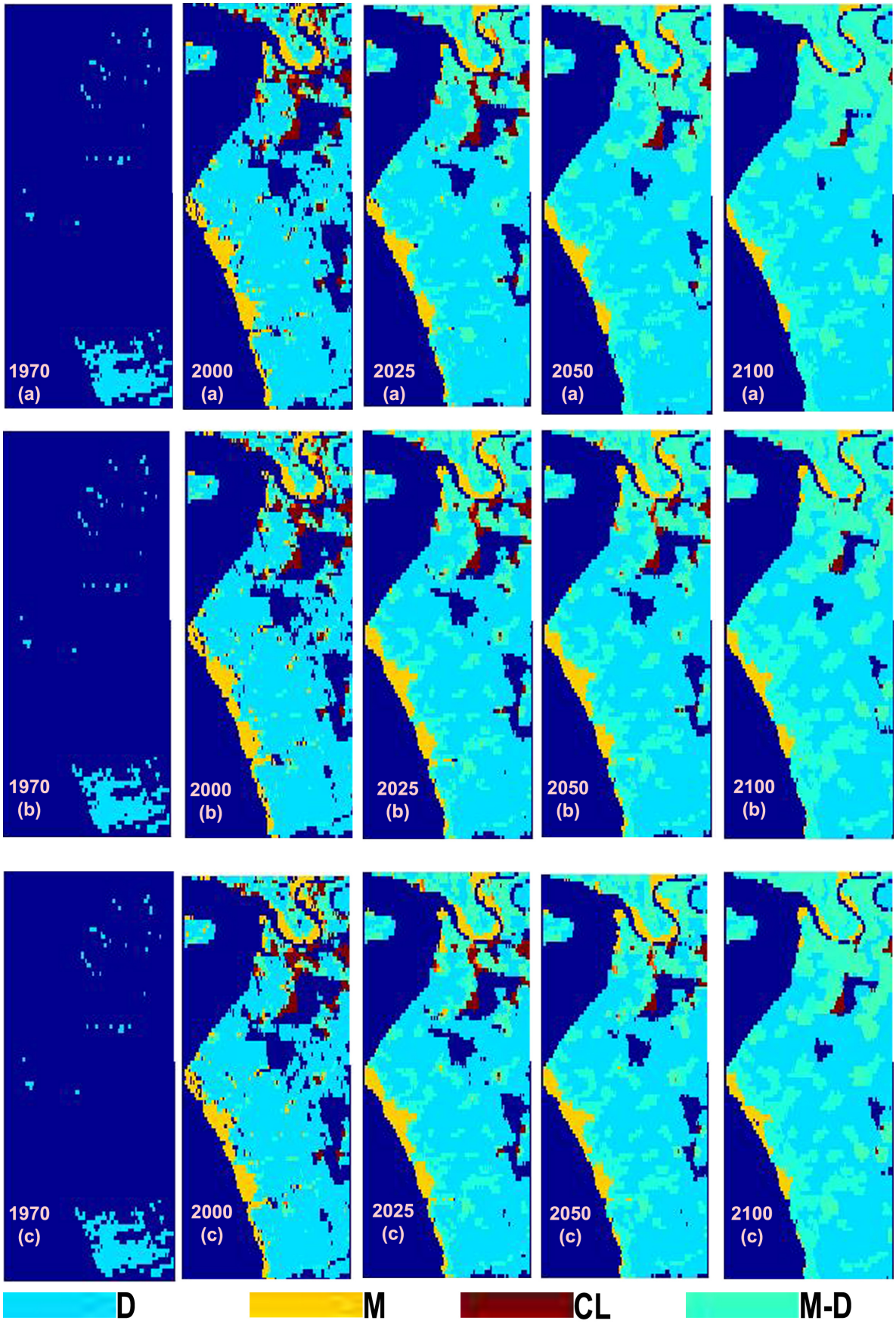

Figure 4.6.: *Species distribution resulted from simulations of three scenarios. Symbol 'D' denotes R.apiculata, symbol 'M' denotes A.alba, symbol 'CL' denotes P.paludosa, symbol 'M-D' denotes A.alba and R.apiculata.*

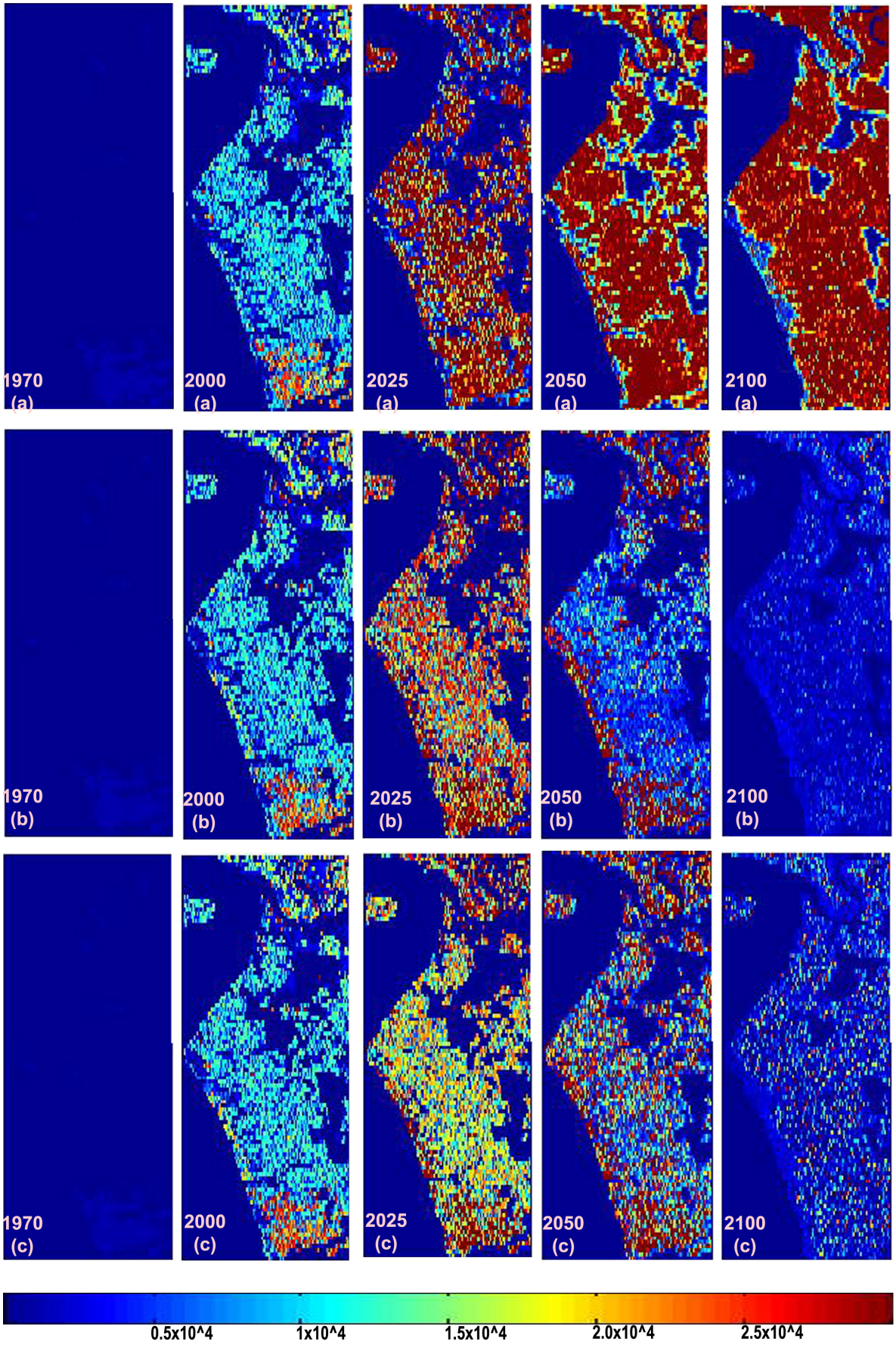

Figure 4.7.: *Biomass ($kg/900m^2$) distribution resulted from simulations of three scenarios.*

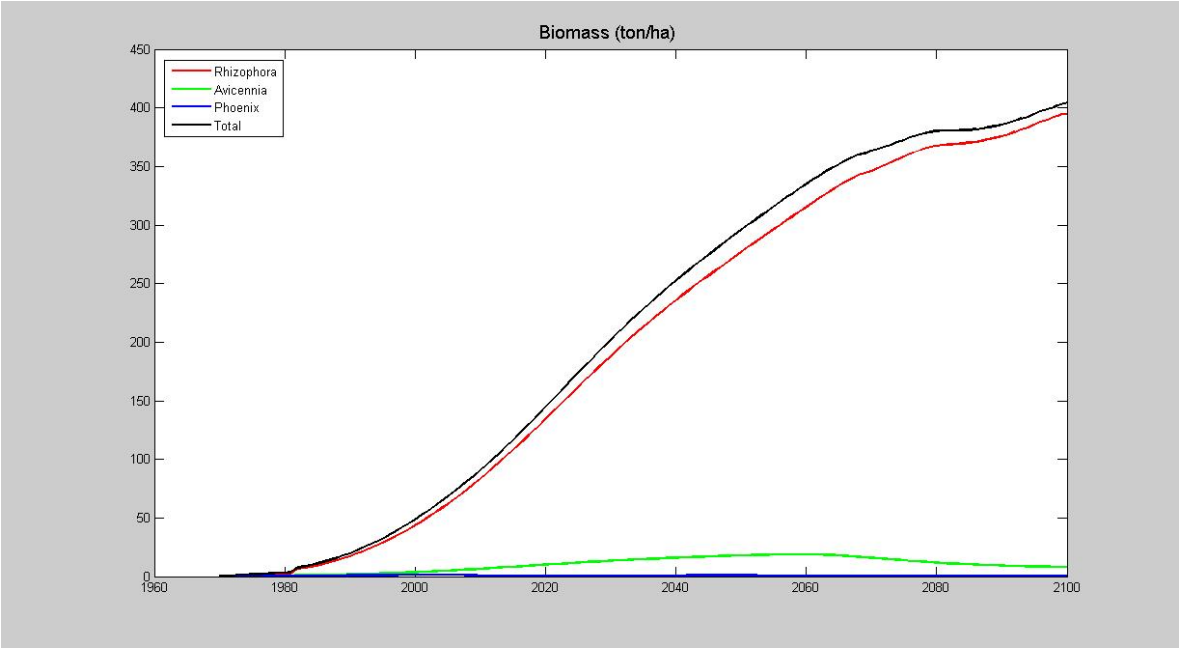

Figure 4.8.: *Time course of biomass resulted from the simulations of stable environmental condition.*

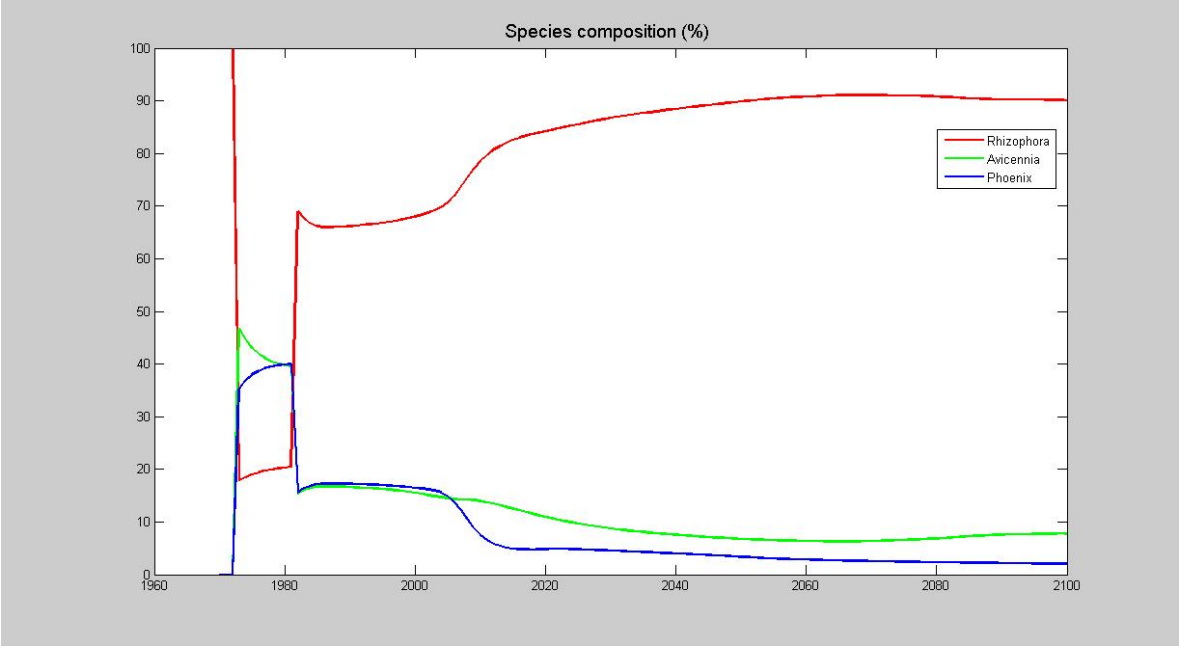

Figure 4.9.: *Time course of species composition resulted from the simulations of stable environmental condition.*

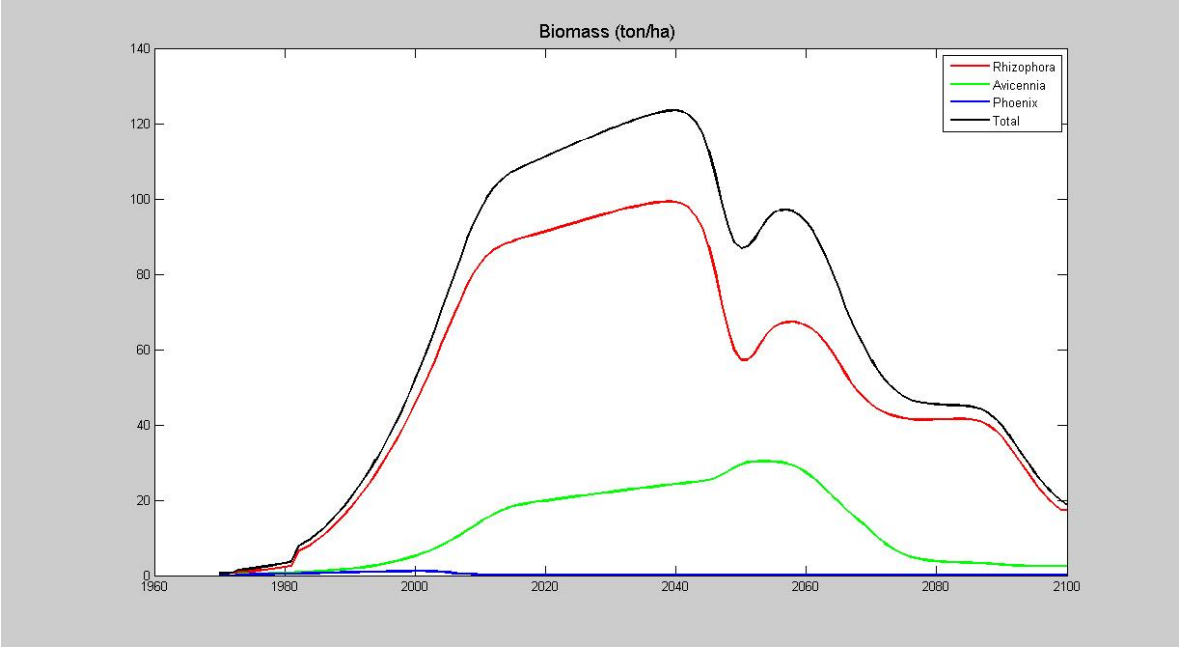

Figure 4.10.: *Time course of biomass resulted from the simulations of the sea level increase 65 cm scenario.*

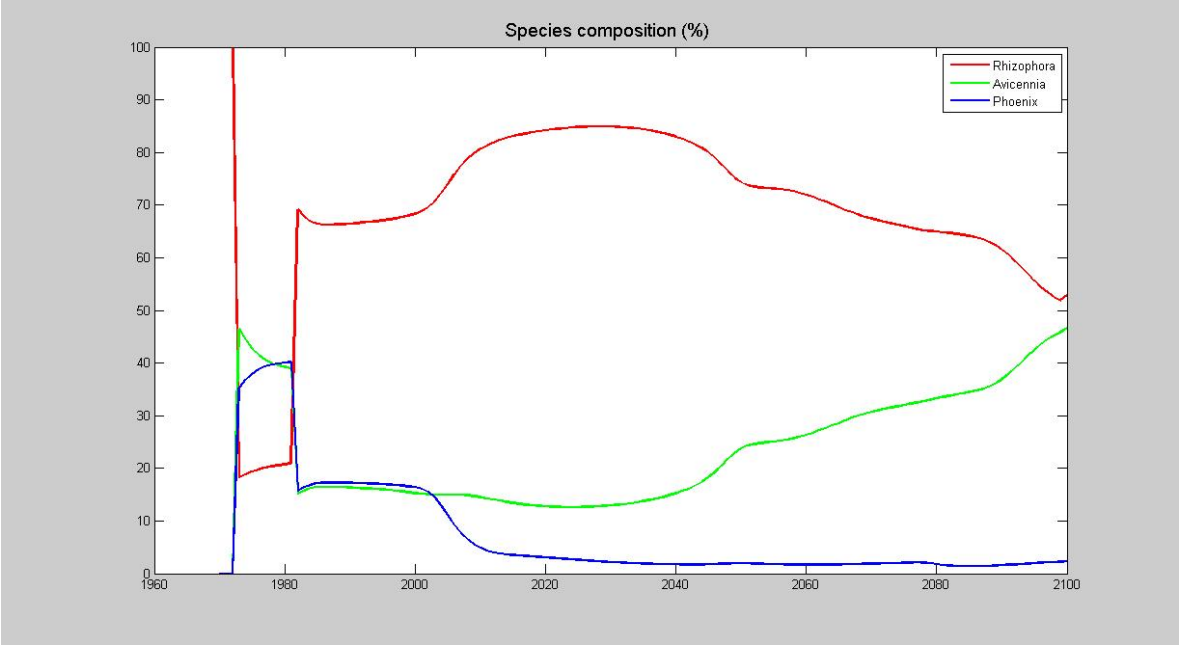

Figure 4.11.: *Time course of species composition resulted from the simulations of the sea level increase 65 cm scenario.*

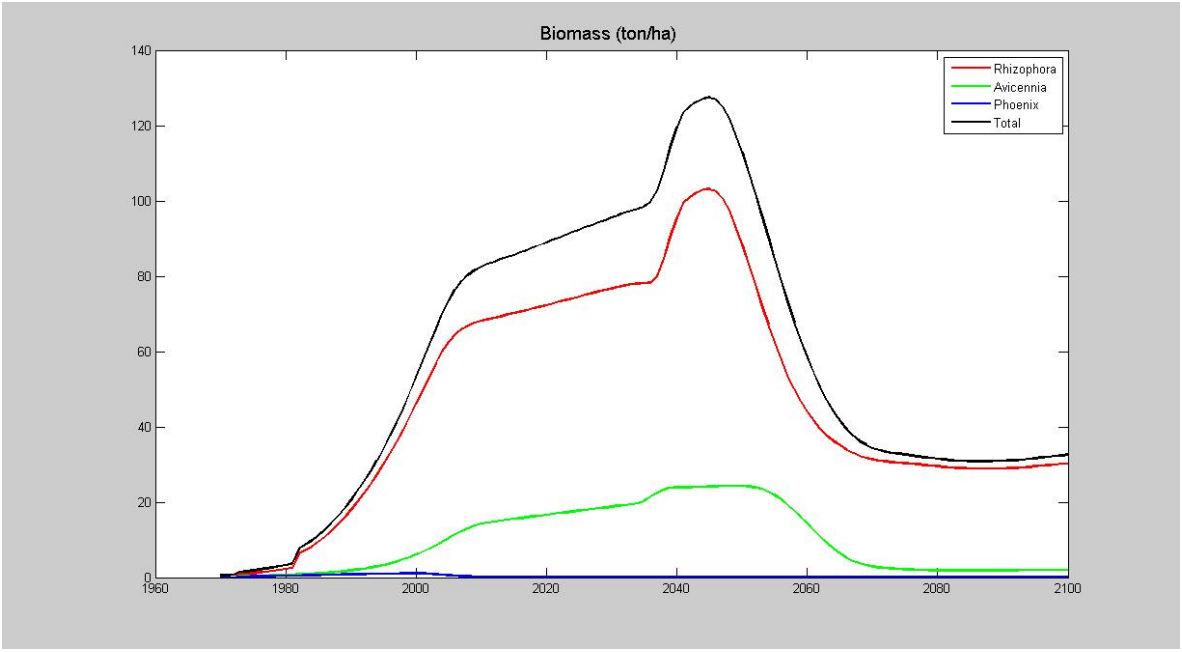

Figure 4.12.: *Time course of biomass resulted from the simulations of the sea level increase 100 cm scenario.*

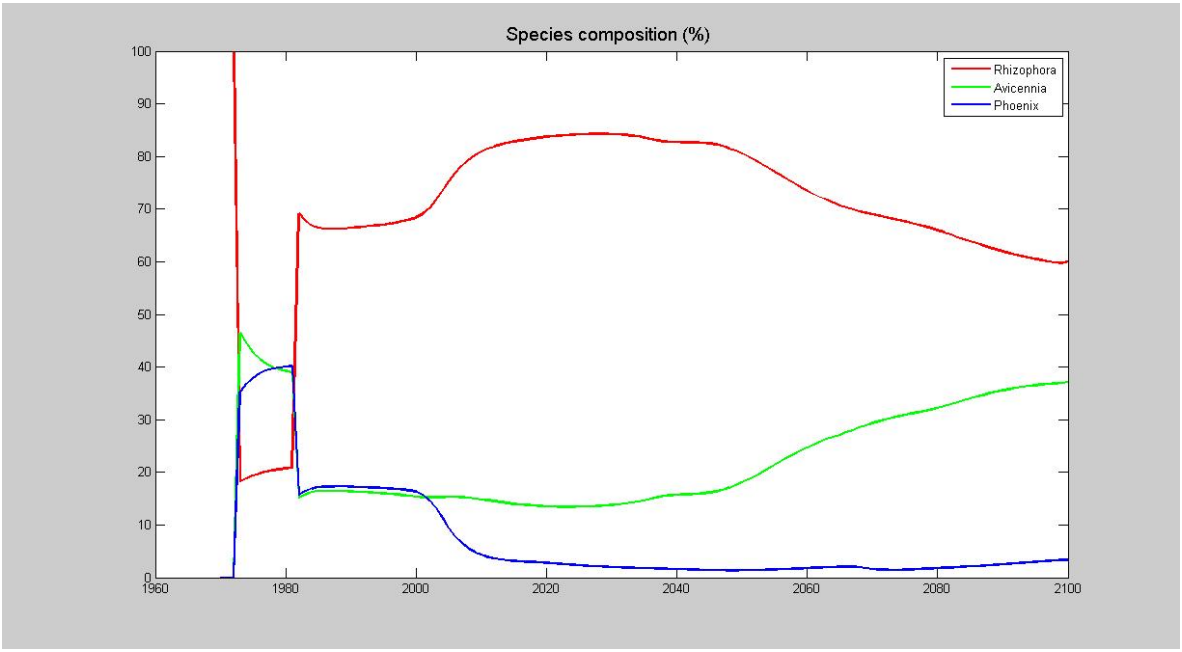

Figure 4.13.: *Time course of species composition resulted from the simulations of the sea level increase 100 cm scenario.*

For the scenario of sea level increases 65 cm, biomass of all three species decreases after 131 years. However, biomass of *A.alba* remains rather stable in the last phase (from 2080 to 2010). Species composition of *A.alba* increases while the other two species show the decreasing trend.

For the scenario of sea level increases 100 cm, biomass and composition of *R.apiculata* and *A.alba* decrease strongly for a period (15 years, from 2045 to 2070, Figs. 4.12 and 4.13) then remain rather stable in the last phase from 2070 to 2100. In this scenario, *R.apiculata* shows the stronger ability of survival than *A.alba*.

4.5. CGMM validation

The simulated results of the stable environmental condition (6 years as equivalent to satellite images) are compared to the NDVI values of satellite images. NDVI images were calculated to achieve the sequence of mangrove changes in the study area. Six satellite images are processed (geo-correction and radiant calibration) to extract NDVI values (Figure 4.14). Since NDVI values represent a normalized ratio of reflected visible and near-infrared energy as expressed by the following equation, it is used for analysis of vegetation monitoring.

$$NDVI = (NIR - RED)/(NIR + RED) \tag{4.23}$$

where NIR denotes near-infrared energy and RED represents visible energy.

Correlation between mean NDVI and simulated biomass is shown in Fig. 4.15. It shows a rather correlate relationship with $R^2 = 0.663$ for linear relationship and $R^2 = 0.745$ for polynormial relationship.

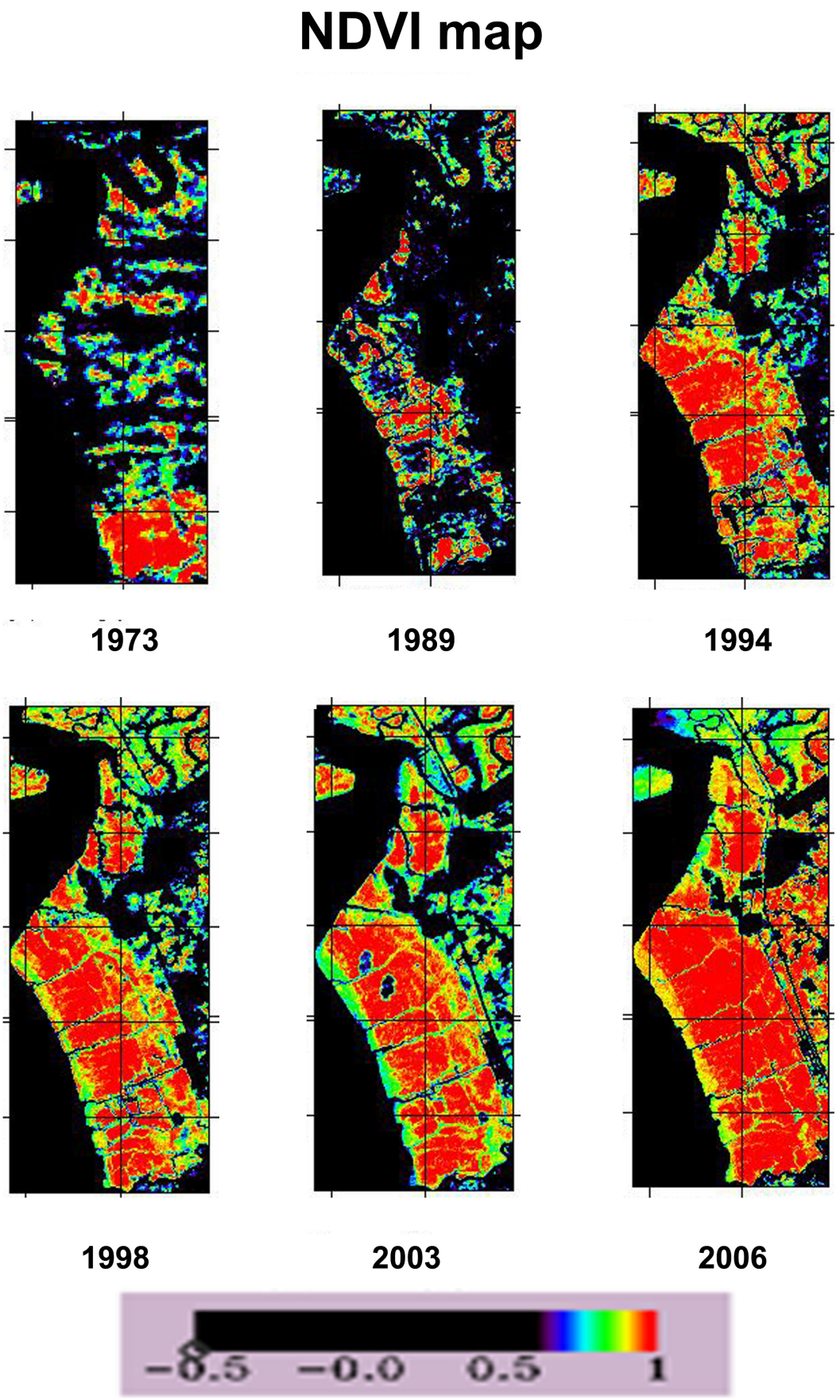

Figure 4.14.: *NDVI images of the study area.*

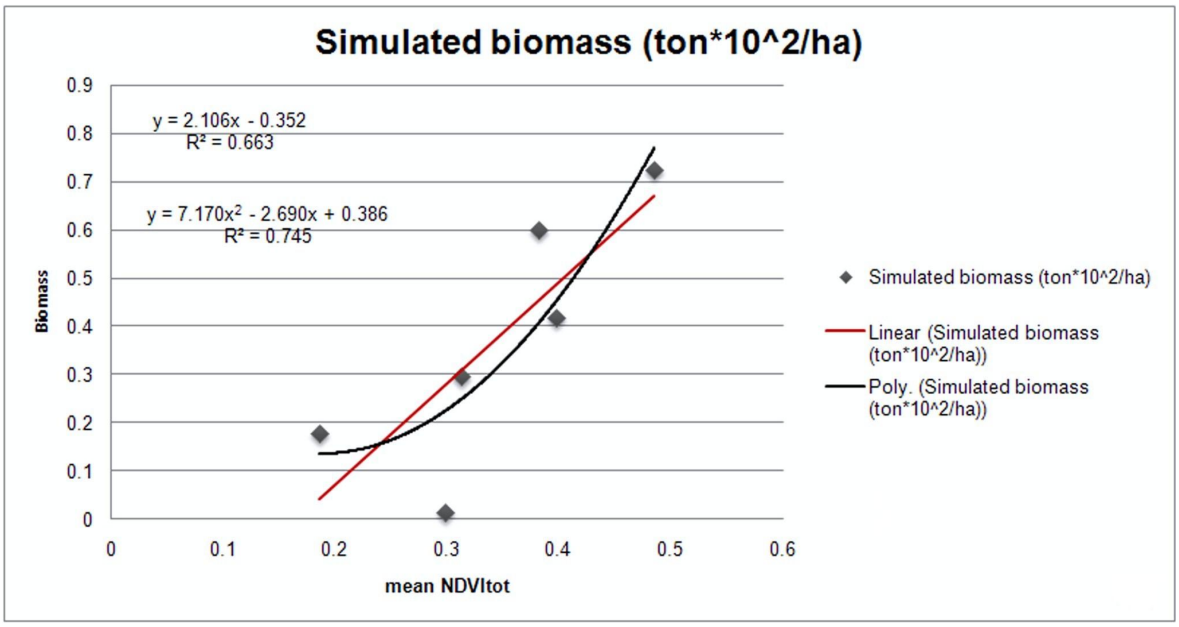

Figure 4.15.: *Correlation between mean NDVI values and mean simulated biomass values.*

5. Proposing a coupled model for mangrove modelling

5.1. Limitations of ecological models

Accuracy of ecological models Ecological models have become effective tools for supporting the managers in managing the natural resources and ecosystems, because they embedded the driving mechanisms that influence the ecological processes. Individual based models can account for the feedback between stand structure and individual growth while landscape based models supply the ecological succession in the context of expanding to the landscapes. The more the accuracy of model predictions, the more the support for decision making process of the managers.

A model however, is just a special situation that allows us to test a theory or an assumption. Models do not represent all possible real world cases. We can only understand to a certain degree, we can not cover all aspects. Since a thorough and comprehensive understanding about the complex mechanisms which cause the dynamics of the ecosystems, from which we can formularize and create a model, is a difficult task.

Difficulty in the parameter estimation Ecological models generally have many parameters, multiple outputs of interest and a small underlying empirical database. Parameter estimation for ecological models is also a major obstacle especially when dealing with the data of long term complicated processes of the forest. Because in forest ecology it is not feasible to apply the designed and controlled experiments as what we can do in the laboratory. Thus, reliability in explaining the complicated ecological processes by mathematical models is still a question. When choosing a model for a certain application, it is important to consider its ability to parameterize from the data so that it could correctly simulate the desired scenarios.

Difficulty in the measuring, monitoring and data collection Data obtaining in ecology is another difficult problem. Field inventory for species discrimination, map interpretation, collateral and ancillary data analysis, ... are not effective to acquire because they require intensive field work and are time consuming.

5.2. Another approach for obtaining data: Remotely sensed data

There have been a large number of studies and applications of remote sensing in monitoring, assessing the changes and distribution of forests, in general, and mangrove forests, in particular. The technology of remote sensing offers a practical and economical means to study vegetation cover changes, especially over large areas.

Kuenzer et al. (2011) reviewed in detail a large numbers of studies which applied remote sensing in monitoring and mapping mangroves during the last 20 years. More than 100 publications were reviewed. Following that, the applications of remote sensing techniques in the detection of mangrove distribution in recent 20 years have achieved considering achievement together with the outstanding development of the remote sensors. Initiated by the applications of air photo interpretation for mapping mangrove distribution using 'visual-interpretation techniques' in the early 1990s then developed to the application of automatic interpretation method using 'unsupervised ISODATA classification'.

The first Landsat Multispectral Scanner System (MSS) launched in 1972 began the modern era of land remote sensing from space. Since then, there have been other branches of satellite imagery launched such as medium-resolution imagery, high-resolution imagery (QuickBird, IKONOS) and detailed spectral data (Airborne Hyperspectral Data). The applications of those data to mangrove interpretation started to develop in the late of 1990s with different sensors used and different methods applied (Kuenzer et al., 2011).

The rapid advancement of remote sensing technology reinforces our identification of the potential and effectiveness in using space-born data in the detection of land surface changes, including changes in mangrove ecosystems.

The feasibility of applying remote sensing in mangrove studying Compared to other types of tropical forests, mangroves have fewer species, thus the identification of different species base on remotely sensed data is simpler and easier.

Mangroves often occur in species zonation, this is also an advantage when distinguishing different mangrove species on satellite images.

Spectral reflectance of mangrove species can be detected (see Figure 5.1).

Remote sensing of mangroves provides important information for detecting:

- Extent and change of mangrove following time (Thu and Populus (2007))
- Species distribution (Hang and Anh (2002), Hirose et al. (2004), Anh (2007))
- Productivity assessment
- Prompt information supply for disaster management

5.3. Proposing a coupled model for mangrove modelling

Plummer (2000) proposed four alternative strategies in combining remotely sensed data with ecological models include: (i) to use remotely sensed data to provide estimates of variables required to drive ecological process models, (ii) to use remotely sensed data to test, validate or verify predictions of ecological process models, (iii) to use remotely sensed data to update or adjust ecological process model predictions and (iv) to use ecological process models to understand remotely sensed data. Because remote sensing can contribute the timely, up-to-date

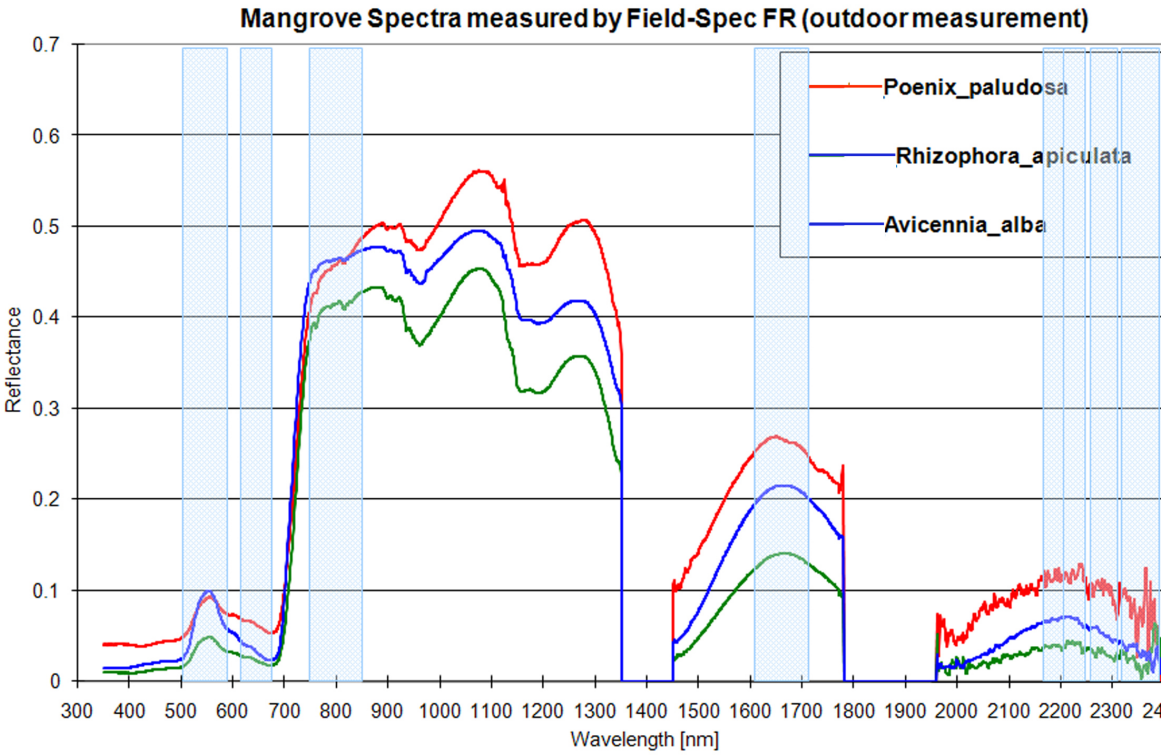

Figure 5.1.: *Spectral characteristics of 3 mangrove species (Source: ERSDAC).*

and relatively accurate information of land surfaces: surface climate, vegetation cover, vegetation structures (species and stages) and health (LAI and biomass), land use changes, and so forth. And its digital data can be easily integrated into GIS for more analysis.

The feasibility in distinguishing different mangrove species (Fig. 5.1) together with the correlation between simulated biomass values and NDVI of satellite data (as discussed in Section 4.5 of Chapter 4) demonstrate that remotely sensed data can be used in coupling with the ecological model.

We explore the changes of NDVIs from 1973 to 2006 (Fig. 5.2). NDVI changes during this period do not follow a consistent trend while our simulated reusults show this trend. Because of that, the coupling model (couple remote sensing and ecological model) will help in these aspects: (i) calibrate against information on agent history, (ii) capture progression of agents, (iii) characterize learning by memory of agents based on experience, or strong history dependence of agents.

We propose a conceptual structure of the coupling model as shown in Figure 5.3. Following this conceptual structure, field inventory data are used to estimate parameters for the IBM, they are also used as 'training data' for the steps of satellite image interpretation. The results from remote sensing imagery analysis will be used as input data for the LBM. A constructed mechanism to 'learn the data' will be developed for the LBM. This ecological model will be

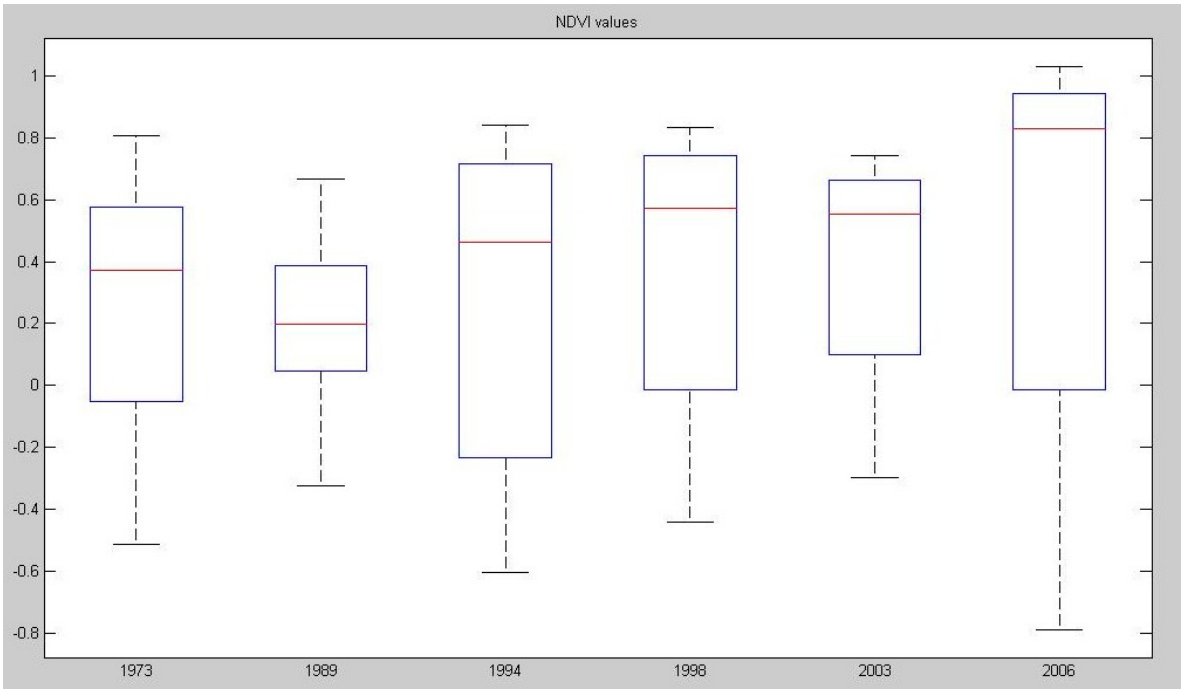

Figure 5.2.: *NDVI distribution following tiem in the study area.*

'trained' to understand the input data, then, this model will simulate and forecast future changes of ecological processes base on real input data.

5.4. Conclusion

The accuracy of ecological mathematical models is limited, because of the complexity of ecological processes which we can not fully detect. Therefore, simulation results just give the representative meaning. To achieve more accurate results, further studies need to be conducted. The coupling of remote sensing data and ecological models is a promising research direction.

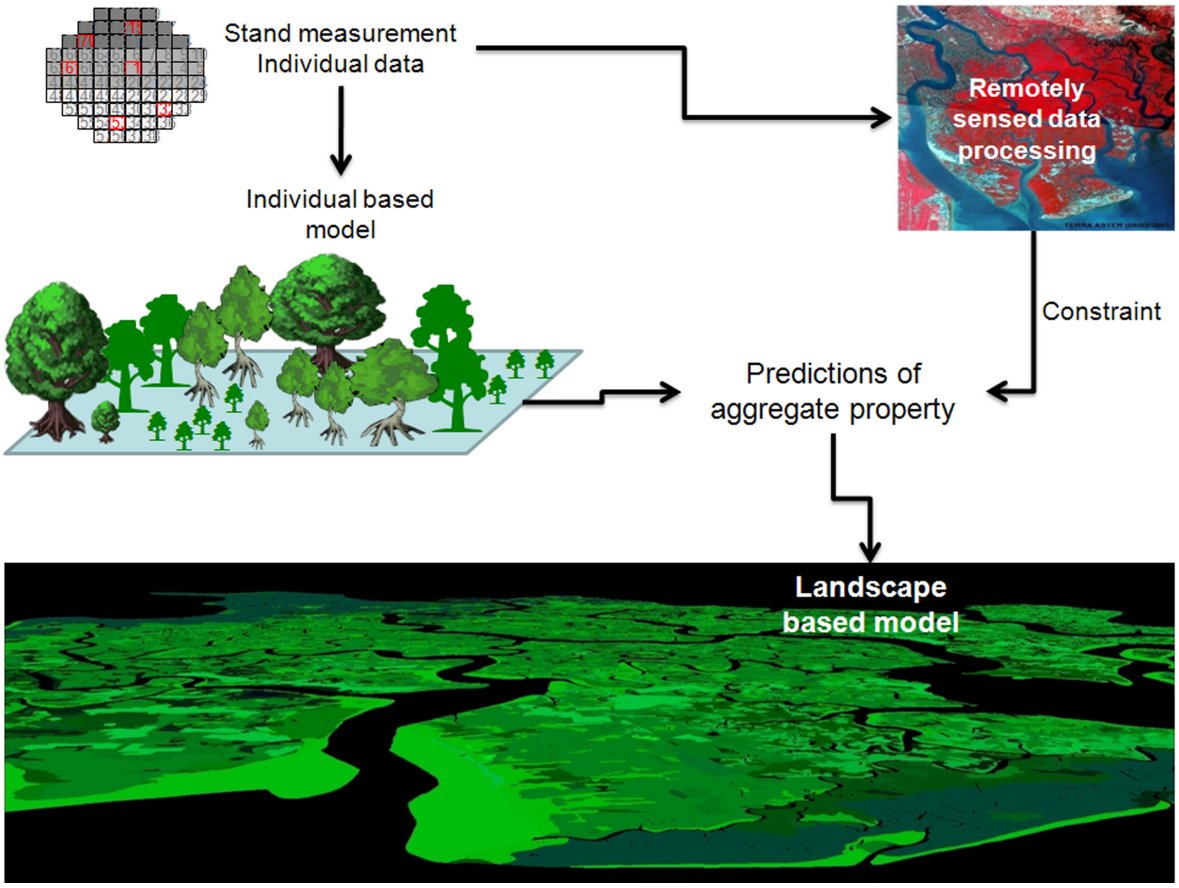

Figure 5.3.: *Conceptual structure proposed for a coupling model to predict mangrove future.*

6. Summary

The mangrove ecosystems play very important roles in coastal areas of (sub)-tropical regions and are being largely occupied with high level of stress and disturbance. However, the mangrove ecosystems management is quite a difficult undertaking because of its geographic conditions and its complex bio-geological processes.

Mathematical ecological models that simulate the underlying processes governing the growth of mangrove in dependence of environmental factors are effective tools for supporting the mangrove ecosystem management. The wide application of ecological models have proved their effectiveness. They are useful because they help to learn some about the systems they represent, and help in making decisions related to them.

Effective use of simulation modelling in the analysis of complex systems requires knowledge of key driving processes, and a means of expressing the relationships between these processes. Thus, a well-constructed model is more than simply a descriptive tool; it also possesses explanatory power through its integration of empirical work on ecological processes, and provides insight into the dynamics of complex ecological systems.

In this work, we construct the model (CGMM) by the integration from many disciplines: from applying spatial point statistics to generate artificial data to add into the data set for parameter estimation; to applying hierarchy theory to design the procedure of parameter estimation, and then to construct a larger scale model (CGMM) from a smaller scale model (the IBM).

The CGMM, which still includes the heterogeneity of simulated objects while can extent to a large spatial area, has been constructed to simulate the development of mangrove attributes under influences of environmental factors and applied to the CanGio Mangrove Biosphere Reserve in Vietnam.

CGMM simulations show encouraging results. However, for the long term, the model should integrate more other processes which affect the changes of mangrove and should be constructed to have the ability to 'learn' the input data or in another meaning, to capture progression of simulated objects.

A. Appendix A: Calculation of Multiplier from the data

$$\frac{d(dbh)}{dt} = \frac{G_{opt} \cdot dbh \cdot (1 - dbh \cdot H/D_{max}/H_{max})}{2b_1 + 3b_2 \cdot dbh - 4b_3 \cdot dbh^2} \times MUL \tag{A.1}$$

$$MUL = f_s \times f_{el} \times f_c \tag{A.2}$$

To extract MUL, first we need to extract the parameters for the optimal growth part: G_{opt}, D_{max}, H_{max}, b_1, b_2, b_3. This process was discussed in Chapter 3. Assume that we have known those parameters, then MUL is calculated as follows:

A.0.1. When we know the age of trees in a stand

Let $G = G_{opt} \times MUL$, Eq. (A.1) becomes:

$$\frac{d(dbh)}{dt} = G \cdot \frac{dbh(1 - \frac{dbh \times H}{D_{max} H_{max}})}{2b_1 + 3b_2 \cdot dbh - 4b_3 \cdot dbh^2} \tag{A.3}$$

Given (from Botkin (1993), p.33):

$$b_2 = \frac{2(H_{max} - b_1)}{D_{max}} \tag{A.4}$$

$$b_3 = \frac{(H_{max} - b_1)}{D_{max}^2} \tag{A.5}$$

and let: $a = H_{max} - b_1$, $x = ln(dbh/D_{max})$, then:

$$G = \frac{2H_{max} \times \left[\int \frac{b_1 + a(3e^x - 2e^{2x})}{a + b_1 - e^x(b_1 + a(2e^x - e^{2x}))} dx - C\right]}{t} \tag{A.6}$$

where C is an integration constant. From Eq. (A.6), we can get G from dbh and t (age of tree), then calculating MUL by G/G_{opt}

A.0.2. We don't know the age of trees, but we know the increment of dbh

dbh increment in one year ($\Delta t = 1$), under stress condition: $\Delta dbh = dbh_2 - dbh_1$ or

$$\Delta dbh = G_{opt} \times dbh_1 \times \frac{1 - (dbh_1 \cdot H_1/D_{max}/H_{max})}{2b_1 + 3b_2 \cdot dbh_1 - 4b_3 \cdot dbh_1^2} \times MUL \tag{A.7}$$

Under optimal environmental condition, MUL is equal to 1, then we have: $\Delta dbh_{opt} = dbh_{opt} - dbh_1$ or

$$\Delta dbh_{opt} = G_{opt} \times dbh_1 \times \frac{1 - (dbh_1 \cdot H_1/D_{max}/H_{max})}{2b_1 + 3b_2 \cdot dbh_1 - 4b_3 \cdot dbh_1^2} \tag{A.8}$$

divide Eq. (A.7) by Eq. (A.8), we get:

$$\frac{\Delta dbh}{\Delta dbh_{opt}} = MUL \tag{A.9}$$

B. Appendix B: Reconstruction of spatial point pattern

Data analysis of point patterns corresponds to studies where the interest lies in where events of interst occur. A fundamental question of interset in this context is whether or not the points of interest are occurring at random, or do the points cluster in some manner, or perhaps the points of interest are occurring with some sort of regularity. Moller and Waagepetersen (2007) explained some typical processes of spatial point processes. Following that, *the Poisson process* and *the Cox process* have many applications in situations where the objects (or points) are mutually independent of each other, i.e. are not interacting. In Poisson processes the points are independently distributed in space S and in Cox processes they are conditionally independent given the intensity function.

However, in many cases the analysis of a spatial point pattern focuses on the detection and characterisation of interaction among the points. This interaction is often a mutual repulsion leading to patterns of some regularity. Since many different assumptions are possible, different point process models can be formed in this way, leading to the class of *Gibbs processes* which we apply to construct the point patterns for our forest.

In our forest, we know the number of trees (points) in the stands, thus we just observe the *Gibbs processes with fixed number of points* (Illian et al. (2008), p.139).

Gibbs processes with fixed number of points Consider n points randomly distributed in S, where n is fixed. Assume that their positions are given by a multivariate probability density, the location density function

$$f_n(x_1, ..., x_n) \; for \; x_1, ..., x_n \in S \tag{B.1}$$

which does not depend on the order of the points. This multivariate density defines a point process with exactly n points in S.

Consider the location density function

$$f_n(x_1, ..., x_n) = exp\left[-\sum_{i=1}^{n-1}\sum_{j=i+1}^{n}\phi(\|x_i - x_j\|)\right]/Z_n \tag{B.2}$$

for $x_1, ..., x_n$. The function $\phi(r)$ in this formula is often called the *pair potential*, it measures the 'potential energy' caused by the interaction among pairs of points (x_i, x_j) as a function of their distance $r = \|x_i - x_j\|$.

The pair potential attains values in the range $-\infty < \phi(r) \leq \infty$ within the conventional that $exp(-\infty) = 0$. The term Z_n in (B.2) is the 'configurational partition function', a normalising

factor ensuring that (B.2) is really a probability density.

The double sum over all pairs of different points in the exponent of (B.2)

$$U(x_1, ..., x_n) = \sum_{i=1}^{n-1} \sum_{j=i+1}^{n} \phi(\|x_i - x_j\|) \tag{B.3}$$

is often called the 'total energy' of the system of points with pairwise interaction defined by the pair potential function $\phi(r)$.

Many different types of pair potential functions may be considered, the followings are applied in the thesis:

- *Gibbs hard-core process with fixed number of points.* This process is defined through the pair potential function

$$\phi(r) = \left\{ \begin{array}{ll} \infty & r \leq r_0 \\ 0 & r > r_0 \end{array} \right\} \tag{B.4}$$

  with a fixed *hard-core* distance r_0. There are no pairs of points that are closer than the distance r_0. This results in a 'regular' point pattern.

- *Strauss process with fixed number of points*

$$\phi(r) = \left\{ \begin{array}{ll} \beta & r \leq r_{max} \\ 0 & r > r_{max} \end{array} \right\} \tag{B.5}$$

- *Hard-core Strauss process with fixed number of points*

$$\phi(r) = \left\{ \begin{array}{ll} \infty & r < r_0 \\ \beta & r_0 < r \leq r_{max} \\ 0 & r > r_{max} \end{array} \right\} \tag{B.6}$$

  Hard-core Strauss point pattern denotes that there are no pairs of points that are closer than the distance r_o, a certain number of points can locate (with a probability) within the distance $r_0 < r \leq r_{max}$.

The *'Gibbs Hard-core Strauss'* process is applied to reconstruct the positions of the trees in each stand (data plot) in our forest.

B.1. Reconstruction of point patterns

The main idea is to generate a simulated pattern such that appropriate summary characteristics of real pattern as similar as possible. This reconstruction approach demonstrates the summary characteristics to extract important features in spatial point pattern of data sets.

To generate the *Gibbs Hard-core Strauss point pattern*, an iterative procedure called the Markov chain Monte Carlo (MCMC) method is applied. The approach is iterative with an initial point pattern which is modified in a step-by-step fashion by deleting some points and generating others. This procedure is repeated many times until the algorithm eventually converges and generates the expected patterns.

In the case of even-age stands as in our data, if we assume that environmental condition in one stand is homogeneous, the differentiation in size among individual trees will come from two reasons, the first is from the tree inside itself, the second is due to spatial competition among trees. Therefore, in the case of our data, the smaller trees are overlapped by the bigger trees (they locate inside the zone of influence of bigger trees).

Under this assumption, to generate the *Gibbs Hard-core Strauss point pattern* so that it best explains the data, the first certain number of bigger trees in the plot (75% of total trees with higher *dbh* values) are generated uniformly, then the other smaller trees (the remain 25%) are generated sequentially. If there are existing events within the distance of $dbh/2$ of each event (hard-cord distance), then they are rejected. A certain number of smaller trees can be located (with a probability) within a radius $dbh/2 < r \leq R$ of the bigger tree's location (Eq. B.6).

The steps for generating N trees

- Rank the *dbh*s of trees in a stand from largest to smallest
- Generate $n1$ larger trees (defined as 75% in total number of trees) uniformly in the stand
- Generate the remain 25% ($n2 = N - n1$) smaller trees randomly located in the stand
- Delete the point x_k, if

$$min\left\{\|x_k - x_i\| : i = 1, 2, ..., n2,\ i \neq k\right\} < rbh(x_k) \tag{B.7}$$

  where x_i is the neighbouring point (tree) of x_k
- Generate new point until the proposed point can be accepted

C. Appendix C: Equations, Variables and Constants

We describe the Equations, Variables and Constants follow the structures of submodels that implemented in our models. In the equations presented below, for the IBM, they are applied for each species specific individual tree. For CGMM, they are applied for each *dbh* class of each species.

C.1. Equations

C.1.1. Tree Growth

Increment of *dbh*:

$$\frac{d(dbh)}{dt} = \frac{G_{opt} \cdot dbh \cdot (1 - dbh \cdot H/D_{max}/H_{max})}{2b_1 + 3b_2 \cdot dbh - 4b_3 \cdot dbh^2} \times f_s \times f_{el} \times f_c \tag{C.1}$$

Tree height:

$$H = b_1 + b_2 \cdot dbh - b_3 \cdot dbh^2 \tag{C.2}$$

Tree biomass:

$$Biom = a_1 \cdot dbh^{c_1} \tag{C.3}$$

Multipliers

- Salinity multiplier:

$$f_s = \frac{1 - a_{0s}}{1 + e^{d(x_{1s} - s)}} + a_{0s} \tag{C.4}$$

- Elevation multiplier:

$$f_{el} = \left\{ (a_{maxe} - a_{1e}) \left[1 - e^{-(el/el_1)^{\alpha}} \right] + a_{1e} \right\} e^{-(el/el_2)^{\beta}} + a_{2e} \left[1 - e^{-(el/el_2)^{\beta}} \right] \tag{C.5}$$

C.1.2. Tree - to - tree Competition

$$f_c = (a_{maxc} - a_{0c}) \exp\left[-(FA/FA_{thr})\right] + a_{0c} \tag{C.6}$$

For IBM

$$FA_i = \frac{1}{FON_i} \times \sum_{j=1; j \neq i}^{Nn} \int_O FON_{o,ij} \tag{C.7}$$

Table C.1.: *Processes are implemented in IBM and CGMM.*

Process	**Symmbol**	**IBM**	**CGMM (LBM)**
Growth	dbh, H	Individual tree	Individual dbh class
Factor of tree-to-tree competition	FA	Spatial explicitness, competition between individual trees	Spatial statistics, competition between focused dbh class and other classes
Reproduction	Ns	Total number of seedlings are given by a species specific parent tree	Total number of seedlings of tree species sp at dbh class k in the cell (x, y)
Seedling dispersal	k_s	By a kernel k_s which is the bivariate normal probability density function, the seedlings are dispersed from the position of the parent tree. This process takes into account the hard-core process, a seedling can not grow inside the hard-core distance $dbh/2$ from other trees	By a kernel k_s which is the bivariate normal probability distribution, the seedlings are dispersed from the source cell to target cells
Mortality	Pm	The individual tree will die if it's mortality probability increases beyond a threshold	When the mortality probability of dbh class k increases beyond a threshold, a random number (from 1 to Nc) of trees in dbh class k of species sp will die
Level of interaction		Spatially explicit interaction among trees and between trees and the environment	Two levels of interaction: the local interaction within cell (through growth, competition, reproduction, mortality) and the spatial interaction between cells through seedling dispersal
Abiotic factors		The salinity and elevation values are the functions which are dependent on the coordinates (x, y) in the stand	The salinity and elevation are input from GIS data

$$FON = \left\{ \begin{array}{cc} F_{max} & 0 \leq r \leq rbh \\ \exp\left[-\frac{|log(F_{min})|}{R-rbh}(r-rbh)\right] & rbh < r \leq R \\ 0 & r > R \end{array} \right\} \tag{C.8}$$

$$R = a_2 \times rbh^{c_2} \tag{C.9}$$

For CGMM

$$FA = 1 - exp\left[-(\frac{\bar{R_{nei}}}{R_{thr}})^{\gamma 1}\right] \tag{C.10}$$

$$R_{thr} = a_3 + c_3 \cdot dist \tag{C.11}$$

$$dist = 0.5 \times \sqrt{\frac{Scell}{N}} \tag{C.12}$$

$$\gamma 1 = a_4 \cdot R_f^{c_4} \tag{C.13}$$

C.1.3. Reproduction

$$\frac{dN2}{dt} = r_2 \cdot fRep \cdot Biom \cdot (1 - \frac{N2}{N2_{max}}) \tag{C.14}$$

$$fRep = 1 - exp\left[-(Biom/Ec)^{\gamma 2}\right] \tag{C.15}$$

Biom is calculated from Eq. C.3

C.1.4. Seedling dispersal

$$h(r) = \left\{ \begin{array}{cc} 0 & r \leq rbh \\ k_s(x, y|\mu_1, \mu_2) & r > rbh \end{array} \right\} \tag{C.16}$$

$$r = \sqrt{(x-\mu_1)^2 + (y-\mu_2)^2} \tag{C.17}$$

$$k_s(x, y|\mu_1, \mu_2) = \frac{1}{2\pi \cdot \sigma_1 \cdot \sigma_2 \sqrt{1-\rho^2}} exp\left[-\frac{1}{2(1-\rho^2)} \cdot \left(\frac{(x-\mu_1)^2}{\sigma_1^2} - \frac{2\rho(x-\mu_1)(y-\mu_2)}{\sigma_1 \cdot \sigma_2} + \frac{(y-\mu_2)^2}{\sigma_2^2}\right)\right] \tag{C.18}$$

C.1.5. Tree mortality

$$\frac{dE}{dt} = r_1 \cdot \frac{dBiom}{dt} - r_3 \cdot N2 - \mu \cdot Biom \tag{C.19}$$

$$\mu = \mu 0 \times exp[-(\frac{t}{t_{thr}})^{\alpha_\mu}] \tag{C.20}$$

$$P_m = P0 \times exp(-r_4 \cdot E) \tag{C.21}$$

C.2. Parameters

All the parameters for growth equation are estimated (as described in Chapter 3) from the data of two species: *Rhizophora apiculata* and *Avicennia alba*, for *Phoenix paludosa* we use assumed parameters.

The parameters for other processes (reproduction, seedling dispersal, tree mortality) are assumed parameters for all three species.

Table C.2.: *Parameters of growth equation*

Parameters	**Description**	*R.apiculata*	*A.alba*	*P.paludosa*
G_{opt}	species specific growth constant, under optimal growth situation	485.95	390	550.95
D_{max}	maximum diameter of tree	70	65	60
H_{max}	maximum height of tree	4200	4000	3200
b_1	height value of seedling	100	100	100
b_2	species specific growth constant	117.1429	120	103.33
b_3	species specific growth constant	0.8367	0.923	0.8611
a_1	scaling factor of biomass function	0.6353	0.128	0.3
c_1	scaling factor of biomass function	1.9264	2.4171	0.3

Table C.3.: *Parameters of growth multiplier of salinity factor*

Parameters	**Description**	*R.apiculata*	*A.alba*	*P.paludosa*
a_{0s}	minimum value of salinity factor multiplier	0.3	0.3	0.3
d	constant that describing the steepness of salinity factor multiplier	-0.4	-0.18	-0.6
x_{1s}	the salinity threshold	24	30	20

Table C.4.: *Parameters of growth multiplier of elevation factor*

Parameters	**Description**	*R.apiculata*	*A.alba*	*P.paludosa*
a_{maxe}	maximum value of elevation factor multiplier	1	1	1
a_{1e}	minimum value of elevation factor multiplier	0.04	0.15	0
a_{2e}	minimum value of elevation factor multiplier	0.15	0.03	0.3
el_1	factor that define the optimal elevation range	-1	-2.3	0.9
el_2	factor that define the optimal elevation range	2.5	0.5	6.2
α	scaling parameter	20	20	20
β	scaling parameter	20	20	20

Table C.5.: *Parameters of growth multiplier of competition factor (for IBM)*

Parameters	**Description**	*R.apiculata*	*A.alba*	*P.paludosa*	**Comments**
a_{maxc}	maximum value of competition factor multiplier	1	1	1	estimated
a_{0c}	minimum value of competition factor multiplier	0.15	0.15	0.15	estimated
FA_{thr}	threshold value of competition factor FA	0.3	0.3	0.3	estimated
a_2	scaling parameter for calculating the zone of influence R	21.994	39.174	11	estimated
c_2	scaling parameter for calculating the zone of influence R	0.8764	0.5486	0.8764	estimated
F_{min}	min. value of the FON	0.1	0.1	0.1	from Berger and Hildenbrandt (2000)
F_{max}	max. value of the FON	1	1	1	from Berger and Hildenbrandt (2000)

Table C.6.: *Parameters of growth multiplier of competition factor (for CGMM)*

Parameters	**Description**	*R.apiculata*	*A.alba*	*P.paludosa*
a_3	scaling parameter for calculating the threshold of R	6.552	6.552	6.552
c_3	scaling parameter for calculating the threshold of R	0.996	0.996	0.996
a_4	scaling parameter for calculating the threshold of $\gamma 1$	239.5	239.5	239.5
c_4	scaling parameter for calculating the threshold of $\gamma 1$ in	-0.75	-0.75	-0.75

Table C.7.: *Parameters of reproduction function*

Parameters	**Description**	*R.apiculata*	*A.alba*	*P.paludosa*
E_c	threshold value of Biomass	3.75	3.75	3
$\gamma 2$	scaling factor	3.6	3.6	6
r_2	rate of reproduction	0.005	0.004	0.02
$N2_{max}$	maximum number of seedling a tree produce	15	20	25

Table C.8.: *Parameters of mortality probability function*

Parameters	**Description**	*R.apiculata*	*A.alba*	*P.paludosa*
$P0$	Mortality probability at zero growth	1	1	1
r_4	decay rate	0.04	0.04	0.04

D. Appendix D: List of Symbols

Symbols	Description
f_c	competition factor (multiplier) that influences the growth rate of tree
f_{el}	elevation factor (multiplier) that influences the growth rate of tree
f_s	salinity factor (multiplier) that influences the growth rate of tree
G_{opt}	species specific growth constant, under optimal growth situation
G	tree's growth rate under integrated conditions
dbh	diameter at breast height of tree
H	height of tree
H_{max}	maximum height of tree
D_{max}	maximum diameter of tree
b_1	height value of seedling
b_2	species specific growth constant
b_3	species specific growth constant
ppt	part per thousand
MUL	mutiplier
a_{0s}	min. value of salinity factor multiplier
d	constant for salinity factor multiplier
x_{1s}	salinity value effects on growth
s	salinity in ppt
a_{maxe}	max. value of elevation factor multiplier
a_{1e}	min. value of elevation factor multiplier
el	elevation in meter
el_1	constant for elevation effect on growth
el_2	constant for elevation effect on growth
α	constant for elevation effect on growth
β	constant for elevation effect on growth
a_{maxc}	max. value for competition effect on growth
a_{0c}	min. value for competition effect on growth
FA	competition factor that effects on growth
FA_{thr}	constant for competition effect on growth
FON	Field of Neighbourhood

FON_o	area of Field of Neighbourhood is overlapped by neighbouring trees
R	radius of Zone of influence
$Biom$	biomass of tree
a_1	scaling parameter for calculating biomass
c_1	scaling parameter for calculating biomass
a_2	scaling parameter for calculating diameter of Zone of influence
c_2	scaling parameter for calculating diameter of Zone of influence
R_{thr}	threshold value of R
a_3	scaling parameter for calculating R threshold
c_3	scaling parameter for R threshold
$\gamma 1$	scaling factor takes into account the steepness of the curve FA in CGMM
a_4	scaling parameter for calculating $\gamma 1$
c_4	scaling parameter for calculating $\gamma 1$
$dist$	mean distance among trees in the stand
R_f	zone of influence of focused tree
Ec	threshold value of biomass
k_s	dispersal kernel
Ns	total number of seedlings in one stand
$N1$	number of seedlings are planted on a unit area
$N2$	number of seedlings are regenerated by adult trees in a stand
Nd	number of young fatalities in a stand
Pm	probability of mortality
res	residual sum of squares

References

Adler, F. R. (1996). A model of self-thinning through local competition. *Population Biology 93*, 9980.

Allen, T. H. F. and T. B. Starr (1982). *Hierarchy: Perspectives for Ecological Complexity.* The University of Chicago Press, Chicago.

Alongi, D. M. (2008). Mangrove forests: Resilience; protection from tsunamis and responses to global climate change. *Estuarine, Coastal and Shelf science 76*, 1–13.

Andrew Royle, J. and R. M. Dorazio (2008). *Hierarchical modelling and Inference in Ecology. The Analysis of Data from Populations, Metapopulations and Communities.* Academic Press, San Diego.

Anh, N. H. (2007). Assessing the impacts of man-made topography on mangrove forest - case study of cangio area, hochiminh city, vietnam. Master's thesis, Institute for Environment & Resources, VNU-HCMC, Vietnam.

Berger, U. and H. Hildenbrandt (2000). A new approach to spatially explicit modelling of forest dynamics: spacing, ageing and neighbourhood competition of mangrove trees. *Ecological Modelling 132*, 287 – 302.

Berger, U., V. H. Rivera-Monroy, T. W. Doyle, F. Dahdouh-Guebas, N. C. Duke, M. L. Fontalvo-Herazo, H. Hildenbrandt, N. Koedam, U. Mehlig, C. Piou, and R. R. Twilley (2008). Advances and limitations of individual-based models to analyze and predict dynamics of mangrove forests: A review. *Aquatic Botany 89*, 260.

Berninger, F. and E. Nikinmaa (1997). Implications of varying pipe model relationships on scots pine growth in different climates. *Functional Ecology 11*, 146.

Botkin, D. B. (1993). *Forest dynamics. An Ecological Model.* Oxford University Press.

Bunt, J. S. (1996). Mangrove zonation: An examination of data from seventeen riverine estuaries in tropical australia. *Annals of Botany 78*, 333–341.

Chen, R. and R. R. Twilley (1998). A gap dynamic model of mangrove forest development along gradients of soil salinity and nutrient resources. *Journal of Ecology 86*, 37–51.

Clough, B., D. Tan, D. Phuong, and D. Buu (2000). Canopy leaf area index and litter fall in stands of the mangrove rhizophora apiculata of different age in mekong delta, vietnam. *Aquatic Botany 66*, 311–320.

Costanza, R. and A. Voinov (2004). *Landscape simulation modelling: A spatially explicit dynamic approach.* Springer-Verlag.

Dale, V., T. Doyle, and H. Shugart (1985). A comparison of tree growth models. *Ecological Modelling 29*, 145.

FAO (2005). *Global forest resources assessment. Thematic study on Mangroves. Vietnam.* Forestry Department, FAO, Rome (Italy).

Fujimoto, K., T. Miyagi, T. Adachi, H. andMurofochi, M. Hiraide, T. Kumuda, N. H. Phan, S. T. Mai, X. Do, and N. N. Vien (2000). *Belowground carbon sequestration of mangrove forests in Southern Vietnam. In: Organic material and sea level change in mangrove habitat.* Grant in Aid for International Scientific Research.

Furukawa, K. and E. Wolanski (1996). Sedimentation in mangrove forests. *Mangroves and Salt Marshes 1*, 3–10.

Garman, S. L. (2004). Design and evaluation of a forest landscape change model for western oregon. *Ecological Modelling 175*, 319–337.

Grimm, V. (1999). Ten years of individual-based modelling in ecology: what have we learned and what could we learn in the future? *Ecological Modelling 115*, 129.

Grimm, V., U. Berger, D. L. DeAngelis, J. Gary Polhill, J. Giske, and S. F. Railsback (2010). The odd protocol: A review and first update. *Ecological Modelling 221*, 2760–2768.

Hamzah, L., K. Harada, and F. Imamura (1999). Experimental and numerical study on the effect of mangrove to reduce tsunami. *tohoku Journal of Natural Disaster Science 35*, 127–132.

Hang, H. T. M. and N. H. Anh (2002). Study on using vegetation indicator in monitoring the change of soil features in cangio area with the help of remote sensing (in vietnamese). *Journal of Science & Technology Development, Vietnam 5.*

Hang, H. T. M. and N. H. Anh (2003). Geoinformatics and landuse planning for the wetland - case study of cangio - hochiminh city- south vietnam. *Environmental Informatics (ISEIS) 1.*

Hang, H. T. M. and N. H. Anh (2006a). Geoinformatics application in saigon – dongnai river basin management – some achievements (in vietnamese). *Journal of Science of Technology Development, Environment Resources, Vietnam 9*, 14.

Hang, H. T. M. and N. H. Anh (2006b). Sustainable urbanization for the coastal wetland – cangio district – hochiminh city (in vietnamese). *ournal of Science of Technology Development, Environment Resources, Vietnam 9*, 40.

Hang, H. T. M., D. V. Quy, T. Triet, N. H. Anh, K. Hirose, Y. Maruyama, and S. Y. (2003). Geo–environmental research for cangio mangrove forest, vietnam. *Asian Journal of Geoinformatics 1*, 3.

Harada, K. and F. Imamura (2005). *Effects of coastal forest on tsunami hazard mitigation - A preliminary investigation. In: Tsunamis: Case studies and recent developments.* Springer, the Netherlands.

Hirose, K., M. Syoji, H. T. M. Hang, N. H. Anh, T. Triet, and V. N. Nam (2004). Mangrove mapping using aster vnir and swir data. In *Proceedings of the 36th Conference of the remote sensing society of Japan.*

Hong, P. N. (1991). *Mangrove Ecology in Vietnam.* Ph. D. thesis, HaNoi University of Education, Vietnam.

Hong, P. N. (2004). *Effects of mangrove restoration and conservation on the biodiversity and environment in Can Gio District. In: Mangrove management and conservation: present and future.* United Nations University Press, New York.

Hong, P. N. and Q. Q. Dao (2003). *Mangrove reforestation in Vietnam - Achievements and Challenges. In: Evaluation of effects of mangrove reforestation on the environment and coastal life (JRC Funded Project areas).* Proceedings of the JRC/MERD mangrove reforestation project. Agricultural Publishing House, HaNoi.

Hong, P. N., N. B. Quynh, and N. H. Tri (1988). *Mangrove Forest, potential and use.* Agricultural Publishers, Vietnam.

Hope, J. C. E. (2003). *Modelling forest landscape dynamics in Glen Affric, northern Scotland.* Ph. D. thesis, University of Stirling.

Illian, J., A. Penttinen, H. Stoyan, and D. Stoyan (2008). *Statistical Analysis and Modelling of Spatial Point Patterns.* John Willey & Sons.

Kimmins, H., J. A. Blanco, B. Seely, C. Welham, and K. Scoullar (2010). *Forecasting Forest Futures. A Hybrid Modelling Approach to the Assessment of Sustainability of Forest Ecosystems and their Values.* Earthscan.

Kuenzer, C., A. Bluemel, S. Gebhardt, Q. T. Vo, and S. Dech (2011). Remote sensing of mangrove ecosystem: A review. *Remote sensing 3*, 878–928.

Le Roux, X., A. Lacointea, A. Escobar-Gutiérrez, and S. Le Dizèsa (2001). Carbon-based models of individual tree growth: a critical appraisal. *Annals of Forest Sciences 58*, 469.

Li, B. L., H. i. Wu, and G. Zou (2000). Self-thinning rule: a causal interpretation from ecological field theory. *Ecological Modelling 132*, 167.

Lischke, H., T. J. Löffler, and A. Fischlin (1998). Aggregation of individual trees and patches in forest scucession models: capturing variability with height structure, random, spatial distributions. *Theoretical population biology 54*, 213.

Lischke, H., T. J. Löffler, P. E. Thornton, and N. E. Zimmermann (2007). *Model up-scaling in landscape research. In: A changing World. Challenges for Landscape Research.* Springer. The Netherlands.

Lischke, H., N. E. Zimmermanna, J. Bolliger, S. Rickebusch, and T. J. Löffler (2006). Treemig: A forest-landscape model for simulating spatio-temporal patterns from stand to landscape scale. *Ecological Modelling 199*, 409 – 420.

Liu, J. and P. Ashton (1995). Individual-based simulation models for forest succession and management. *Forest Ecology and Management 73*, 157.

López-Hoffman, L., D. D. Ackerly, N. P. R. Anten, J. L. Denoyer, and M. Martinez-Ramos (2007). Gap-dependence in mangrove life-history strategies: a consideration of the entire life cycle and patch dynamics. *Journal of Ecology 95*, 1222–1233.

Luan, J., R. I. Muetzelfeldt, and J. Grace (1996). Hierarchical approach to forest ecosystem simulation. *Ecological Modelling 86*, 37.

Lugo, A. E. and S. C. Snedaker (1974). The ecology of mangroves. *Ann. Rev. Ecol. Systematics 5*, 39–64.

Macnae, W. (1966). Mangroves in eastern and southern australia. *Australian Journal of Botany 14*, 67 – 104.

Manson, F. J., N. R. Loneragan, G. A. Skilleter, and S. R. Phinn (2005). An evaluation of the evidence for linkages between mangroves and fisheries: A synthesis of the literature and identification of research directions. *Oceanography and Marine Biology: An Annual Review 43*, 485–515.

Mazda, Y., D. Kobashi, and S. Okada (2005). Tidal - scale hydrodynamics within mangrove swamps. *Wetland and Management 13*, 647–655.

Mladenoff, D. and W. Baker (1999). *Spatial modeling of forest landscape change: approaches and applications*. Cambridge University Press.

Mladenoff, D. J. (2004). Landis and forest landscape models. *Ecological Modelling 180*, 7.

Mochida, Y., S. Ichihara, T. Miyagi, Y. Hirabuki, K. Fujimoto, T. Murohushi, P. Duc, N. N. Vien, V. S. Le, and N. H. Phan (2000). *Ecological study of mangrove forest in CanGio, HoChiMinh City, Vietnam. In: Organic material and sea level change in mangrove habitat.* Grant in Aid for International Scientific Research.

Moller, J. and R. P. Waagepetersen (2007). Modern statistics for spatial point processes. *Scandinavian Journal of Statistics 34*, 643–684.

Monserud, R. A. (2003). Evaluating forest models in a sustainable forest management context. *FBMIS 1*, 35–47.

Munro (1974). *Forest growth models - a prognosis. In: Growth models for tree and stand simulation, 7-21.* Royal College of Forestry, Stockholm, Sweden.

Nagelkerken, I., S. J. Blaber, S. Bouillon, P. Green, M. Haywood, L. G. Kirton, J. O. Meynecke, J. Pawlik, H. M. Penrose, A. Sasekumar, and P. J. Somerfield (2008). The habit function of mangroves for terrestrial and marine fauna: A review. *Aquatic Botany 89*, 155–185.

Nakajima, T., M. Matsumoto, and N. Shiraishi (2011). Modeling diameter growth and self-thinning in planted sugi (cryptomeria japonica) stands. *The Open Forest Science Journal 4*, 49.

Nam, V. N. (2000). *Study on biomass and productivity of natural Avicennia alba community in CanGio District, HoChiMinh City. In: Organic material and sea level change in mangrove habitat.* Grant in Aid for International Scientific Research.

Nam, V. N. (2003). *Biomass and primary productivity of natural population of Avicennia alba BL. in CanGio, HoChiMinh City.* Ph. D. thesis, Forest Science Institute of Vietnam (FSIV).

Nam, V. N., T. V. My, and M. Jensen (1992). *Mangrove for production and protection. A changing resource system: Case study in CanGio District, Southern Vietnam. In: Field document No 35 RWEDP in Asia.* FAO.

Nam, V. N., N. D. Quy, and N. S. Thuy (1996). Research on biomass and primary productivity of planted rhizophora apiculata in cangio, hochiminh city. Technical report, Department of Science and Technology of HoChiMinh City, Vietnam.

Nam, V. N. and N. S. Thuy (1998). Vegetation in cangio mangrove forest, hochiminh city. *Journal of Forestry, Vietnam 1*, 29.

Ngan, P. and C. Q. Hien (1987). *Mangroves in Vietnam (in Vietnamese).* Viet Nam Education Publishing House.

Nguyen, P. K. (2009). Climate change, sea level rise scenarios for vietnam. Technical report, Ministry of Natural Resources and Environment.

Oliver, J. (1982). *The geographic and environmental aspects of mangrove communities: climate. In: Mangrove ecosystems in Australia - structure, function and management.* ANU Press, Canberra.

Plummer, S. E. (2000). Perspectives on combining ecological process models and remotely sensed data. *Ecological Modelling 129*, 169–186.

Pool, D. G., S. C. Snedaker, and A. E. Lugo (1977). Structure of mangrove forests in florida, puerto rico, mexico and costa rica. *Biotropica 9*, 195–212.

Ratzé, C., F. Gillet, J. P. Müller, and K. Stoffel (2007). Simulation modelling of ecological hierarchies in constructive dynamical systems. *ecological complexity 4*, 13.

Saenger, P. (2002). *Mangrove Ecology, Silviculture and Conservation.* Kluwer Academic Publishers.

Shugart, H. (1984). *A Theory of Forest Dynamics: the Ecological Implications of Forest Succession Models.* Springer-Verlag, New York.

Shugart, H. and D. West (1980). Forest succession models. *Bioscience 30*, 308.

Sinoquet, H. and X. Le Roux (2000). Short-term interactions between tree foliage and the aerial environment: an overview of modelling approaches available for tree structure-function models. *Annals of Forest Sciences 57*, 477.

Snedaker, S. C. (1982). *Mangrove species zonation: why?. In: Tasks for vegetation Science.* The Hague: Dr W. Junk.

Sternberg, L. d. S. L., S. Y. Teh, S. M. L. Ewe, F. M. Wilhelm, and D. L. DeAngelis (2007). Competition between hardwood hammocks and mangroves. *Ecosystems 10*, 648–660.

Teh, S. Y., D. L. DeAngelis, L. d. S. L. Sternberg, F. R. Miralles-Wilhelm, T. J. Smith, and H.-L. Koh (2008). A simulation model for projecting changes in salinity concentrations and species dominance in the coastal margin habitats of the everglades. *Ecological Modelling 213*, 245–256.

Thom, B. G. (1982). *Mangrove ecology - a geomorphological perspective. In: Mangrove ecosystems in Australia.* Australian National Unversity Press, Canberra.

Thu, P. M. and J. Populus (2007). Status and changes of mangrove forest in mekong delta: Case study in tra vinh, vietnam. *Estuarine, Coastal and Shelf science 71*, 98–109.

Tomlinson, P. B. (1986). *The Botany of Mangrove.* Cambridge University Press.

Twilley, R. R., V. H. Rivera-Monroy, R. Chen, and L. Botero (1999). Adapting an ecological mangrove model to simulate trajectories in restoration ecology. *Mar. Pollut. Bull. 37*, 404–419.

Valiela, I., B. J. L., and J. K. York (2001). Mangrove forests: One of the world's threatened major tropical environments. *Bioscience 51*, 807–815.

Vanclay, J. K. (1994). *Modelling forest growth and yield : applications to mixed tropical forests.* ePublications@SCU.

Waring, R. and S. Running (1998). *Forest Ecosystems: analysis at multiple scales. 2nd edition.* Academic Press, San Diego.

Xi, W., R. N. Coulson, A. G. Birt, Z. B. Shang, J. D. Waldron, C. W. Lafon, D. M. Cairns, M. D. Tchakerian, and K. D. Klepzig (2009). Review of forest landscape models: Types, methods, development and applications. *Acta Ecologica Sinica 29*, 69.